

GRID POWER QUALITY WITH VARIABLE SPEED TURBINES (HYDRO TURBINES AND/OR WIND TURBINES)

A DISSERTATION

*Submitted in partial fulfillment of the
requirements for the award of the degree*

of

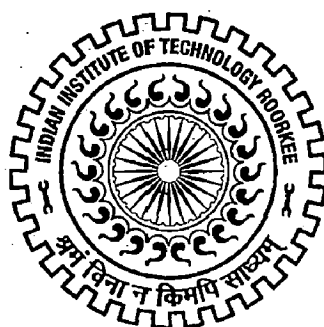
MASTER OF TECHNOLOGY

in

ALTERNATE HYDRO ENERGY SYSTEMS

By

A.V.SESHAGIRI ANANTH



**ALTERNATE HYDRO ENERGY CENTRE
INDIAN INSTITUTE OF TECHNOLOGY ROORKEE
ROORKEE - 247 667 (INDIA)**

JUNE, 2007

CANDIDATE'S DECLARATION

This is to certify that the work which is being presented in the form of this report in this dissertation entitled, "**Grid power quality with variable speed turbines (hydro turbines and/or wind turbines)**", in partial fulfillment of the requirements for the award of the degree of **Master of Technology** in "**Alternate Hydro Energy Systems**", submitted in Alternate Hydro Energy Centre, Indian Institute of Technology, Roorkee is an authentic record of my own work carried out during the period from July, 2006 to June, 2007 under the able guidance of **Prof Dr. J.D.Sharma**, Professor, **Department of Electrical Engineering**, Indian Institute of Technology, Roorkee.

The matter embodied in this Dissertation has not been submitted by me for the award of any other degree or diploma.

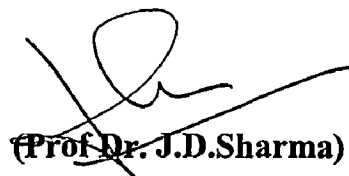
Date: 29 June, 2007

Place: Roorkee



(A.V.SESHAGIRI ANANTH)

This is to certify that the above statement made by the candidate is correct to best of my knowledge.



(Prof Dr. J.D.Sharma)

Professor,

Department of Electrical Engineering,

Indian Institute of Technology,

Roorkee-247667

ACKNOWLEDGEMENT

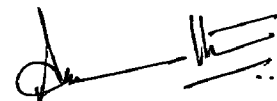
First of all, I take this opportunity to express my foremost and deep sense of gratitude to **Prof Dr.J.D.Sharma**, Professor, **Department of Electrical Engineering**, Indian Institute of Technology Roorkee, for his proficient and enthusiastic guidance, useful criticism, encouragement and immense help. The valuable hours of discussions and suggestions that I had with him have undoubtedly helped in supplementing my thoughts in the right direction for attaining the desired objective. Working under his guidance will always remain a cherished experience in my memory and I will adore it throughout my life.

My very special thanks and gratitude are due to **Shri Arun Kumar**, Head of the Department, **Alternate Hydro Energy Centre**, who stood by me and supported when I have had difficult times. I am greatly indebted to him and such was the rare parental care and support I received from him not only in the past six months but through out my stay at IIT Roorkee. The suggestions he has given me about getting along with life have changed my lifestyle significantly. Not only this, I have also seen and worked closely with him and produced two sponsored “**Sectoral Overview Reports on Hydropower Development in India**”. That had given me the exposure of working for a company under stress. For this, I am thankful to him once again.

It is a great pleasure to acknowledge the help of **Ms. Anubhuti Bansal**, my junior at **Alternate Hydro Energy Centre** in preparing this report. She is a great teacher and a wonderful person. I consider myself fortunate to have a friend like her.

I am very much indebted to **Mr. M. Sekhar Babu**, my fellow batch mate of Chemical Engineering Department, for providing great mental support through out the period of my dissertation without which I would not have completed this work.

Finally, I would like to record my thanks to the entire **Faculty of Alternate Hydro Energy Centre**, my fellow class-mates, friends and **my family** for their constant support and encouragement.



(ANANTH, A.V.SESHAGIRI)

ABSTRACT

As the title of this dissertation indicates, variable-speed wind turbines are equipped with special synchronous generator drives which can run at any speed apart from their rated synchronous speed. This can be achieved with the help of the field rotor excitation control system of the generator which adapts the rotational speed of the wind turbine rotor (or the generator rotor, since there is no gearbox) to the wind speed over a relatively wide speed range, so as to produce a variable frequency voltage waveforms. But the electrical system should have a fixed frequency which should be equal to the grid frequency for the system to run in synchronism with the grid. A generator drive connecting a variable-speed mechanical system with a fixed frequency electrical system must therefore contain some kind of a slip or decoupling mechanism between the two systems for the variable speed operation to be possible. This mechanism is provided by the rectifier and the inverter circuit block in the present work. The main principle of this block is to convert the variable frequency (due to the variable speed) into a fixed frequency by rectifying and then inverting to a desired frequency:

In wind turbine technology, the doubly-fed induction generator drive (Type C) and the full load converter connected generator drive (Type D) are the two most frequently applied variable speed generator drive concepts. There are also other variable-speed generator drive types, but they are currently not generally applied in wind turbines. It would probably also be possible to use written pole synchronous generators as a way of obtaining variable-speed capability in a generator drive [23].

The Type D variable-speed generator drive which is selected in this dissertation, consist of a traditional synchronous generator combined with power electronics to provide the slip or decoupling mechanism as said before. This configuration is relatively simple to implement and has many advantages over the only other configuration, i.e., Type C where a doubly fed induction generator is used.

As far as the computer simulation is concerned, as yet, most simulation programs do not include such models as standard. There may be standard models of the individual components (i.e. generators, excitation system, comparators, pulse generators and universal bridge blocks) but they are not integrated into a unified model needed in a

universal bridge blocks) but they are not integrated into a unified model needed in a variable-speed generator drive. Hence, in the present work, a synchronous generator model, an IEEE Type 1 excitation system model, a voltage comparator model which is used in the control system to produce required gate pulses for the inverter to generate a frequency of 50 Hz, a pulse generator and the universal bridge blocks of MATLAB/Simulink environment have been used.

To briefly explain the concept, the output of this gearless variable speed synchronous generator will be given to the frequency converter to convert variable frequency into a fixed frequency. In this context, it is made sure that the generator always produces the EMF even at other speeds other than the synchronous speed. The other speeds are the different wind speeds. This has been achieved by controlling the excitation system of the generator to produce variable flux linkage corresponding to the speed of the generator at that particular time for the purpose of maintaining constant magnitude output voltage waveform. The control is done by the feedback circuit which feeds back the voltage components V_d and V_q to the excitation system and the control system present in the excitation system does the rest of the work.

The effort has been put to build the rest of the components required to make the full system and integrate these individual components into a unified model with the necessary internal control systems needed in a variable-speed generator drive by giving well-fit appropriate specifications. Later, this modeled and integrated experimental set up is connected to a 10000 MVA, 230 kV grid through a 2.35 MVA transformer and a 100 km transmission line. The loads have been connected and then the model has been simulated to produce very good results.

The grid power quality of these variable speed wind turbines is an inherent advantage of variable speed operation. Hence, the power quality is maintained in the system itself eliminating the need for installing new PE devices directly saving the cost.

Later the system protection studies through fault analysis are also done to check the system's performance under those faulted conditions and almost perfect results have been produced.

CONTENTS

S.No.	ITEM	Page No
	CANDIDATE'S DECLARATION	i
	ACKNOWLEDGEMENT	ii
	ABSTRACT	iv
	CONTENTS	vi
	LIST OF FIGURES	vii
	LIST OF TABLES	x
CHAPTER 1	INTRODUCTION	
1.1	Overview	1
1.2	Recent advances in wind power generation	1
1.3	Variable speed wind turbines	1
1.4	Various configurations of wind turbines	2
1.5	Fixed vs. variable speed turbines	4
1.6	Comparisons of the two variable speed designs	5
1.7	Power control concepts of wind turbine in general	5
1.8	Generator	7
1.9	Types of installations of wind turbines	8
CHAPTER 2	LITERATURE REVIEW	
2.1	Overview	12
2.2	Literature	12
CHAPTER 3	VARIABLE SPEED WIND TURBINE-GENERATOR SYSTEM	
3.1	Overview	16
3.2	Variable speed wind turbine	16
	3.2.1 Efficiency of the wind turbine in general	20
	3.2.2 Efficiency of variable speed turbines	21
	3.2.3 Performance assessment of variable speed turbines	23
	3.2.4 Power curve	24
	3.2.5 Power coefficient C_p	24

3.3.1	Park's transformation	28
3.3.2	Load angle	30
3.3.3	Power factor determination	31
3.4	Rectifiers and Inverters	32
CHAPTER 4 MODELLING AND SIMULATION		
4.1	Overview	34
4.2	Introduction to modelling and simulation	34
4.3	Model verification of wind turbine	35
4.4	Model verification of the generator	39
4.5	Complete model	45
4.6	Grid power quality	54
4.7	Variable speed hydro turbines	55
CHAPTER 5 FAULT ANALYSIS		
5.1	Overview	55
5.2	Purpose of fault calculation	55
5.3	Types of faults	56
5.4	Switching transients	58
5.5	Simulation results and discussion	59
5.5.1	LLLG Fault	60
5.5.2	LL Fault	63
5.5.3	LG Fault	66
5.5.4	LLG Fault	68
5.5.5	LL Fault and LG Fault on the third phase	71
5.5.6	Short circuit fault current calculation	74
5.6	Results in a tabulated form	75
CHAPTER 6 CONCLUSIONS AND FUTURE SCOPE		
6.1	Conclusions	76
6.2	Future scope of work	77
REFERENCES		78
APPENDIX A	DESIGN OF SNUBBER CIRCUITS	81
APPENDIX B	CONCEPT OF CONTROL SYSTEM OF THE INVERTER	85
APPENDIX C	PARAMETERS	88

LIST OF FIGURES

S.No.	ITEM	Page No.
1.1	Typical wind turbine configurations	3
1.2	Enercon's E-82 wind turbine : Onshore installation	8
1.3	Thirty V80-2.0 MW turbines of Vestas' Offshore installation	9
1.4	The components inside the E-82 wind turbine system	10
3.1	Block diagram of wind turbine	17
3.2	Inside C_p (λ , β) block	17
3.3	The C_p - λ Characteristics for various β values	19
3.4	Wind power for a particular wind turbine at various efficiencies	21
3.5	Efficiency vs. rotational speed for variable speed 2 MW wind turbine	22
3.6	Plot of the power curve	26
3.7	Plot of the power coefficient curve	26
3.8	Block representation of park's transformation	29
3.9	Block representation of inverse park's transformation	29
3.10	Torque vs. load angle	30
3.11	Schematic block diagram for power factor determination	32
4.1	Model of the wind turbine	35
4.2	Specifications of the wind turbine	36
4.3	Turbine power characteristics	37
4.4	Power output in p.u. with respect to time	37
4.5	Torque output in p.u. with respect to time	38
4.6	Model of the synchronous generator	39
4.7	Specifications of the generator	40
4.8	SG : Mechanical power output of wind turbine in p.u. vs. time in secs	41
4.9	SG : Mechanical torque output of wind turbine in p.u. vs. time in secs	42
4.10	SG : 3 phase load voltages in volts vs. time in secs	43
4.11	SG : 3 phase load currents in amps vs. time in secs	43
4.12	SG : Rotor speed in rads/sec vs. time in secs	44
4.13	SG : Load angle in degs vs. time in secs	45
4.14	Model of the synchronous generator with the rectifier and the inverter	45
4.15	Inside the rectifier and inverter block	46
4.16	Specifications of the rectifier	46
4.17	Circuit model of a three phase PWM inverter	47
4.18	Specifications of the inverter	48
4.19	Inside the grid block	49
4.20	SGRI: Mechanical power output of wind turbine in p.u. vs. time in secs	49
4.21	SGRI: Mechanical torque output of wind turbine in p.u. vs. time in secs	50
4.22	SGRI : 3 phase load voltages in volts vs. time in secs	50
4.23	SGRI : 3 phase load currents in amps vs. time in secs	51
4.24	SGRI : Rotor speed in rads/sec vs. time in secs	52
4.25	SGRI : Load angle in degs vs. time in secs	53
4.26	SG with RI block: Power factor $\cos\phi$ vs. time in secs	53

5.1	Representation of the faults in power system	57
5.2	LLLGfault: Three phase load voltages before, during and after the fault	60
5.3	LLLG fault: Three phase load voltages (for zooming)	60
5.4	LLLGfault: Three phase load currents before, during and after the fault	61
5.5	LLLG fault: Three phase load currents (for zooming)	61
5.6	LLLG fault: Load angle before, during and after the fault	62
5.7	LL fault: Three phase load voltages before, during and after the fault	63
5.8	LL fault: Three phase load voltages (for zooming)	63
5.9	LL fault: Three phase load currents before, during and after the fault	64
5.10	LL fault: Three phase load currents (for zooming)	64
5.11	LL fault: Load angle before, during and after the fault	65
5.12	LG fault: Three phase load voltages before, during and after the fault	66
5.13	LG fault: Three phase load currents before, during and after the fault	67
5.14	LG fault: Load angle before, during and after the fault	68
5.15	LLG fault: Three phase load voltages before, during and after the fault	68
5.16	LLG fault: Three phase load voltages (for zooming)	69
5.17	LLG fault: Three phase load currents before, during and after the fault	70
5.18	LLG fault: Three phase load currents (for zooming)	70
5.19	LLG fault: Load angle before, during and after the fault	71
5.20	LL&LG fault: 3 phase load voltages before, during and after the fault	71
5.21	LL&LG fault: Three phase load voltages (for zooming)	72
5.22	LL&LG fault: 3 phase load currents before, during and after the fault	72
5.23	LL&LG fault: Three phase load currents (for zooming)	73
5.24	LL&LG fault: Load angle before, during and after the fault	73
A1	Representation of the snubber circuit of a single diode of the rectifier	82
A2	Representation of the snubber circuit of a single IGBT of the inverter	83
A3	Inside the control system block of fig 4.15	85
A4	PWM wave forms	86

LIST OF TABLES

S.No.	ITEM	Pag No
1.1	Technical data of Enercon E-82 wind turbine	11
3.1	Data of V_{wind} and P_{output} of E 82 wind turbine to calculate P_{input} and C_p	25
5.1	Results in a tabulated form	75

CHAPTER 1

INTRODUCTION

1.1 Overview

This introduction chapter briefly introduces everything about variable speed generation which include the recent advances of wind turbine generation, introduction to variable speed wind turbines, generator drives etc. The advantages of variable speed wind turbine-generator drives over fixed speed drives have been highlighted. In addition to this, the variable power control concepts of variable speed drives have been explained. Various configurations of wind turbines used and suitable generator drives for those turbines have been introduced. Comparison of the two variable speed designs and types of installations has also been touched.

1.2 Recent advances in wind power generation

The development of wind turbine power generation has grown during the past ten years. The global market for the electrical power produced by the wind turbine generator (WTG) has been increasing steadily, which directly pushes the wind technology into a more competitive arena. Recently, there have been positive trends shown by the utilities to offer renewable energy to customers. Many customers who are environmentally conscious now have the option of subscribing to clean energy such as wind energy from the power provider. The European market has shown an ever-increasing demand for wind turbines [8].

Variable-speed wind turbine generation has been gaining momentum, as shown by the number of companies joining the variable-speed WTG market.

1.3 Variable speed wind turbines

During the past few years the variable-speed wind turbine has become the dominant type among the installed wind turbines.

Variable-speed wind turbines are designed to achieve maximum aerodynamic efficiency over a wide range of wind speeds. It has become possible continuously to adapt (accelerate or decelerate), the rotational speed ω of the wind turbine to the wind

speed v , with a variable-speed operation. To achieve that, the tip speed ratio λ is kept constant at a predefined value that corresponds to the maximum power coefficient.

The electrical system of a variable-speed wind turbine is more complicated than that of a conventional fixed speed wind turbine. It is typically equipped with an induction or synchronous generator and connected to the grid through a power converter. The power converter controls the generator speed, i.e., the power fluctuations caused by wind variations are absorbed mainly by changes in the rotor generator speed and consequently in wind turbine rotor speed.

The advantages of variable-speed wind turbines are an increased energy capture, improved power quality [5] and reduced mechanical stress on the wind turbine. The disadvantages are losses in power electronics, the use of more components and increased cost of equipment because of the power electronics [1].

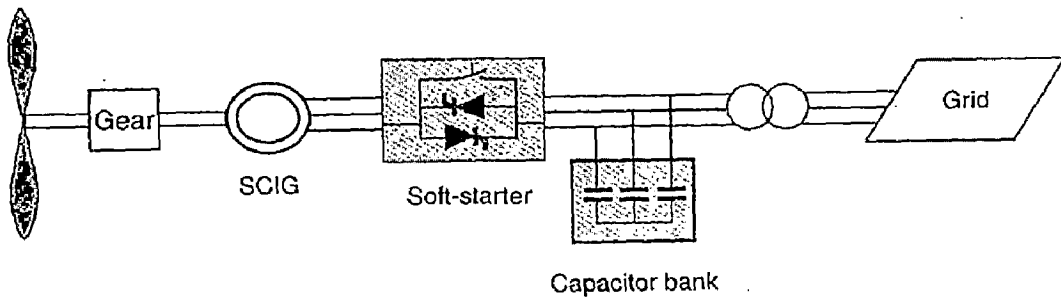
1.4 Various configurations of wind turbines

There are four typical wind turbine configurations which are shown in Fig 1.1. They are classified as Type A, Type B, Type C and Type D configurations.

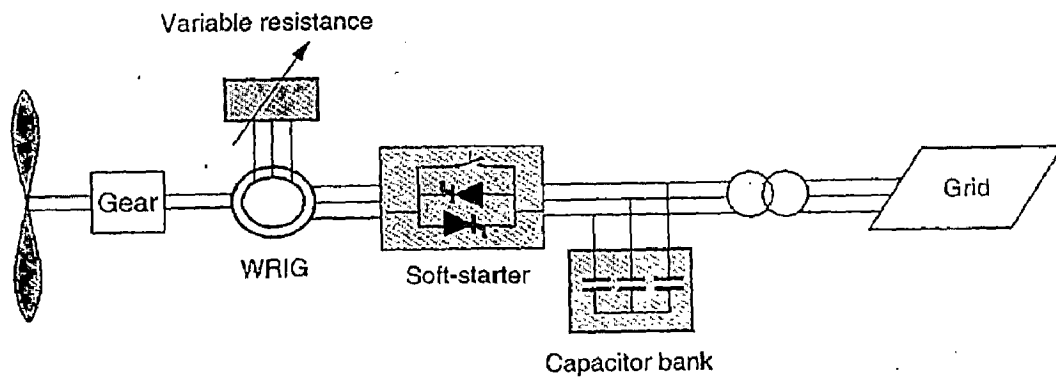
The Type A configuration denotes the fixed-speed wind turbine. It consists of a rotor with an asynchronous squirrel cage induction generator (SCIG) with a gearbox connected to the grid via a transformer. The generator stator winding is connected to the grid. The generator slip varies with the generated power, so the speed is not, in fact, constant. However, as the speed variations are very small (just 1-2%), it is commonly referred to as a fixed speed turbine. A squirrel cage generator always draws reactive power from the grid, which is undesirable, especially in weak networks. The reactive power consumption of squirrel cage generators is therefore nearly always compensated by capacitors.

The Type B configuration corresponds to the limited/ semi-variable speed wind turbine. Vestas and Nordic wind power supply a variation of this design, in which the rotor resistance of the squirrel cage generator can be varied instantly using fast power electronics. So far, Vestas alone has succeeded in commercializing this system, under the trade name OptiSlip. A number of turbines, ranging from 600 kW to 2.75 MW, have now been equipped with this system.

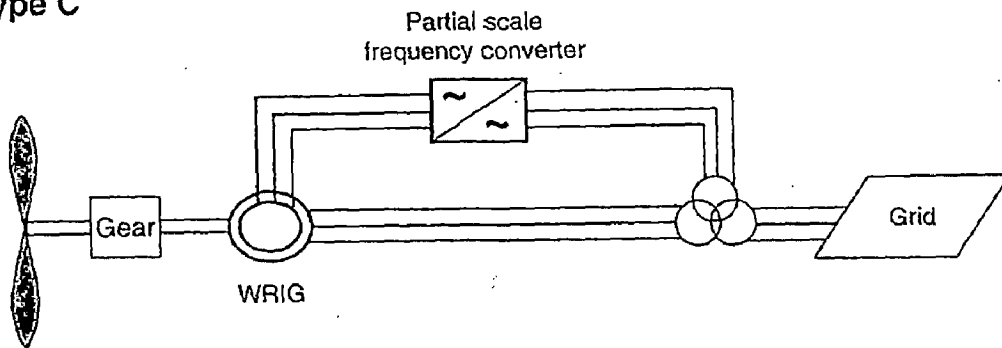
Type A



Type B



Type C



Type D

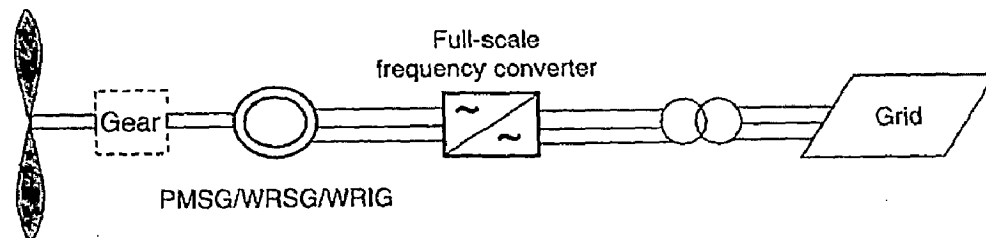


Fig 1.1 Typical wind turbine configurations [1]

All the configurations have been shown in fig 1.1 where Type A and Type B configurations have already been discussed. Type C and Type D configurations are the variable speed configurations. The Type C configuration is known as the doubly fed induction generator (DFIG) concept and the Type D configuration corresponds to the variable speed wind turbine, with the generator connected to the grid through a full-scale frequency converter. In a variable speed turbine with doubly fed induction generator, the converter feeds the rotor winding, while the stator winding is connected directly to the grid. The electrical rotor frequency can be varied by this converter, thus decoupling mechanical and electrical frequency and making variable speed operation possible. In a variable speed turbine with direct drive synchronous generator, the generator and the grid are completely decoupled by means of a power electronic converter, also allowing variable speed operation. The frequency converter performs the reactive power compensation and the smoother grid connection. The generator can be excited electrically [wound rotor synchronous generator (WRSG)]. The other generators which can be used for Type D configuration are wound rotor induction generator (WRIG) and permanent magnet synchronous generator (PMSG). Some full variable-speed wind turbine systems have no gearbox (see the dotted gearbox in Fig 1.1). In these cases, a direct driven multi pole generator with a large diameter is used [1].

1.5 Fixed vs. Variable speed turbines

The advantage of a fixed speed turbine is that it is relatively simple and therefore the price tends to be slightly lower. These turbines have to be more mechanically robust than other designs, because of the higher structural loads involved and since the rotor speed cannot be varied, fluctuations in wind speed translate directly into drive train torque fluctuations. Depending on the strength of the grid connection, the resulting power fluctuations may result in grid voltage fluctuations, which can cause unwanted fluctuations in bulb brightness, the phenomenon commonly known as flicker.

The advantages of variable speed turbines are that they generate more energy for a given wind speed regime, and that the active and reactive power generated can be easily controlled. There is also less mechanical stress, and rapid power fluctuations are scarce, because the rotor acts as a flywheel (storing energy temporarily as a buffer). In general,

no flicker problems occur with variable speed turbines. Variable speed turbines also allow the grid voltage to be controlled, as the reactive power generation can be varied. Variable speed systems can also give major savings since it can afford lighter foundations in offshore applications [21].

The drawbacks of variable speed are that the built-in power electronics are sensitive to voltage dips caused by faults and/or switching.

1.6 Comparisons of the two variable speed designs

Comparing the two variable speed designs, one advantage that can be observed in designs based on the doubly fed induction generator, is that a fairly standard generator of a small size and hence cheaper power electronics converter can be used. The cost of the semiconductor components used in AC-DC-AC converters has fallen sharply in the last five to seven years, reducing the latter advantage. A drawback of designs with the doubly fed induction generator, when compared with direct drive variable speed turbines, is that

- They still need a maintenance intensive and potentially unreliable gearbox in the drive train.
- Because they are wired directly to dual IGBT's, the generator can induce stray currents in the rotor shaft, commonly damaging slip rings and brushes.
- The stray currents induced, are also responsible for pitting generator bearings which many times can lead to costly generator failures.

The drawbacks of the direct drive design are the large and relatively heavy and complex ring generator and a larger electronic converter through which the full 100% of the power generated has to pass, compared with about one third of the power in the case of the doubly fed induction generator-based wind turbine [21]. Due to the use of the 100% frequency converter and the usage of LC filters, not only the cost becomes more but it absorbs much of the reactive power also reducing the power factor which directly affects the system's efficiency. So an additional cost has to be met to install the power factor correction devices.

1.7 Power control concepts of wind turbines in general

All wind turbines are designed with some sort of power control. There are different ways to control aerodynamic forces on the turbine rotor and thus to limit the power in very high winds in order to avoid damage to the wind turbine.

The simplest, most robust and cheapest control method is the stall control (passive control), where the blades are bolted onto the hub at a fixed angle. The design of rotor aerodynamics causes the rotor to stall (lose power) when the wind speed exceeds a certain level. Thus, the aerodynamic power on the blades is limited. Such slow aerodynamic power regulation causes less power fluctuations than a fast-pitch power regulation. Some drawbacks of the method are lower efficiency at low wind speeds, no assisted startup and variations in the maximum steady-state power due to variations in air density and grid frequencies.

Another type of control is pitch control (active control), where the blades can be turned out or into the wind as the power output becomes too high or too low, respectively. Generally, the advantages of this type of control are good power control, assisted startup and emergency stop. From an electrical point of view, good power control means that at high wind speeds the mean value of the power output is kept close to the rated power of the generator. Some disadvantages are the extra complexity arising from the pitch mechanism and the higher power fluctuations at high wind speeds. The instantaneous power will, because of gusts and the limited speed of the pitch mechanism, fluctuate around the rated mean value of the power.

The third possible control strategy is the active stall control. As the name indicates, the stall of the blade is actively controlled by pitching the blades. At low wind speeds the blades are pitched similar to a pitch-controlled wind turbine, in order to achieve maximum efficiency. At high wind speeds the blades go into a deeper stall by being pitched slightly into the direction opposite to that of a pitch-controlled turbine. The active stall wind turbine achieves a smoother limited power, without high power fluctuations as in the case of pitch-controlled wind turbines. This control type has the advantage of being able to compensate variations in air density. The combination with the pitch mechanism makes it easier to carry out emergency stops and to start up the wind turbine [1].

1.8 Generator

In general, the synchronous generator is much more expensive and mechanically more complicated than an induction generator of a similar size. However, it has one clear advantage compared with the induction generator, namely, that it does not need a reactive magnetizing current. The magnetic field in the synchronous generator can be created by using permanent magnets or with a conventional field winding. If the synchronous generator has a suitable number of poles (a multipole WRSG or a multipole PMSG), it can be used for direct-drive applications without any gearbox.

The synchronous machine is probably most suited for full power control as it is connected to the grid through a power electronic converter. The converter has two primary goals which are as follows.

- To act as an energy buffer for the power fluctuations caused by an inherently gusting wind energy and for the transients coming from the net side,
- To control the magnetization and to avoid problems by remaining synchronous with the grid frequency [1].

For the variable speed operation, the Type D configuration has been selected and a direct drive wound rotor synchronous generator has been used in this work because of its more advantages over a doubly fed induction generator.

The wound rotor synchronous generator (WRSG) is the workhorse of the electrical power industry. The rotor winding is excited with direct current using slip rings and brushes or with a brushless exciter with a rotating rectifier. Unlike the induction generator, the synchronous generator does not need any further reactive power compensation system. The rotor winding, through which direct current flows, generates the exciter field, which rotates with synchronous speed. The speed of the synchronous generator is determined by the frequency of the rotating field and by the number of pole pairs of the rotor.

The wind turbine manufacturers Enercon and Lagerwey use the wind turbine concept Type D with a multipole (low-speed) WRSG and no gearbox. It has the advantage that it does not need a gearbox. But the price that has to be paid for such a gearless design is a large and heavy generator and a full-scale power converter that has to handle the full power of the system.

1.9 Types of installations of wind turbines

There are two types of installations. They are

- Onshore wind turbine installations and
- Offshore wind turbine installations

The following pictures are the examples for Onshore and Offshore installations of Enercon and Vestas respectively. Both the wind turbines' capacity is of 2 MW.



Fig 1.2 Enercon's E-82 wind turbine : Onshore installation [17]

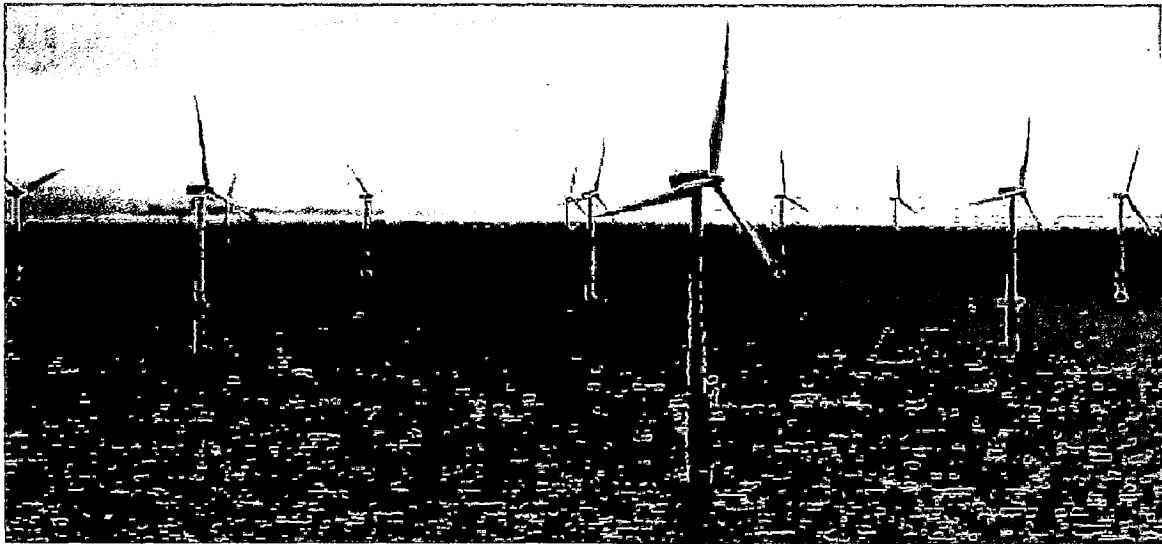


Fig 1.3 Thirty V80-2.0 MW turbines of Vestas' Offshore installation [25]

The world's leading wind turbine manufacturing companies are Enercon and Vestas. There are few others for example Nordic, GE, Lagerwey etc which develop wind turbines of capacity around 1.5 MW. Enercon and Vestas are the best in the business developing turbines up to 6 MW capacity.

Vestas installed more than 30,000 wind turbines all over the world the highest capacity of a single wind turbine being 3 MW by name V-90 at Meroicinha, Portugal. The turbines with more MW capacity are yet to be installed/ being installed.

Enercon installed 10,722 wind turbines all over the world with a total power reaching 11.1 GW. The highest capacity of a single wind turbine installed by Enercon is 2 MW and the name of the turbine is E-82.

A model of an E-82 turbine has been considered in the present work. The components inside the E-82 wind turbine system have been shown in fig 1.4. The technical data of Enercon E-82 wind turbine is shown below in table 1.1 and the data has been taken from [17].

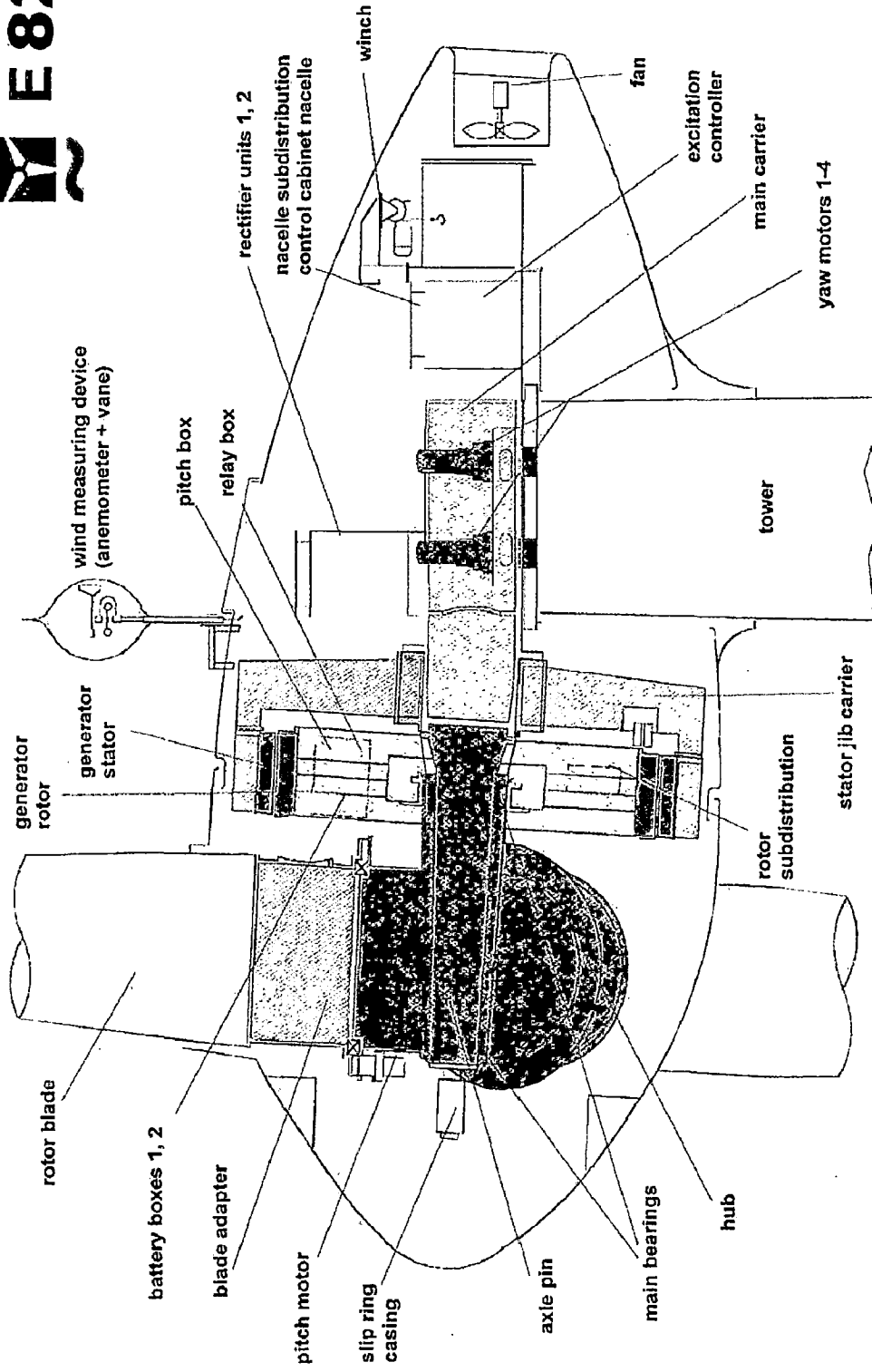


Fig 1.4 The components inside the E-82 wind turbine system [1]

Parameter	Details
Power of generator, P	2000 kW
voltage of generator	400 V
Type of generator	Enercon direct drive synchronous generator
Grid feeding	Enercon converter
Number of blades	3
blade material	GRP (epoxy); integrated lightning protection
Rotor type	Upwind rotor
Direction of rotation	Clockwise
Rotor diameter	82 m
Blade length	38.8 m
Swept area	5281 m ²
Turbine concept	Gearless, variable single blade pitch control, variable speed

Table 1.1 Technical data of Enercon E-82 wind turbine [17]

CHAPTER 2

LITERATURE REVIEW

2.1 Overview

A lot of work has been done in the past two decades on variable speed wind turbines and thus a lot of literature is available at IEEE and in various journals and other publications on variable speed technology. Some of the important literature relating to this work is presented as follows.

2.2 Literature

A total of 10 technical papers had been reviewed and their brief summaries are presented as follows.

Wind turbine manufacturers are today adapting their equipment to comply with increasingly strict transmission integration requirements. One class of the new turbines being developed is the synchronous machine (either wound field or permanent magnet excited) with full AC/DC/AC power electronic conversion. The topology of the new machines differs considerably from that of more conventional forms of power generation with synchronous generator technology and must be considered when modelling the interaction of the turbines with the transmission system. Hence in paper [2], Behnke, M.R. and Muljadi, E. focused on the simulation of the response of a variable-speed wind turbine with a synchronous generator and full power electronics to transmission system disturbances using reduced order models compatible with positive sequence phasor time-domain analysis software (e.g., PSS/E or PSLF). They investigated and analyzed the voltage ride through capability of the wind turbine. They also presented the dynamic behavior of the wind turbine under different transient conditions.

Chen, Z. in paper [4] presented the performance study of several compensation schemes for a line-commutated SCR converter operating under a wide range of DC voltage. The studied reactive power and harmonic compensation schemes include passive filters, active filters, and hybrid compensation methods for a SCR interfaced permanent magnet generator based variable speed wind turbine. He investigated the effectiveness of the compensation schemes in terms of reactive power and harmonics. Later he presented

the required compensation current ratings of these schemes. He also considered the effects of higher pulse number of the converter on the compensation schemes.

Chen, Z. and Spooner, E. in paper [5], discussed appropriate modeling and simulation techniques for studying the voltage fluctuation and harmonic distortion in a network to which variable speed wind turbines are connected. They have made case studies on a distribution network in which they showed that the voltage fluctuation and harmonic problems can be minimized with the proposed power electronics interface and control system while the wind energy conversion system captures the maximum power from the wind as wind speed varies. The studies which they made have also demonstrated the ability of the advanced converter to assist the system voltage regulation.

Chen, Z. and Spooner, E. in paper [6] compared the two of the most promising types of power converter applicable to the task of interfacing variable-voltage DC energy sources to the grid. The converters studied are first a DC/DC converter with a current-controlled Voltage Source Inverter and, secondly, the line-commutated SCR with an active compensator for reduction of harmonic current and reactive power demand. The comparison is drawn with particular reference to use with variable-speed permanent-magnet wind turbine generators. They addressed the optimal power transfer, reactive power / voltage regulation and harmonic minimization. They presented experimental results from laboratory models alongside simulation results, which are in good agreement, to demonstrate the power control and harmonic performance of these systems. They also discussed power losses and semiconductor costs.

Renewable sources of electricity generation, of which the most promising for the UK is wind energy, are becoming increasingly important due to concern over the environment. Conner, B. and Leithead, W.E. in paper [7] assessed the performance of variable speed wind turbines for several operational strategies. They considered two contrasting wind turbine rotors and assessed their performance by simulation.

Eduard, M. and Butterfield, C.P. in paper [8] described the operation of variable-speed wind turbines with pitch control. The system they considered is controlled to generate maximum energy while minimizing the loads. In low to medium wind speeds, the generator and the power converter control, the wind turbine is controlled to capture maximum energy from the wind. In the high-wind-speed regions, the wind turbine is

controlled to maintain the aerodynamic power produced by the wind turbine. They investigated the two methods to adjust the aerodynamic power. They are the pitch control and the generator load control, both of which are employed to regulate the operation of the wind turbine. Their analysis and simulation showed that the wind turbine can be operated at its optimum energy capture while minimizing the load on the wind turbine for a wide range of wind speeds.

Mullane, A., Lightbody, G., Yacamini, R. and Simon, G. in paper [11] examined the simulation and control of a horizontal axis variable speed wind turbine. They developed appropriate mathematical models for the wind turbine induction generator and voltage sourced converter. They implemented the developed models using Simulink S-Functions with some of the simulation difficulties which are later examined. They developed a simple controller to extract maximum power from the wind, by varying the load torque supplied by the generator. They implemented the controller using some of the developed models and they verified the viability of such a control scheme.

Müller, H., Pöller, M. and Basteck, A., Tilscher, M. and Pfister, J. in paper [12] analyzed the grid integration aspects of a new type of variable-speed wind turbine, the directly coupled synchronous generator with hydro-dynamically controlled gearbox. In contrast to existing wind generators using synchronous generators, the generator of this concept is directly connected to the AC grid, without the application of any power electronics converter. Variable speed operation of the turbine is mechanically achieved by a gear box with continuously controllable variable gear box ratio. In this paper, they focussed on the compatibility of the new concept with existing connection standards, such as the E.ON grid code. They also studied typical stability phenomena of synchronous generators, such as transient and oscillatory stability as well as power quality issues like voltage flicker. They presented the results of stability studies and discussed possible advantages of the new concept with special focus on offshore applications.

Pieter, S., Tim, G. in paper [14] developed an advanced generator control algorithm and implemented in ECN's control design tool for wind turbines. For wind speeds above nominal the algorithm limits power and rotor speed to the common bounds of constant power control in variable speed turbines, while the electromagnetic torque

varies half as much as found in literature. They simultaneously avoided production dips at above nominal wind speeds. They examined the algorithm by the aero-elastic wind turbine code Phatas. They are now preparing the application on a commercial wind turbine.

The increasing size of wind farms requires power system stability analysis including dynamic wind generator models. For turbines above 1MW, doubly-fed induction machines are the most widely used concept. However, especially in Germany, direct-drive wind generators based on converter-driven synchronous generator concepts have reached considerable market penetration. Hence, Pöller, M. and Sebastian, A. in paper [15] presented the converter driven synchronous generator models of various order that can be used for simulating transients and dynamics in a very wide time range.

VARIABLE SPEED WIND TURBINE GENERATOR SYSTEM

3.1 Overview

The drafting of this chapter is necessary for performing the present computer simulation. This chapter focuses on the explanation of each component with various design concepts and details of the wind turbine, the synchronous generator, the rectifier and the inverter etc. Various plots have been shown such as the C_p - λ Characteristics for various β values, efficiency plots, power curve plots etc.

In this dissertation, an attempt has been made to implement a variable speed wind turbine-generator system in MATLAB/ Simulink graphical user interface. A wind turbine-generator drive of capacity 2 MW, 400V is taken inspired from the modern E-82 turbine of Enercon.

3.2 Variable speed wind turbine

The variable speed wind turbine can be built using the blocks in MATLAB/ Simulink as shown below in fig 3.1 by implementing the following power equation of wind turbines as appropriate blocks.

$$P_m = c_p(\lambda, \beta) \frac{\rho A}{2} v_{wind}^3 \text{-----} (3.1)$$

Where

P_m = Mechanical output power of the turbine (W)

C_p = Power coefficient or power efficiency of the turbine. It is also known as the Betz limit. It dictates that at most 59% of the wind power can be captured. In this case, the value of C_p is taken as 0.48, i.e 48% only.

ρ = Air density (kg/m^3)

A = Turbine swept area (m^2)

v_{wind} = Wind speed (m/s)

λ = Tip speed ratio which is defined as the ratio of the rotor blade tip speed or the generator speed in $\frac{m}{sec}$ to wind speed in m/s

β = Blade pitch angle (deg)

The above equation (3.1) can be normalized. In the per unit (p.u.) system, the equation 3.1 becomes:

$$P_{m_pu} = k_p c_{p_pu}(\lambda, \beta) v_{wind_pu}^3 \quad (3.2)$$

This is the equation which is used to create the block diagram in MATLAB/ Simulink is as shown below in fig 3.1.

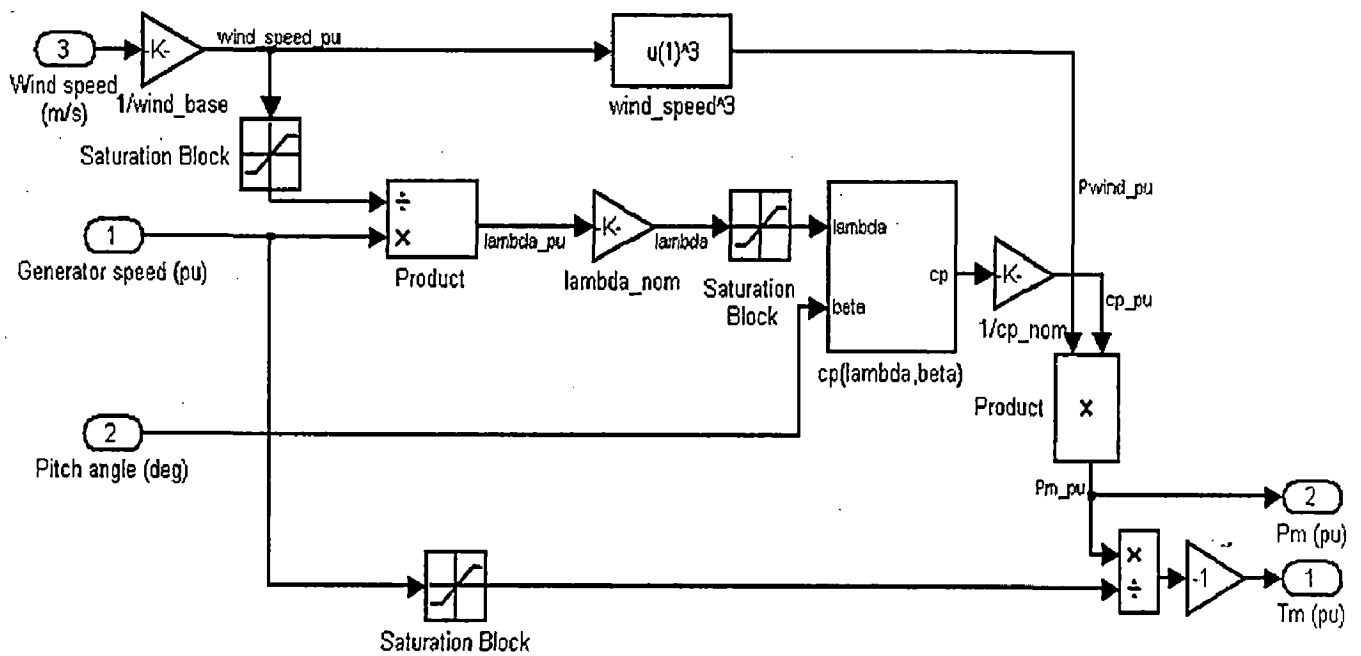


Fig 3.1 Block diagram of wind turbine

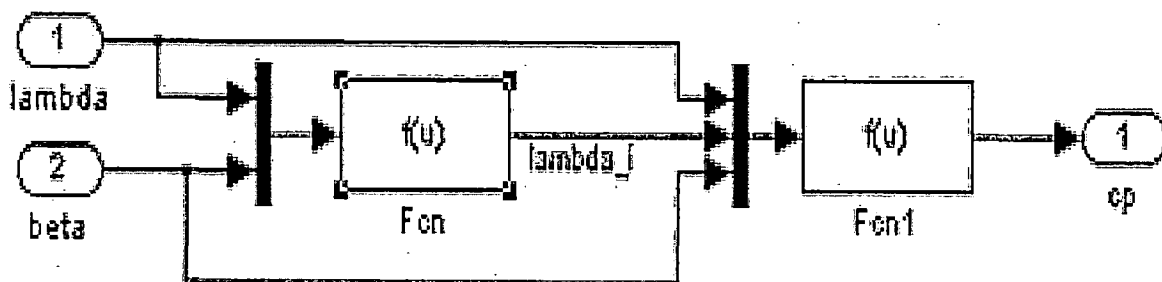


Fig 3.2 Inside $C_p(\lambda, \beta)$ block

Where

P_{m_pu} = Power in p.u. of nominal power for particular values of ρ and A

C_{p_pu} = Power coefficient or power efficiency in p.u. of the maximum value of C_p

v_{wind_pu} = Wind speed in p.u. of the base wind speed. The base wind speed is the mean value of the expected wind speed in m/s.

k_p = Power gain for $C_{p_pu} = 1$ p.u. and $v_{wind_pu} = 1$ p.u.,

k_p is less than or equal to 1. It is taken as 1 in this case.

The below formulas are used to find out the C_p value of a particular wind turbine.

$$\text{Fcn} : \frac{1}{\lambda_i} = \frac{1}{\lambda + 0.08\beta} - \frac{0.035}{\beta^3 + 1} \text{ in fig 3.2} \text{-----} (3.3)$$

$$\text{Fcn1} : c_p(\lambda, \beta) = c_1 \left(\frac{c_2}{\lambda_i} - c_3\beta - c_4 \right) e^{\frac{-c_5}{\lambda_i}} + c_6\lambda \text{ in fig 3.2} \text{-----} (3.4)$$

The coefficients c1 to c6 are: c1 = 0.5176, c2 = 116, c3 = 0.4, c4 = 5, c5 = 21 and c6 = 0.0068 [22].

The Simulink model of the turbine is illustrated in fig 3.1. The three inputs are the generator speed (ω_{r_pu}) in p.u. of the nominal speed of the generator ω_s , the blade pitch angle β in degrees and the wind speed v_{wind} in m/s. The tip speed ratio λ in p.u. of λ_{nom} is obtained by the division of the rotational speed in p.u. of the base rotational speed and the wind speed in p.u. of the base wind speed. Hence as shown in the fig 3.1, the outputs of the turbine are mechanical power output P_{m_pu} and mechanical torque output T_{m_pu} . Either of the outputs can be applied to the generator shaft depending on the requirement of the system.

The c_p - λ characteristics, for different values of the blade pitch angle β are illustrated below in fig 3.3. The maximum value of C_p ($C_{p_max} = 0.48$) is achieved for $\beta = 0$ degree and for $\lambda = 8.1$ from the graph. This particular value of λ is defined as the nominal value (λ_{nom}).

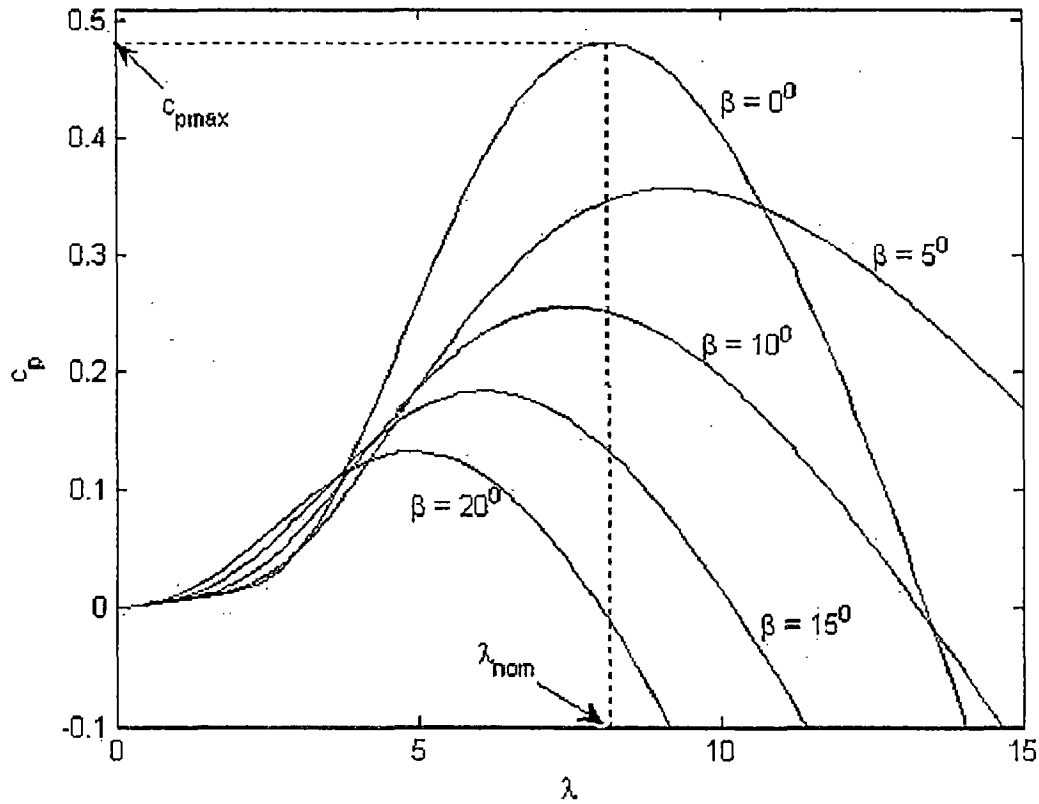


Fig 3.3 The C_p - λ Characteristics for various β values [22]

With the help of equation 3.1, the nominal value of P_m can be calculated. Hence, to calculate the input power of the turbine for a given wind speed of 13 m/s in a given location the following derivation is done.

$$P_m = c_p(\lambda, \beta) \frac{\rho A}{2} v_{wind}^3$$

W.K.T the maximum value of C_p ($C_{p_max} = 0.48$) is achieved for $\beta = 0$ degree and for $\lambda = 8.1$ from fig 3.3. Hence,

$$\begin{aligned} P_m &= 0.48 \times \frac{1.225 \times 3.14159 \times 82^2}{2 \times 4} \times 13^3 \\ &= 3411104.1 \text{ W} \\ &= 3.41 \text{ MW} \end{aligned}$$

Where

Air density ρ for a given location is taken as 1.225 kg/m^3 by assuming the location's average temperature as 10°c through out the year.

The website [18] gives the value of the air density ρ when the temperature of a given location is known. The diameter of the rotor blade of E 82 turbine is given as 82 m [17].

This means that the wind turbine is capable of generating about three and a half mega watts of power at its maximum efficiency theoretically. But the manufacturers rated the turbine to only 2 MW because of many other complex practical considerations which limit the turbine's output power to a maximum of 2 MW.

In this case, the maximum efficiency of the wind turbine is obtained to be only 48% (fig 3.3).

3.2.1 Efficiency of the wind turbine in general

A turbine is said to be 100% efficient if it could convert all the wind's power to mechanical power. But it is practically impossible to achieve that efficiency. To even achieve 50% efficiency is unlikely, and would be a very efficient machine. A 50% efficient turbine would convert half of the power in the wind to mechanical power.

A given wind turbine has a design point that generally defines its peak efficiency at the wind speed for which the system is designed. At wind speeds above and below the design speed the efficiency is the same or less (maybe much less). If a turbine's best efficiency is 48% (as in section 3.2) at a wind velocity of 13 m/s, it will be 48% only at that wind speed. At all other wind speeds it will be something worse. That wind turbine will generally operate at lower than its best efficiency, because wind speeds are never constant or average. The electric power actually produced will be still lower because the generator efficiencies are also less than 100% (generally in the mid- or low-90's at best), and there are further losses in the conversion electronics and lines. In practical terms, each power transfer stage has certain efficiency. When all these efficiencies are figured in, the total system's efficiency can get best at maximum of around 35% or even less of the wind's energy actually delivered as useful electrical energy to the end user in the very best conditions. Therefore, each power transfer stage presents an opportunity to reduce the cost of energy from a wind turbine [20].

The graph in fig 3.4 shows the power versus velocity with several different lines:

- The power in the wind
- The power that could be extracted at 59% efficiency
- The power that could be extracted at 50% efficiency (that is, if the wind turbine were good enough to be considered excellent)
- The actual power output from the wind turbine.

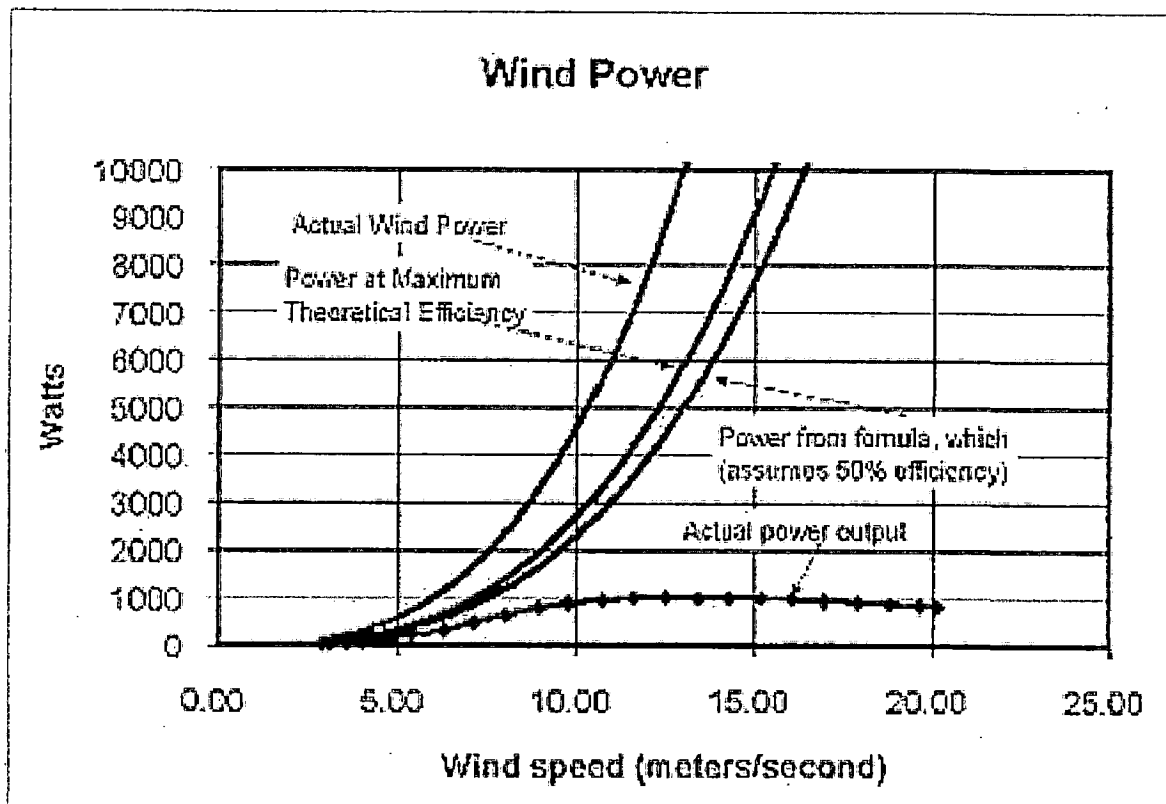


Fig 3.4 Wind Power for a particular Wind Turbine at Various Efficiencies [19]

3.2.2 Efficiency of variable speed turbines

The optimal rotating speed differs due to the wind speed. The variable speed gearless wind turbines can maintain the optimal rotating speed because of the high inertia of the generator rotor. Even if the speed differs due to different wind speeds, the frequency converter is used to produce desired output frequency. So, the power efficiency is improved as illustrated below.

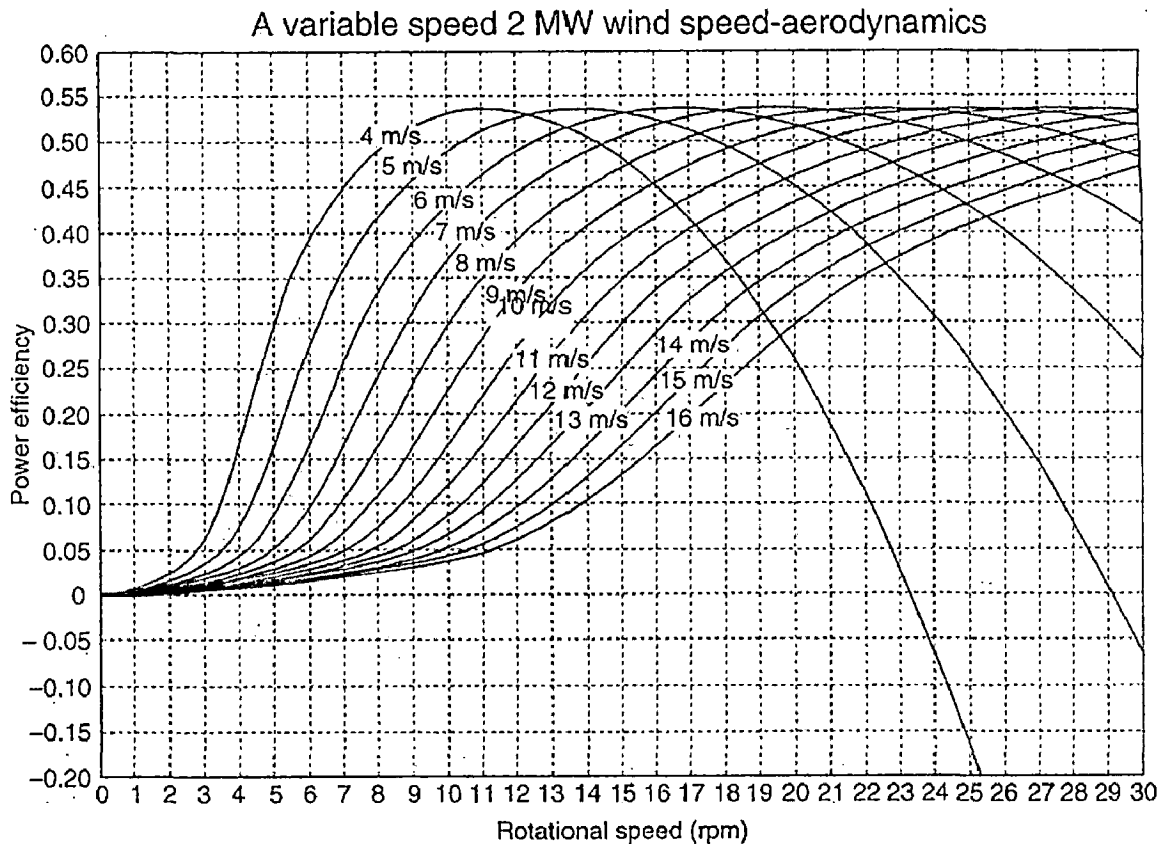


Fig 3.5 Power efficiency C_p vs. Rotational speed for variable speed 2 MW wind turbine [1]

The above graph in fig 3.5 shows the power efficiency graphs with respect to the rotational speed of the generator at different wind speeds. It is the proof that the variable speed turbines achieve higher efficiencies than fixed speed turbines. It is clearly seen that the maximum efficiency all the speeds is around 54% compared to the 48% efficiency of the fixed speed wind turbines.

Apart from this power efficiency, there is an other efficiency known as the aerodynamic efficiency. This aerodynamic efficiency has two definitions - one for the below-rated wind speed and the other for the above-rated wind speed [7].

The aerodynamic efficiency, η , is defined for the below-rated operation as the ratio, expressed as a percentage, of energy capture to the energy capture that would be attained when C_p always had its maximum value, that means, if the turbine's energy capture is at C_{p_max} , then that turbine is considered as a 100% aerodynamically efficient turbine.

$$\eta = \frac{C_p}{C_{p_max}} \times 100 \text{ -----(3.5)}$$

Where C_p is the mean power coefficient.

In the above-rated operation, efficiency has a different definition since it is not required to extract all the power from the wind. In this case, the efficiency is defined as the ratio of the mean power attained to the rated power of the wind turbine, that means, if the turbine generates its normal rated power, then that turbine is considered as a 100% aerodynamically efficient turbine.

$$\eta = \frac{P}{P_{rated}} \times 100 \text{ -----(3.6)}$$

Where P is the mean power and P_{rated} is the turbine's rated power.

3.2.3 Performance assessment of variable speed turbines

The ability to vary the rotor speed increases the operating flexibility of variable speed wind turbines and offers several advantages over constant speed machines.

Variable speed wind turbines are perceived to have two main potential advantages. They are

- Increased energy capture in low wind speeds and
- The reduction of drive-train loads in high wind speeds.

Considering the first potential advantage of increased energy capture in below rated wind speeds, it is the increased aerodynamic efficiency which enables a more cost effective design of the wind turbine.

Similarly, for the second potential advantage of reduced drive-train loads in above rated wind speeds, it is the decreased mean drive-train load disturbances which enable a more cost effective design of the wind turbine. The mean loads are essentially the design loads. It follows that the appropriate measures of performance for variable speed wind turbines are

- aerodynamic efficiency in below-rated wind speed
- extent of transient drive-train loads in above-rated wind speed

The performance of a particular strategy is critically dependent on the rotor characteristics and on the wind regime driving the wind turbine [7].

3.2.4 Power Curve

The power curve is a key concept for understanding the efficiency of wind turbines. The power curve of a wind turbine is a graph that indicates how large the electrical power output will be for the turbine at different wind speeds.

As explained by Equation (3.1), the available energy in the wind varies with the cube of the wind speed. Hence a 10 % increase in wind speed will result in a 30 % increase in available energy.

The power curve of a wind turbine follows this relationship between cut-in wind speed (the speed at which the wind turbine starts to operate) and the rated capacity (Fig.3.6). The wind turbine usually reaches rated capacity at a wind speed of between 12-16 m/s, depending on the design of the individual wind turbine.

At wind speeds higher than the rated wind speed, the maximum power production will be limited as said before, or, in other words, some parts of the available energy in the wind will be spilled. The power output regulation can be achieved with pitch-control (i.e. by feathering the blades in order to control the power) or with stall control (i.e. the aerodynamic design of the rotor blade will regulate the power of the wind turbine). Hence, a wind turbine produces maximum power within a certain wind interval that has its upper limit at the cut-out wind speed. The cut-out wind speed is the wind speed where the wind turbine stops production and turns out of the main wind direction. Typically, the cut-out wind speed is in the range of 20 to 25 m/s [1].

3.2.5 Power Coefficient C_p

The power coefficient is a coefficient which explains how efficiently a turbine converts the energy in the wind to electricity. It is hence, also called the power efficiency.

The electrical power output is divided by the wind energy input to measure the technical efficiency of a wind turbine. Hence to obtain the C_p curve, at each wind speed, the power output is divided by the amount of power in the wind per square meter. The data of the power outputs at different wind speeds for an E-82 turbine is given in [17]. Hence, a table can be prepared making four columns as shown in table 3.1,

The mechanical efficiency of the turbine is largest (in this case 48 per cent) at a wind speed of about 10 m/s. This is a deliberate choice by the manufacturers who designed the turbine. At low wind speeds efficiency is not so important, because there is not much energy to harvest. At high wind speeds the turbine must waste any excess energy above for what the generator was designed. Therefore efficiency matters most in the region of wind speeds where most of the energy is to be found [24].

wind speed in m/s	Power output P in kW	Power input $P = \frac{\rho A}{2} V_{wind}^3$ in kW	Power coefficient $C_p = \frac{P_{output}}{P_{input}}$
2	3	25	0.12
3	25	86.2	0.29
4	82	205	0.4
5	174	404.7	0.43
6	321	697.8	0.46
7	532	1108.3	0.48
8	815	1697.9	0.48
9	1180	2458.3	0.48
10	1612	3358.3	0.48
11	1890	4295.5	0.44
12	2000	5555.5	0.36
13	2050	7067	0.29
14	2050	8913	0.23
15	2050	10789.4	0.19
16	2050	13666.6	0.15
17	2050	15769.2	0.13
18	2050	18636.4	0.11
19	2050	22778	0.09
20	2050	25625	0.08
21	2050	29286	0.07
22	2050	34167	0.06
23	2050	41000	0.05
24	2050	51250	0.04
25	2050	58571.4	0.035

Table 3.1 Data of V_{wind} and P_{output} of E 82 wind turbine to calculate P_{input} and C_p

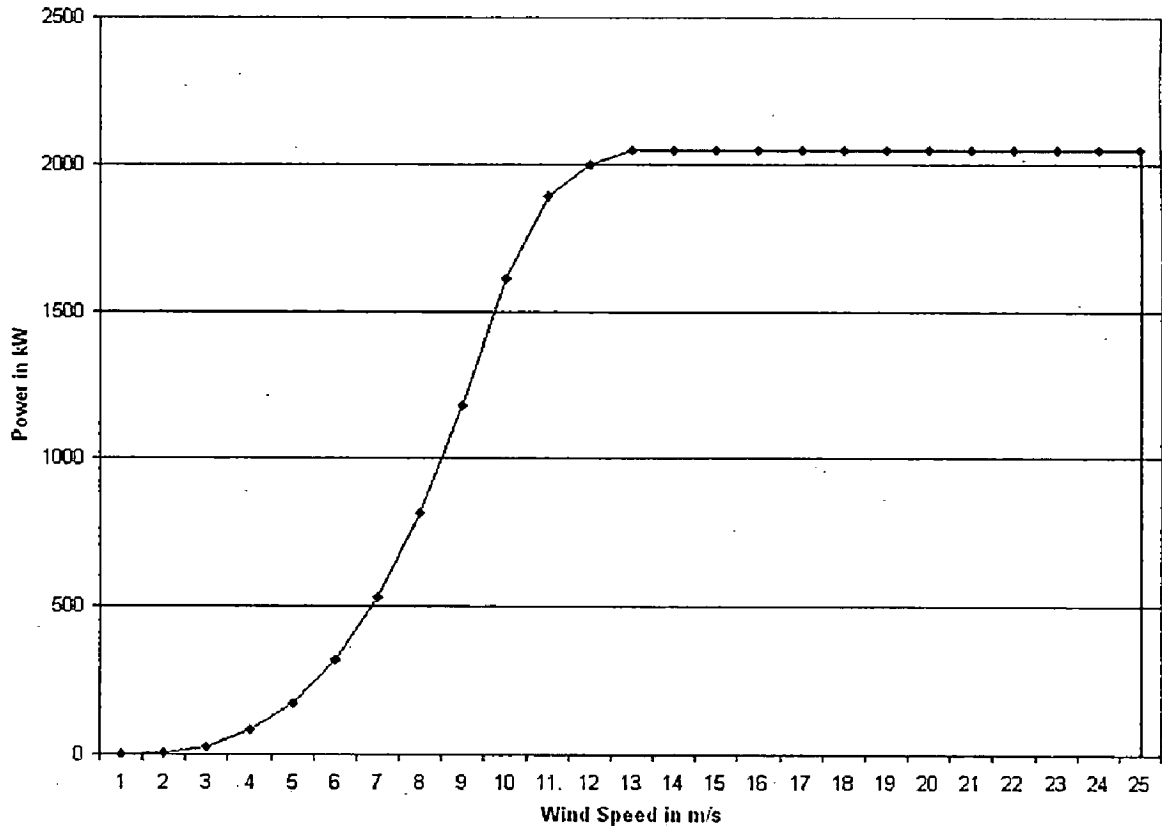


Fig 3.6 Plot of the power curve

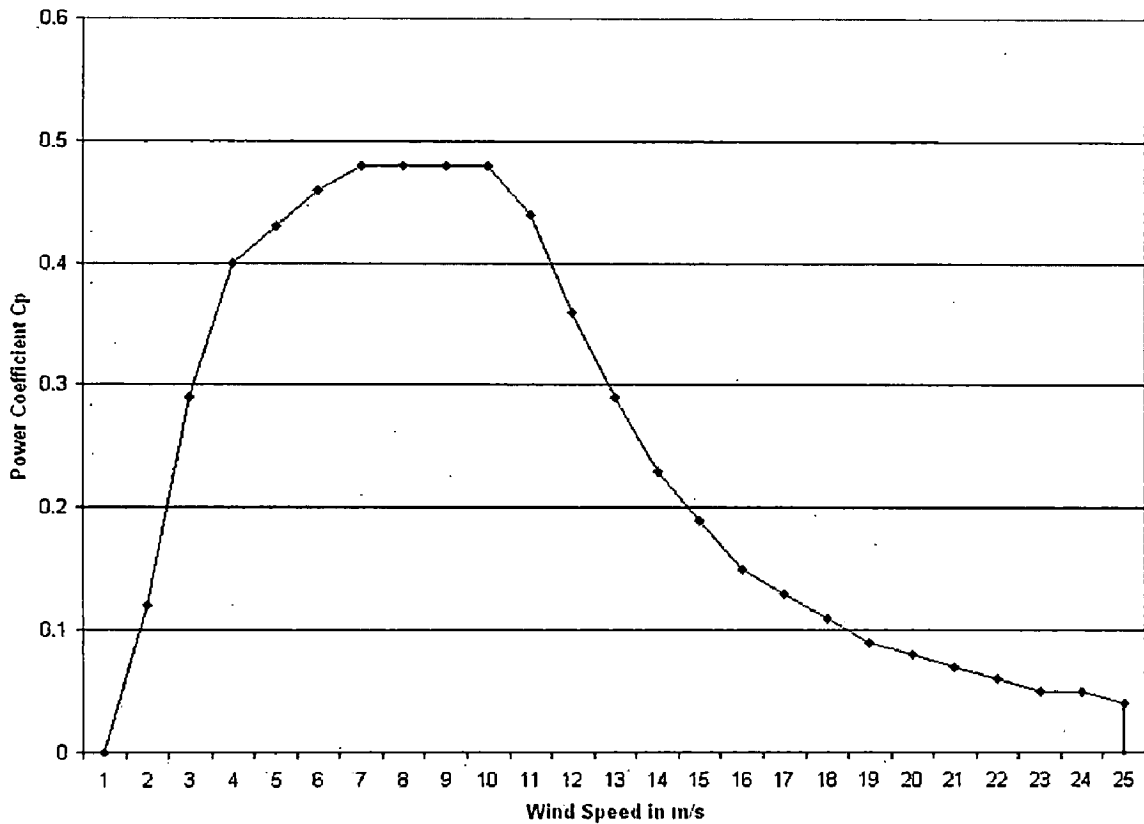


Fig 3.7 Plot of the power coefficient curve

The graphs in figs 3.6 and 3.7 are obtained from the table 3.1. Although it seen that the average efficiency for these turbines is somewhat above 30 per cent, the efficiency varies very much with the wind speed.

3.3 Generator

The two axis (q-d) model for the synchronous generator is an inbuilt model in MATLAB/ Simulink. The model takes into account the dynamics of the stator, field, and damper windings. All rotor parameters and electrical quantities are viewed from the stator. They are identified by primed variables.

The electrical model of the machine with differential equations is as follows [22].

$$V_d = R_s i_d + \frac{d}{dt} \phi_d - \omega_R \phi_q \text{-----(3.7)}$$

$$V_q = R_s i_q + \frac{d}{dt} \phi_q + \omega_R \phi_d \text{-----(3.8)}$$

$$V'_{fd} = R'_{fd} i'_{fd} + \frac{d}{dt} \phi'_{fd} \text{-----(3.9)}$$

$$V'_{kd} = R'_{kd} i'_{kd} + \frac{d}{dt} \phi'_{kd} \text{-----(3.10)}$$

$$V'_{kq1} = R'_{kq1} i'_{kq1} + \frac{d}{dt} \phi'_{kq1} \text{-----(3.11)}$$

$$V'_{kq2} = R'_{kq2} i'_{kq2} + \frac{d}{dt} \phi'_{kq2} \text{-----(3.12)}$$

$$\phi_d = L_d i_d + L_{md} (i'_{fd} + i'_{kd}) \text{-----(3.13)}$$

$$\phi_q = L_q i_q + L_{mq} i'_{kq} \text{-----(3.14)}$$

$$\phi'_{fd} = L'_{fd} i'_{fd} + L_{md} (i_d + i'_{kd}) \text{-----(3.15)}$$

$$\phi'_{kd} = L'_{kd} i'_{kd} + L_{md} (i_d + i'_{fd}) \text{-----(3.16)}$$

$$\phi'_{kq1} = L'_{kq1} i'_{kq1} + L_{mq} i_q \text{-----(3.17)}$$

$$\phi'_{kq2} = L'_{kq2} i'_{kq2} + L_{mq} i_q \text{-----(3.18)}$$

Where

V is electric voltage measured in Volts

R is the electric resistance measured in Ohms

i is electric current measured in Amps

ϕ is magnetic flux linkage measured in Volt-Sec

ω is angular frequency measured in 1/sec

V'_f is electrically excited field voltage measured in Volts

i'_f is field current measured in Amps

V'_k is the damper voltage measured in Volts

i'_k is the damper current measured in Amps

L is the self inductance measured in Henrys

The subscripts used are defined as follows:

- d,q: d and q axis quantity
- R,s: Rotor and stator quantity
- l,m: Leakage and magnetizing inductance
- f,k: Field and damper winding quantity
- x' : Either damper winding quantity or electrically excited quantity

3.3.1 Park's transformation

As the models are developed in rotor reference frame d,q,0, the park's transformation is used to transform the stator phase values (currents, voltages, flux linkages) into the rotor reference frame. And in order to get out of rotor reference frame into the stator phase values, the inverse Park's transformation is used.

By Park's transformation equations as shown, stator phase voltages are transformed to corresponding values in rotor reference frame [22].

$$V_d = \frac{2}{3} \left(V_a \sin \omega t + V_b \sin \left(\omega t - \frac{2\pi}{3} \right) + V_c \sin \left(\omega t + \frac{2\pi}{3} \right) \right) \text{-----(3.19)}$$

$$V_q = \frac{2}{3} \left(V_a \cos \omega t + V_b \cos \left(\omega t - \frac{2\pi}{3} \right) + V_c \cos \left(\omega t + \frac{2\pi}{3} \right) \right) \text{-----(3.20)}$$

$$V_0 = \frac{1}{3} (V_a + V_b + V_c) \text{-----(3.21)}$$

With inverse transformation equations as shown, one gets directly from each component of rotor reference frame into the stator phase values.

$$V_a = \frac{2}{3} \left(V_d \sin \omega t + V_q \cos \omega t + V_0 \right) \text{-----(3.22)}$$

$$V_b = \frac{2}{3} \left(V_d \sin \left(\omega t - \frac{2\pi}{3} \right) + V_q \cos \left(\omega t - \frac{2\pi}{3} \right) + V_0 \right) \text{-----(3.23)}$$

$$V_c = \frac{1}{3} \left(V_d \sin \left(\omega t + \frac{2\pi}{3} \right) + V_q \cos \left(\omega t + \frac{2\pi}{3} \right) + V_0 \right) \text{-----(3.24)}$$

The block representation of the Park's transformation and Inverse Park's transformation are as follows.

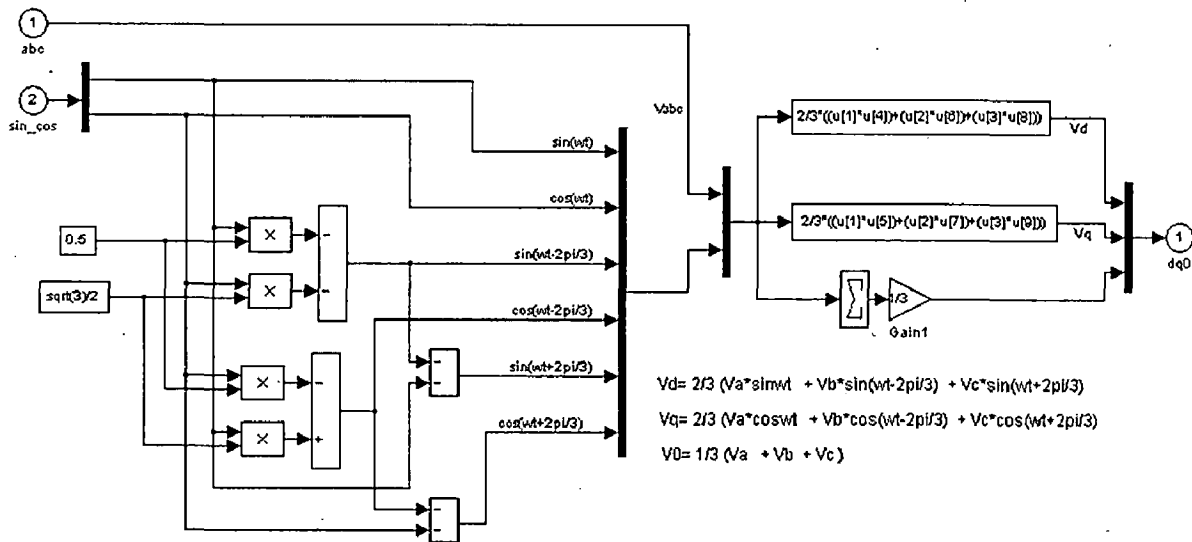


Fig 3.8 Block representation of Park's transformation

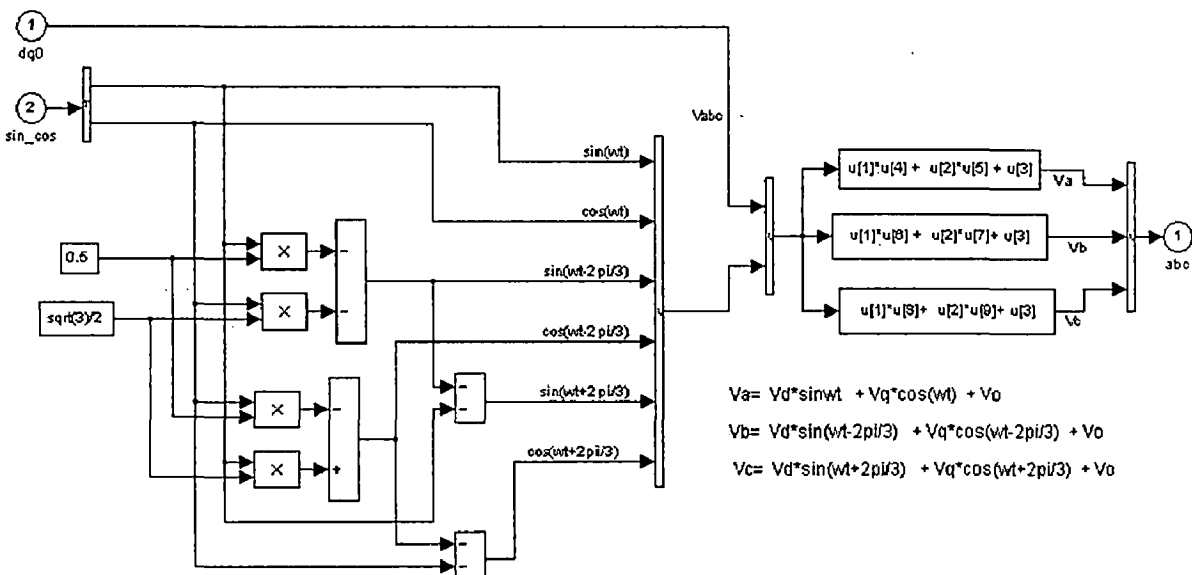


Fig 3.9 Block representation of Inverse Park's transformation

3.3.2 Load angle

In normal operation, the synchronous generator will operate in synchronism, i.e. it generates the same frequency and rotates at a speed which is simply related to number of poles of the machine. When torque is applied to the generator, there is a movement of the rotor with respect to a synchronously rotating reference frame. A synchronously rotating reference may be identified as the rotor pole axes of an unloaded synchronous generator i.e., the generator running at no load will have its rotor pole axes coincident with the reference. When torque is applied, the pole axes move with respect to the reference and synchronous operation is continued with a steady angle between them. This angle is called load angle [13].

If the rotor is driven ahead of the reference by applying the shaft torque, the generator generates electric power and the load angle is positive. If the shaft is loaded mechanically, electric power is absorbed and the rotor moves behind the reference with negative load angle. This is the motoring action as seen in fig 3.10

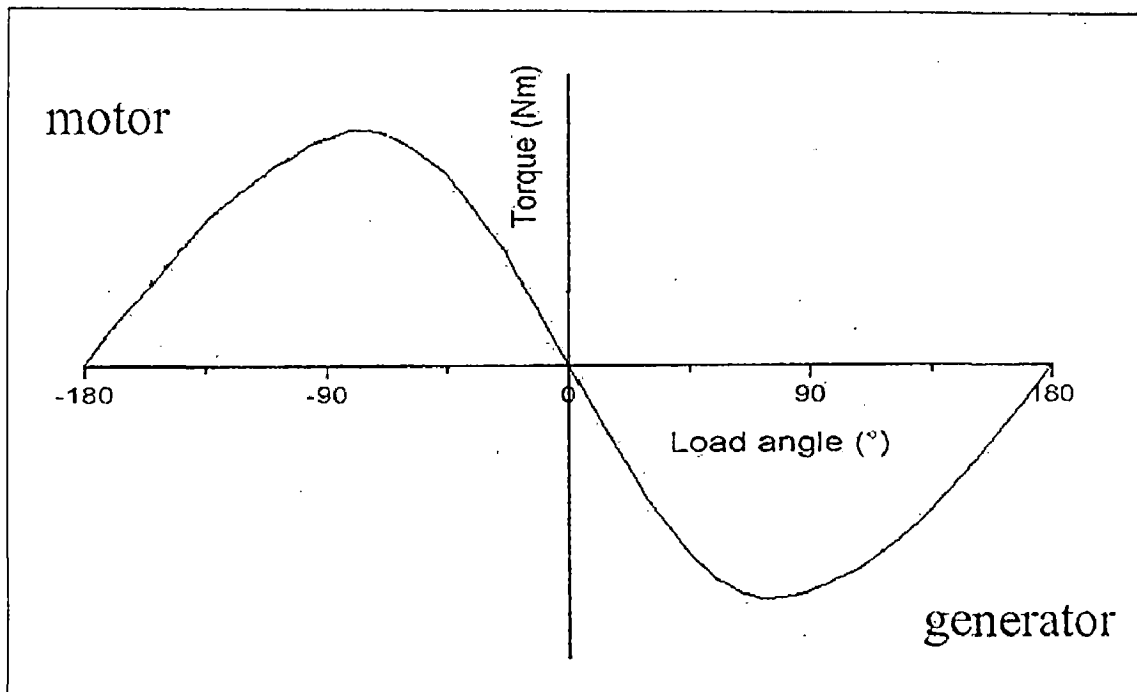


Fig 3.10 Torque vs. Load angle [13]

Similarly if a curve is plotted by replacing the torque with the power in fig 3.10, an exactly opposite waveform will be obtained. This is because of the convention that in generating mode, the torque is absorbed to produce power output and hence torque is negative and power is positive. Similarly in motoring mode, the power is absorbed to produce torque output and hence power is negative and torque is positive.

Generally, maximum power is developed at an angle somewhat less than 90° called the breakdown angle. For load angles greater than the breakdown angle, any further increase in shaft power will result in a decrease in electric power. The generator rotor will then accelerate i.e., the synchronism will be lost and instability results. The generator running below the stability limit may lose synchronism if a sudden alternation in load causes the load angle to exceed the angle for the maximum power by too great a margin.

As the machine synchronizes, the load angle oscillates initially and it steadies at a steady angle after synchronization which is shown in chapter 4.

3.3.3 Power factor determination

The power factor of a machine is defined as the ratio of real power (kW) and apparent power (kVA) of a machine and is given by the cosine of the angle between stator phase voltage and stator phase current of the synchronous generator. In the model it is necessary to determine the real power generated by the generator, thus power factor model was also added to the main model.

$$P = 3V_{ph}I_{ph} \cos \varphi \text{-----(3.25)}$$

The above equation shows the real power of the generator in terms of stator phase voltage, stator phase current and its power factor. The power factor measurement is modeled using the d-q components of stator phase voltage, i.e. V_d, V_q and d-q components of the stator phase current i.e. I_d, I_q .

The formula used for modelling the phase angle is given as in [13]:

$$\varphi = \left[\tan^{-1} \left(\frac{I_d}{I_q} \right) + \tan^{-1} \left(\frac{V_d}{V_q} \right) \right] \text{-----(3.26)}$$

This is done by using the trigonometric function blocks of the MATLAB/Simulink as shown in fig 3.11.

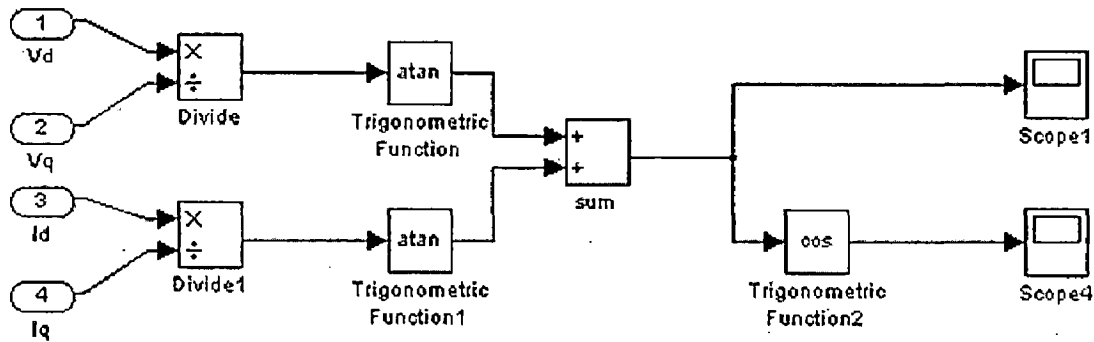


Fig 3.11 Schematic block diagram for power factor determination

3.4 Rectifiers and Inverters

A traditional frequency converter consists of:

- a rectifier (as AC-to-DC conversion unit) to convert alternating current into direct current, while the energy flows into the DC system
- energy storage (capacitors)
- an inverter (DC-to-AC with controllable frequency and voltage) to convert direct current into alternating current, while the energy flows to the AC side.

Diodes can be used only in rectification mode, whereas electronic switches can be used in the rectifying as well as in the inverting mode.

The most common rectifier solution is the diode rectifier, because of its simplicity, its low cost and low losses. It is nonlinear in nature and consequently it generates harmonic currents. These harmonic currents are later filtered with the help of LC filters. Another drawback is that it allows only a unidirectional power flow and it cannot control the generator voltage or current. Therefore, it can be used only with a generator that can control the voltage and with an inverter (e.g. an IGBT) that can control the current.

The thyristor based inverter solution is a cheap inverter, with low losses and, as its name indicates, it needs to be connected to the grid to be able to operate. Unfortunately, it consumes reactive power and produces large harmonics. The increasing demands on

power quality make thyristor inverters less attractive than self-commutated inverters, such as GTO inverters and IGBTs. The advantage of a GTO inverter is that it can handle more power than the IGBT, but this feature will be less important in the future, because of the fast development of IGBTs. The disadvantage of GTOs is that the control circuit of the GTO valve is more complicated.

The generator and the rectifier must be selected as a combination (i.e. a complete solution), while the inverter can be selected almost independently of the generator and the rectifier. A diode rectifier or a thyristor rectifier can be used together only with a synchronous generator, as it does not require a reactive magnetizing current. As opposed to this, GTO and IGBT rectifiers have to be used together with variable-speed induction generators, because they are able to control the reactive power. However, even though IGBTs are a very attractive choice, they have the disadvantages of a high price and high losses. The synchronous generator with a diode rectifier has a much lower total cost than the equivalent induction generator with an IGBT inverter or rectifier [1].

Due to the points mentioned above, the diode rectifier and an IGBT inverter have been selected to carry out further work. An attempt has been made to design a diode rectifier and an IGBT inverter with their respective filters and snubber circuits. The detailed design is explained in the next chapter.

CHAPTER 4

MODELLING AND SIMULATION

4.1 Overview

This chapter briefs about the modelling and simulation in brief and focuses mainly on modelling and model verification of the wind turbine and the synchronous generator and later produces the results of the simulation of the complete model. This chapter presents a number of basic considerations regarding simulations for wind turbines in electrical power systems.

4.2 Introduction to the modelling and simulation

Computer simulation is a very valuable tool in many different contexts. It makes it possible to investigate a multitude of properties in the design and construction phase as well as in the application phase. For wind turbines, the time and costs of development can be reduced considerably, and prototype wind turbines can be tested without exposing physical prototype wind turbines to the influence of destructive full-scale tests. Thus, computer simulations are a very cost-effective way to perform very thorough investigations before a prototype is exposed to real full-scale tests.

However, the quality of a computer simulation can be good only when the quality of the built-in models and the applied data are good. Therefore it is strongly recommended to define clearly the purpose of the computer simulations in order to make sure that the model and data quality are sufficiently high for the problem in question and that the simulations will provide adequate results. Otherwise, the results may be insufficient and unreliable.

There will be an inherent risk that possible insufficiencies and inaccuracies will not be discovered or will be discovered too late and subsequent important decisions may be made on a faulty or insufficient basis unless the built-in models and the applied data are carefully considered. Hence, computer simulations require a very responsible approach.

Computer simulations can be used to study many different phenomena. The requirements that a specific simulation program has to meet, the necessary level of

modelling detail and requirements regarding the model data may differ significantly and depend of the objective of the investigation. Different parts of the system may be of varying importance depending on the objective of the investigation too. All this should be taken into consideration before starting the actual computer simulation work.

However, in order to take into account all this, it is necessary to have a general understanding of the wind turbine-generator drive and how the various parts of the system can be represented in a computer model. This basic overview will be provided in the subsequent sections of this chapter. After that, the different types of simulations and various requirements regarding accuracy will be discussed in more detail with the help of the results obtained.

4.3 Model verification of the wind turbine

The detailed design has been discussed in the previous chapter. The model in the Matlab graphic user interface is shown in fig 4.1. The initial condition here in this simulation is assumed that the wind turbine is already in operation and producing mechanical torque and power in per unit as per the inputs given as shown below.

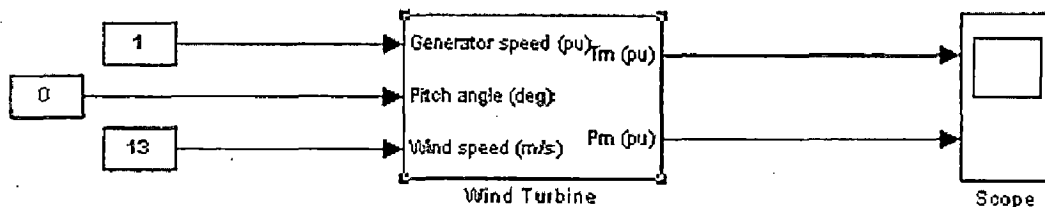


Fig 4.1 Model of the wind turbine

Where

The generator speed is taken as 1 p.u., the pitch angle is taken as 0^0 to get the maximum output power and the wind speed is taken as 13 m/s.

The scope is a block in Matlab which displays its input with respect to the simulation time.

The specifications for the wind turbine in this work are taken as in fig 4.2.

Function Block Parameters: Wind Turbine

Wind Turbine (mask)

This block implements a variable pitch wind turbine model. The performance coefficient C_p of the turbine is the mechanical output power of the turbine divided by wind power and a function of wind speed, rotational speed, and pitch angle (β). C_p reaches its maximum value at zero β . Select the wind-turbine power characteristics display to plot the turbine characteristics at the specified pitch angle.

The first input is the generator speed in per unit of the generator base speed. For a synchronous or asynchronous generator, the base speed is the synchronous speed. For a permanent-magnet generator, the base speed is defined as the speed producing nominal voltage at no load. The second input is the blade pitch angle (β) in degrees. The third input is the wind speed in m/s.

The output is the torque applied to the generator shaft in per unit of the generator ratings.

The turbine inertia must be added to the generator inertia.

Parameters

Nominal mechanical output power (W):
2e6

Base power of the electrical generator (VA):
2e6/0.85

Base wind speed (m/s):
13

Maximum power at base wind speed (pu of nominal mechanical power):
0.91

Base rotational speed (p.u. of base generator speed):
1

Pitch angle β to display wind-turbine power characteristics ($\beta \geq 0$) (deg):
0

Display wind turbine power characteristics

OK Cancel Help Apply

Fig 4.2 Specifications of the wind turbine

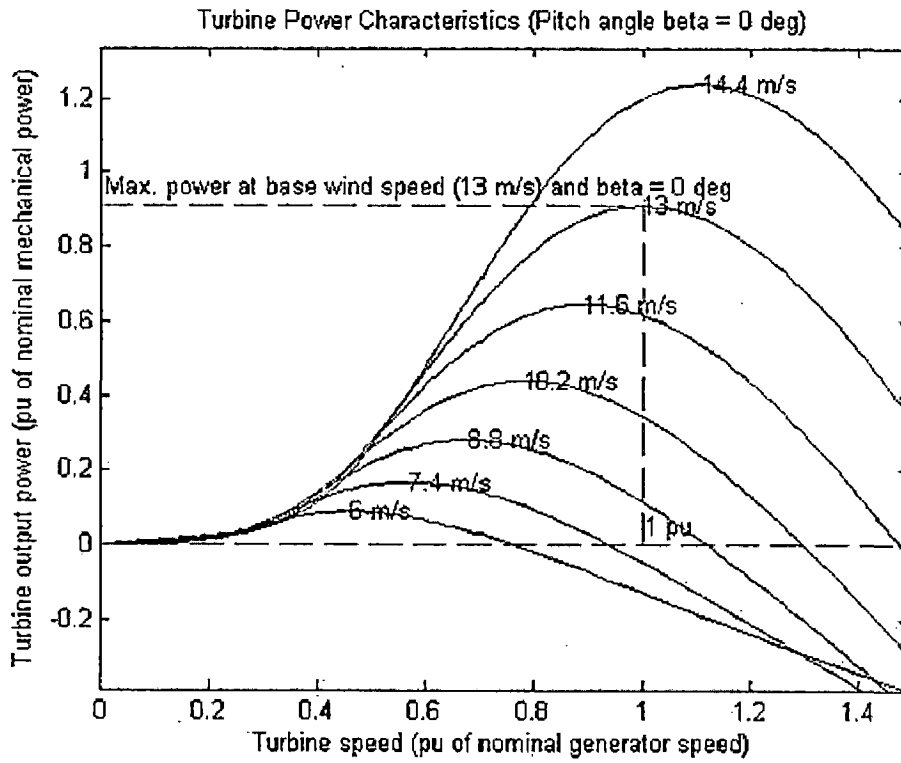


Fig 4.3 Turbine Power Characteristics

The turbine power characteristics as obtained in this particular simulation are displayed as in fig 4.3 which shows the turbine output power with respect to the turbine speed and various graphs are drawn for various wind speeds ranging from 7 m/s to 15 m/s. The results obtained under assumed initial conditions are shown in figs 4.4 and 4.5.

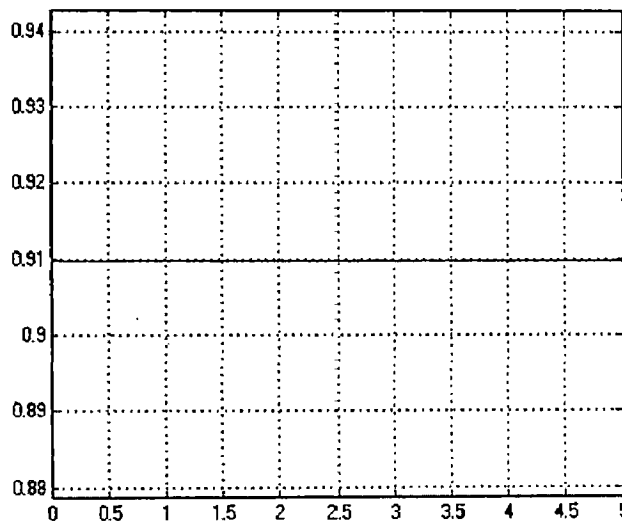


Fig 4.4 Power output in p.u. with respect to time

Fig 4.4 gives the per unit value of the Power output of the wind turbine whose value is specified in fig 4.2 as 0.91. The per unit quantity is defined as the ratio of the actual quantity to its base quantity. Here, the actual quantity is the actual output power produced and the base quantity is the expected output power to be produced. Hence to find out the actual output power produced, the expected output power should be multiplied with the per unit value obtained in the graph. Hence the actual value of the output power is

$$P_{output_actual} = 0.91 \times P_{output_expected}$$

$$P_{output_actual} = 0.91 \times 2MW$$

$$= 1.82 \text{ MW}$$

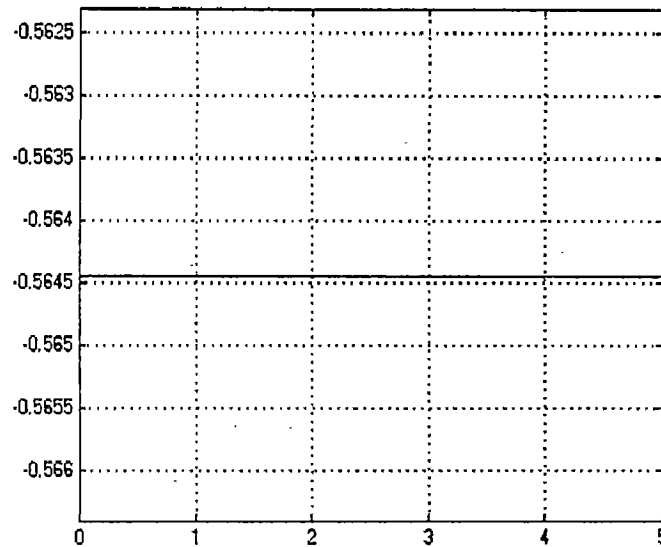


Fig 4.5 Torque output in p.u. with respect to time

The convention of the input mechanical torque is negative for any synchronous machine in generating mode (fig 3.10). This is because, in generating mode, the mechanical torque of the turbine is absorbed to give the electrical power as output where as in motoring mode, the electrical power is absorbed to give mechanical torque as output. Hence in fig 3.1, a gain block of -1 is put just before taking the mechanical torque output from the wind turbine as per the convention that neither power nor torque have the same sign at a time. Here in the fig 4.5 above, the mechanical torque output of the wind turbine is obtained as 0.5645 which is multiplied with -1 to get -0.5645.

4.4 Model verification of the generator

The synchronous generator is coupled to the above wind turbine model and either the power output or the torque output of the wind turbine is given to the generator as one of its input. The synchronous generator then behaves according to the input it gets from the wind turbine. The wind speed of 13 m/s is given as an input to the wind turbine. The wind speed of 13 m/s is given as an input to the wind turbine.

The model of the synchronous generator is shown in fig 4.6.

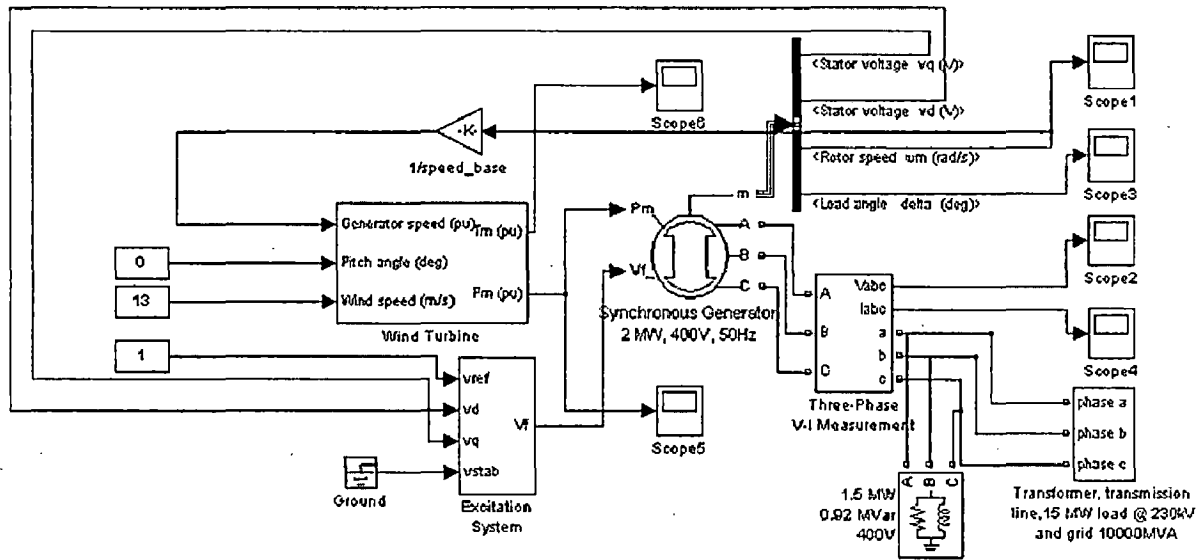


Fig 4.6 Model of the Synchronous Generator

Where

Speed base in the above model is taken as the synchronous speed i.e. for 64 poles and 50Hz, ω_s is 9.817 rad/s.

It is to be noted that the above model is not connected to this work and has been used for the purpose of model verification and comparison with the actual model (Fixed speed wind turbine vs. Variable speed wind turbine) which is shown in the subsequent sections. This is because, the variable speed operation is not possible with the above model due to the generator being directly connected to the grid and there is no frequency conversion at all. So the above model is a fixed speed wind turbine-generator drive model.

The generator specifications of the above model are taken as in fig 4.7.

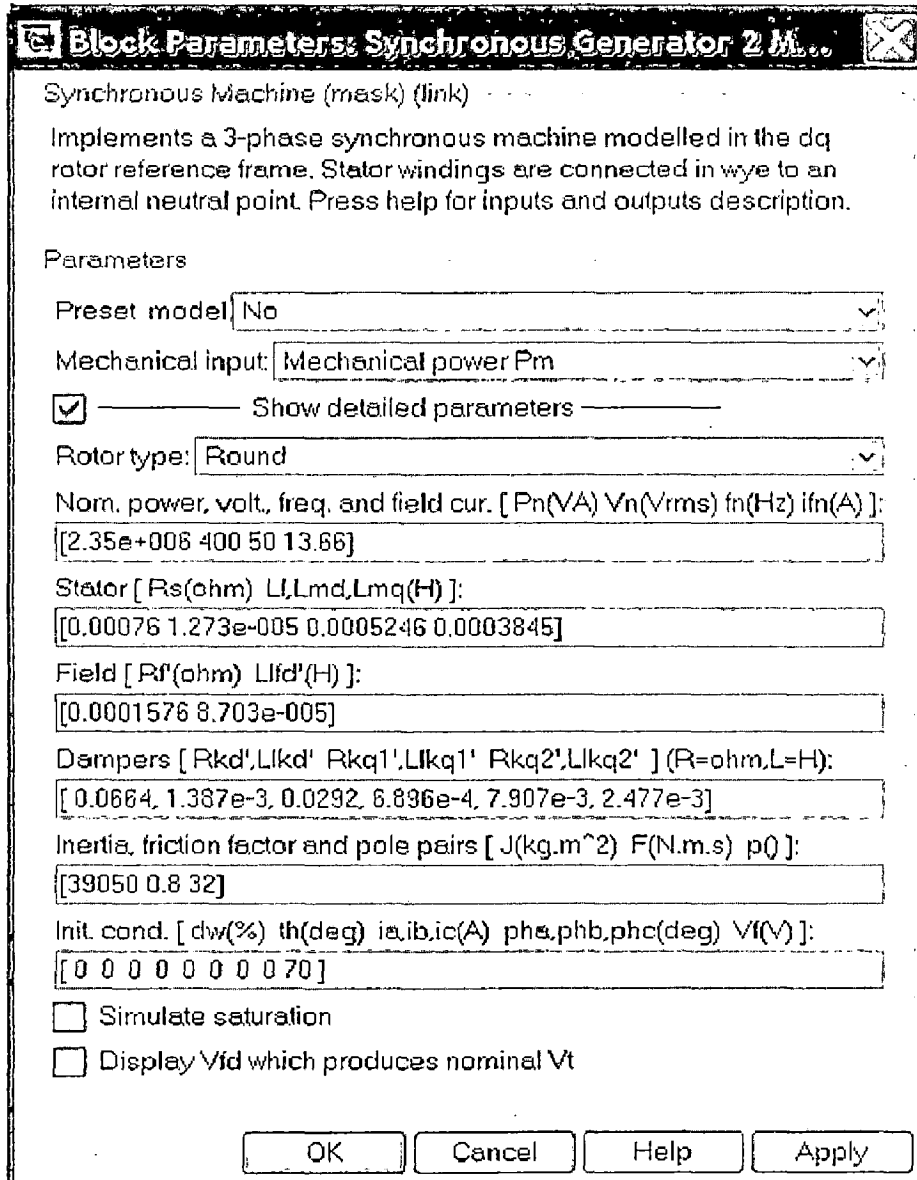


Fig 4.7 Specifications of the Generator

The simulation has been done and various results obtained such as the power output, torque output, three phase voltages, three phase currents, rotor speed and load angle are plotted which prove the genuinity of the model. Figs 4.8 to 4.13 are the results obtained for the above synchronous generator.

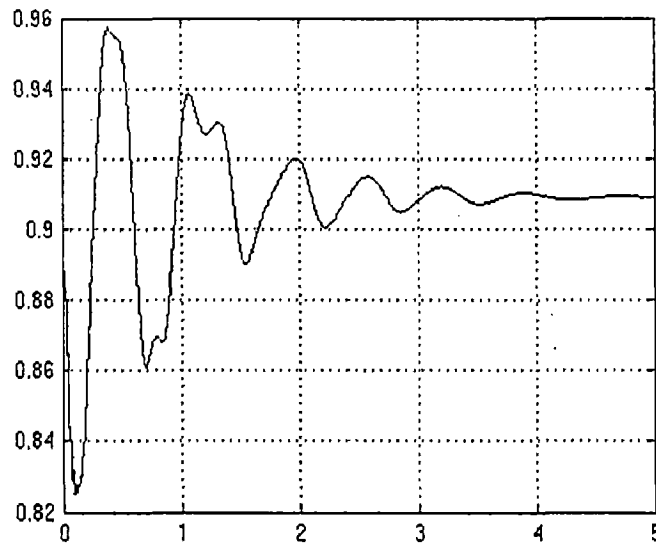


Fig 4.8 Synchronous Generator : Mechanical power output of wind turbine in p.u. vs. time in secs

It is clearly seen that at time $t=0$, the power waveform starts at 0.91 p.u., the specified value and it oscillates for a few seconds before it stabilizes to the same specified value. This is because, a certain initial condition has been specified for the system, i.e. the fixed speed wind turbine of the above fig 4.6 is already in motion producing rated power of 0.91 p.u. at its rated wind speed for the generator's input, before the time $t=0$. Now, as the rotor of the generator is being supplied already an excitation voltage of 70 V initially as shown in fig 4.7 (which produces a certain voltage at the stator terminals), 9.4 rad/sec of rotor speed is produced as shown in fig 4.12. This rotor speed which is obtained, at the output of the generator, is given as a feedback to the input of the wind turbine so as to define the tip speed ratio which is to be maintained constant. Hence there should be some controlling mechanism like pitch control explained in chapter 1 to keep the rotation of the generator rotor at its synchronous speed. A gearbox is also used here if necessary. The pitch control tries to make the speed of its rotor match up with the synchronous speed of the generator so that at varying wind speeds, the rotor with a common shaft (or with a gear box) rotates at a single synchronized speed to achieve a fixed frequency since the generator is directly connected to the grid. It achieves synchronous speed in the steady state (in about 4 secs) because of the development of the rotor field current, before the steady state is achieved, whose rated

value is 13.66 A as specified in fig 4.7. So the initial oscillations are due to the change from initial conditions to the final steady state condition.

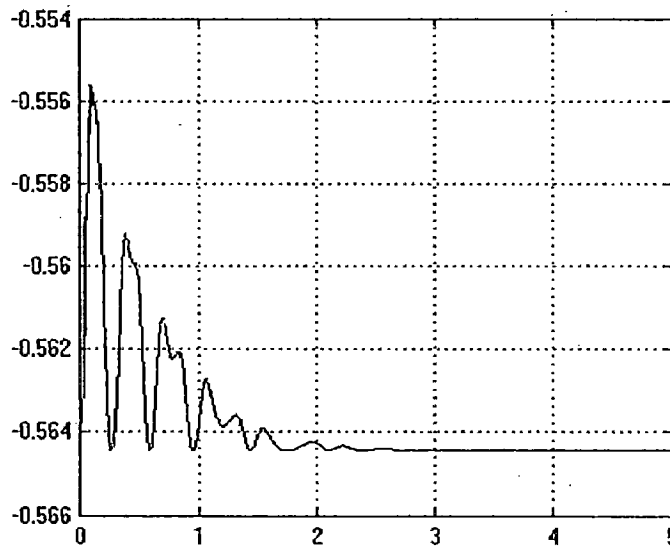


Fig 4.9 Synchronous Generator : Mechanical torque output of wind turbine in p.u. vs. time in secs

The similar reasoning can be given here also as given for the fig 4.8. That is after several initial oscillations, the output mechanical torque settles down at the same constant value of -0.5645 (as in fig 4.5) due to the initial condition. At time $t=0$, the rotor speed which is obtained at the output of the generator is given as a feedback to the input of the wind turbine instead of a constant per unit value of 1 as given in fig 4.1 for maintaining the shaft speed at the synchronous speed. Severe oscillations in the generator's rotor speed and hence in the voltage output can be observed for dynamic variations of the wind speed if the pitch control is not used since there is no frequency conversion. In this case, neither the pitch control nor the variations are included in the model but the excitation control system is present which will maintain the voltage constant in the steady state. Hence no variations are observed in the steady state.

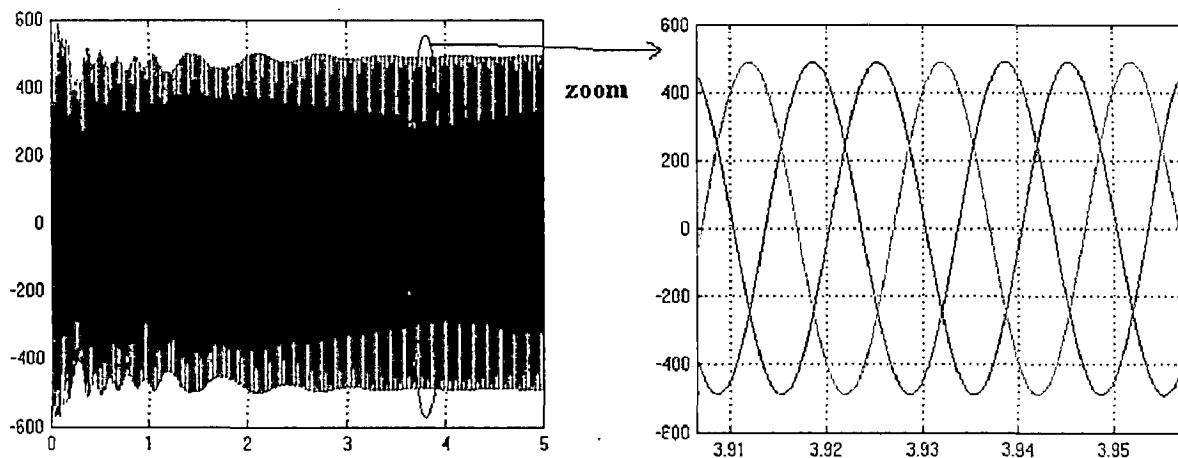


Fig 4.10 Synchronous Generator : Three phase load voltages in volts vs. time in secs

From the previous discussion, it is understood that the shaft speed settles down at its synchronous speed in a few seconds time. We know that the perfect synchronized sinusoidal voltage waveforms can be obtained only when the system is in synchronization when the speed stabilizes to its synchronous speed. Here in fig 4.10, the oscillations in the voltage waveforms are clearly observed when the speed is being brought to synchronous speed. After that, the perfect sinusoidal three phase voltages have been obtained as shown above due to the absence of wind speed variation and the presence of excitation system's feed back control system.

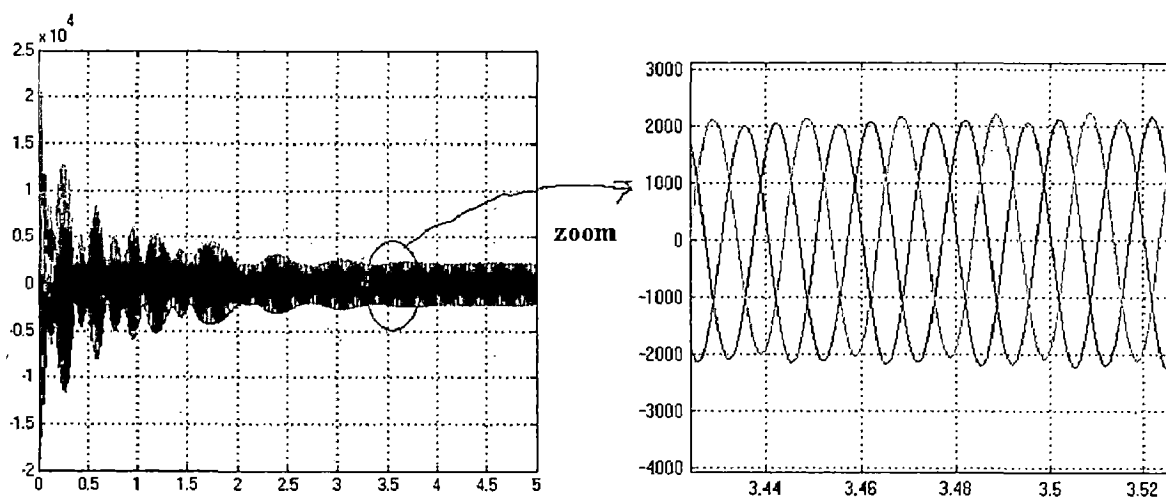


Fig 4.11 Synchronous Generator : Three phase load current in amps vs. time in secs

The similar is the case with the current waveforms. And hence perfect sine current waveforms are obtained in the steady state as shown in fig 4.11.

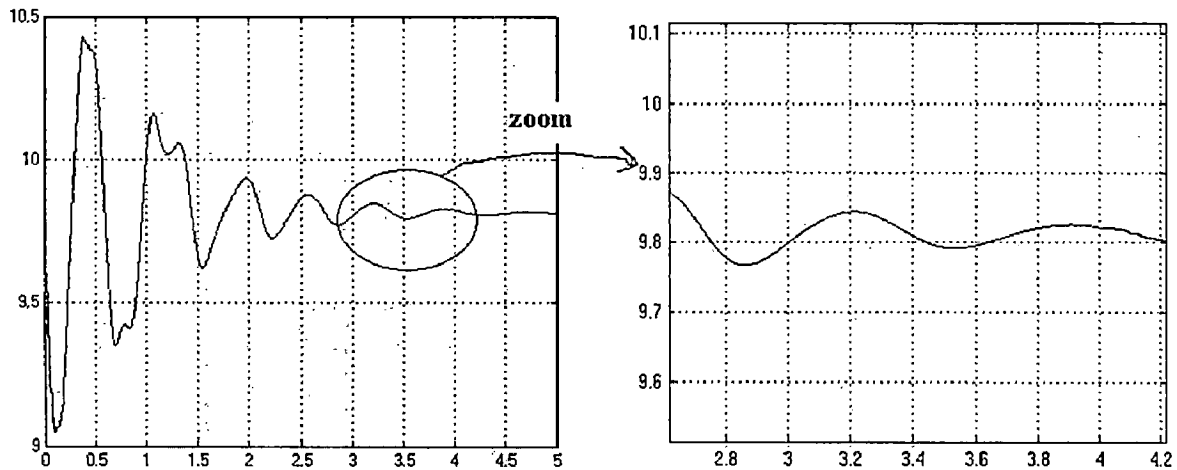


Fig 4.12 Synchronous Generator : Rotor speed in rads/sec vs. time in secs

The synchronous speed of the generator is derived as follows. The generator used here has 32 pole pairs i.e. 64 poles in total. Hence, the synchronous speed in RPM can be derived. And later, this synchronous speed in RPM is converted into rad/sec using the following relation.

$$\begin{aligned}
 N_s &= \frac{120 \times f}{p} \\
 &= \frac{120 \times 50}{64} \\
 &= 93.75 \\
 \omega_s &= \frac{2 \times \pi \times N_s}{60} \\
 &= \frac{2 \times \pi \times 93.75}{60} \\
 &= 9.8174 \text{ rad/sec}
 \end{aligned}$$

The initial condition as said before is that the turbine is already in motion before time $t=0$, and at time $t=0$, it tries to get synchronized to produce desired voltages and currents.

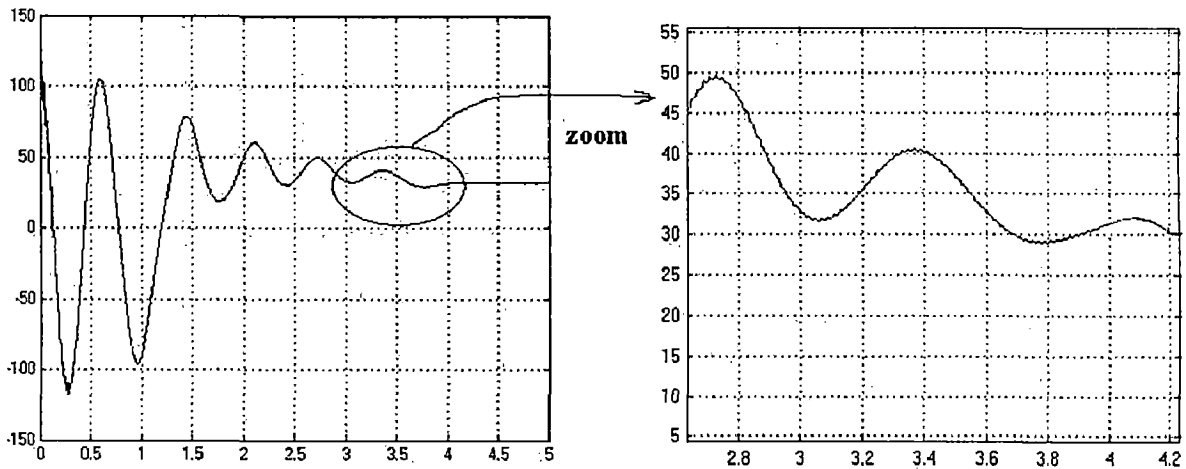


Fig 4.13 Synchronous Generator : Load angle in degs vs. time in secs

The similar is the case with the load angle. It is interesting to see the initial huge oscillations from -100° to 100° . This initial adjustment of the load angle is because the machine cannot drive the load at that speed (below synchronous speed). As the machine tries to steady state, the load angle oscillates and it steadies itself to a steady angle after acheiving the steady state. In this case, the load angle finally settles at around 30° which depend upon the amount of the load.

4.5 Complete model

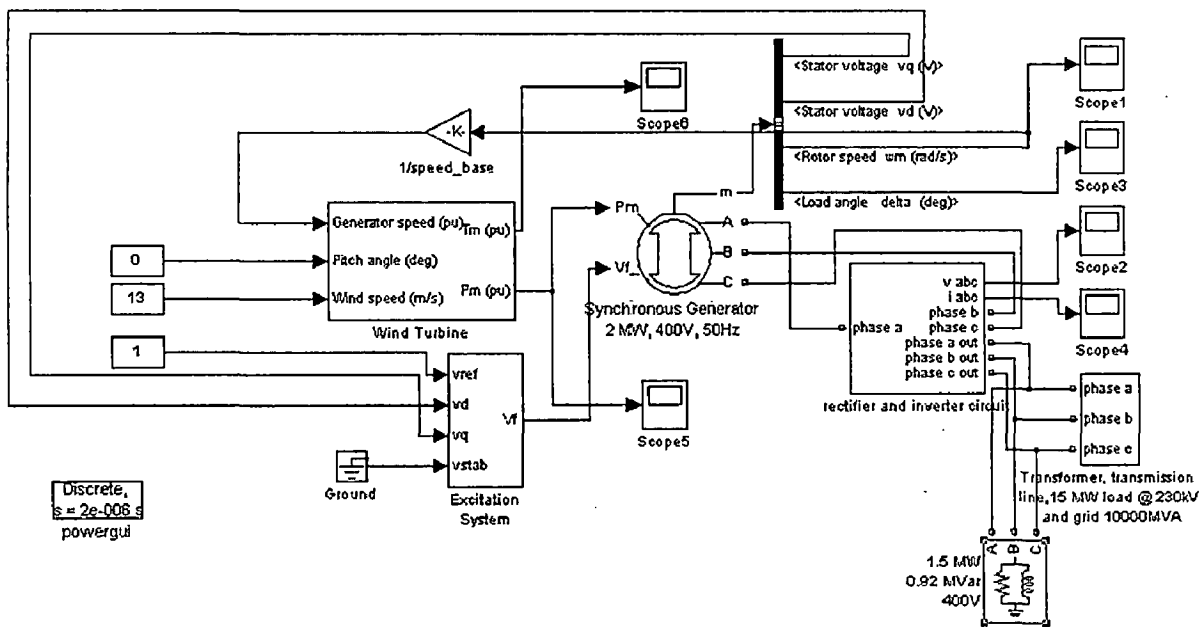


Fig 4.14 Model of the Synchronous Generator with the rectifier and the inverter

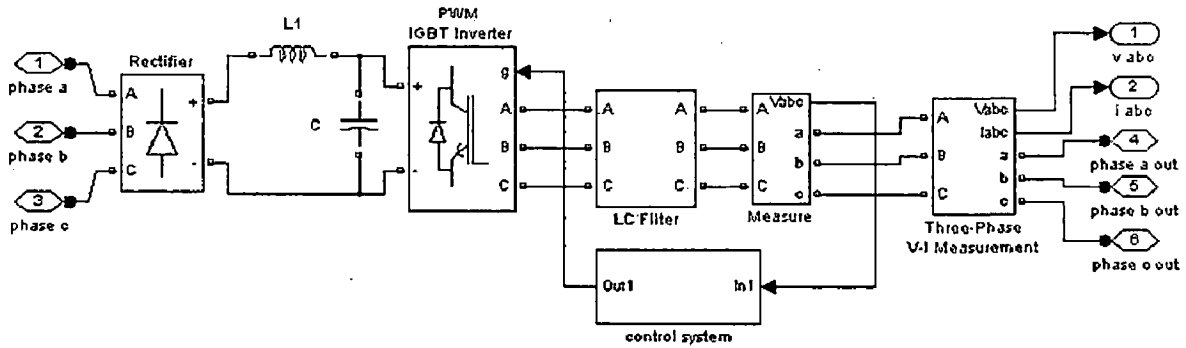


Fig 4.15 Inside the Rectifier and Inverter block

The above model is the variable speed wind turbine-generator drive model.

The output of the generator is given to a rectifier with following specifications for the purpose of full frequency conversion for the variable speed operation to be possible.

Block Parameters: Rectifier

Universal Bridge: (mask) (link)

This block implement a bridge of selected power electronics devices. Series RC snubber circuits are connected in parallel with each switch device. Press Help for suggested snubber values when the model is discretized. For most applications the internal inductance L_{on} of diodes and thyristors should be set to zero.

Parameters:

Number of bridge arms:

Snubber resistance R_s (Ohms):

Snubber capacitance C_s (F):

Power Electronic device:

R_{on} (Ohms):

L_{on} (H):

Forward voltage V_f (V):

Measurements:

Fig 4.16 Specifications of the Rectifier

The snubber resistance R_s and the snubber capacitances C_s have been designed according to some specific requirements. The details of the design for both snubbers used in rectifier and inverter have been mentioned in Appendix A.

The rectified output is then filtered with the help of an LC filter. The values of the filter inductance and capacitance are taken as 0.2 mH and 5 mF respectively.

After the rectification and filtering, the DC output is given to an inverter which will be responsible to convert the DC into AC of a particular frequency. In this case the control system which is responsible to generate gate pulses to the inverter to produce waveforms of voltages of any desired frequency, is set to give waveforms of 50 Hz frequency only. After the inversion, the output waveforms will be of quasi square wave type. So to convert these quasi square waveforms into sinusoidal waveforms, a three phase LC filter is used.

The circuit model of three-phase PWM inverter with IGBTs and a center-taped grounded DC bus is as shown below.

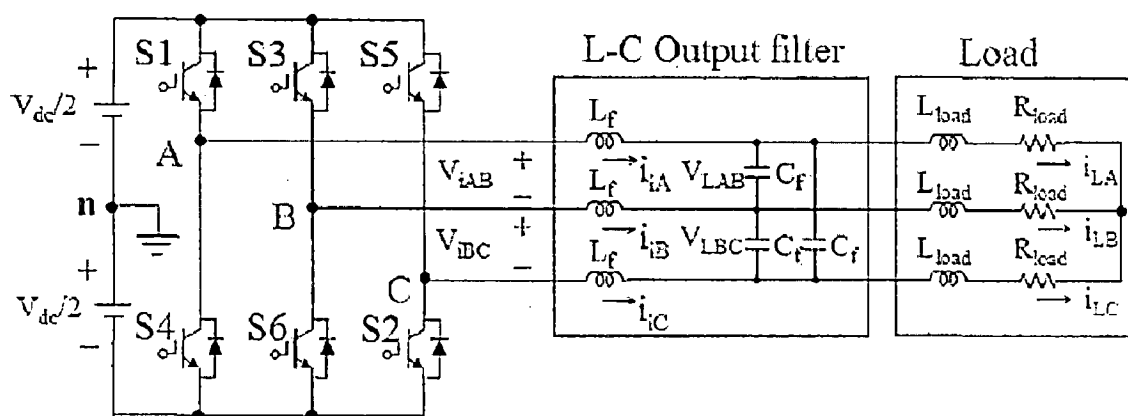


Fig 4.17 Circuit model of three-phase PWM inverter

The specifications of the inverter used are as shown below.

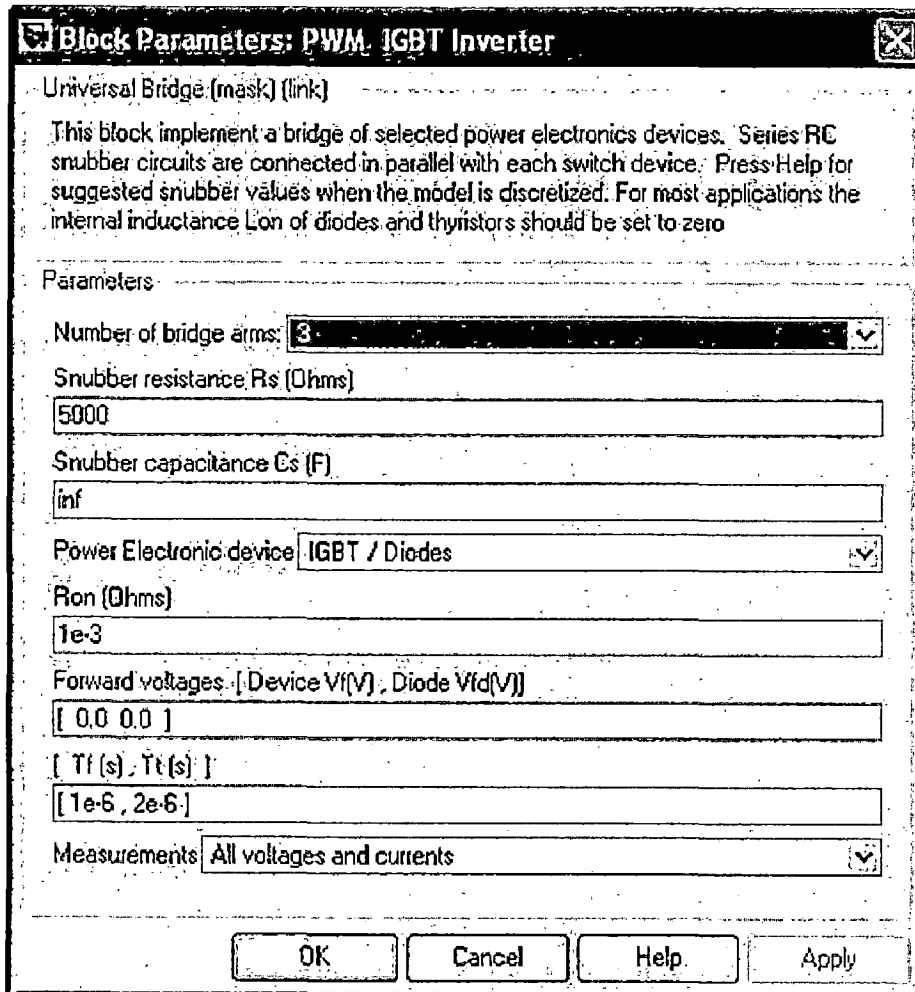


Fig 4.18 Specifications of the Inverter

A resistive snubber is used for this inverter, the design details are given in Appendix A.

The values of the three phase LC filter are taken as follows: inductance of 0.9 mH and capacitance load of 12 kVAR respectively.

The concept of the control system used to generate the required gate pulses is clearly explained in Appendix B.

A 2.35 MVA transformer, 15 MW load, 100 kms transmission line and a grid of 10000 MVA and 230 kV have been used whose parameters have been mentioned in the Appendix C. the block diagram in MATLAB/ Simulink is shown below in fig 4.19.

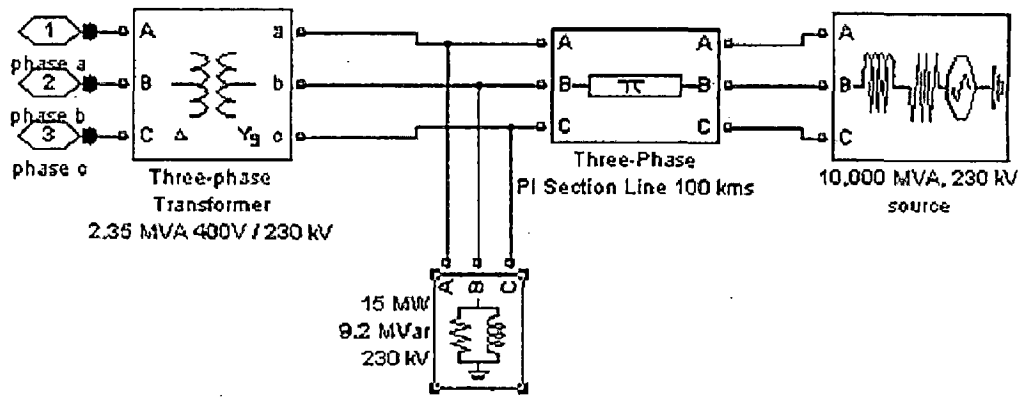


Fig 4.19 Inside the grid block

The simulation has been done with all the above components and various results are obtained similarly as before. Figs 4.20 to 4.25 are the results obtained for the above model. Here, as this is a variable speed drive, the rotor's inertia is increased to accommodate the minute wind speed variations which are absorbed in the rotor eventually. This is the reason why the time taken to reach the steady state from the initial state is very less.

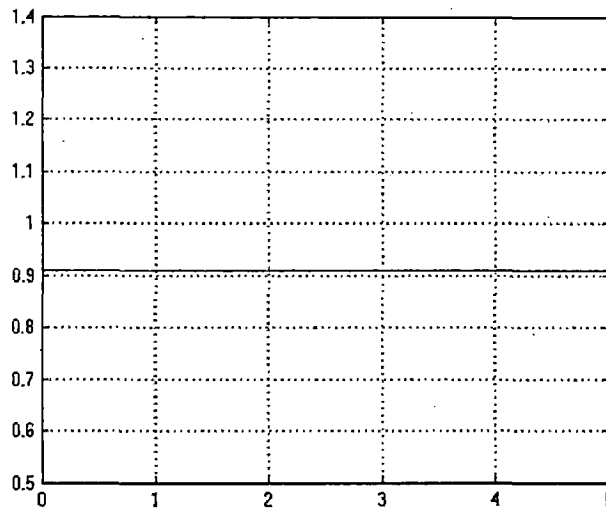


Fig 4.20 SG with RI block : Mechanical power output of wind turbine in p.u. vs. time in secs

The result obtained in fig 4.8 shows several oscillations before reaching to a steady state value after the system gets initiated for achieving synchronous speed. Due to the large inertia of the generator's rotor here in fig 4.20, the initial oscillations are

damped out and will be negligible as said before. Hence a constant power output waveform is obtained.

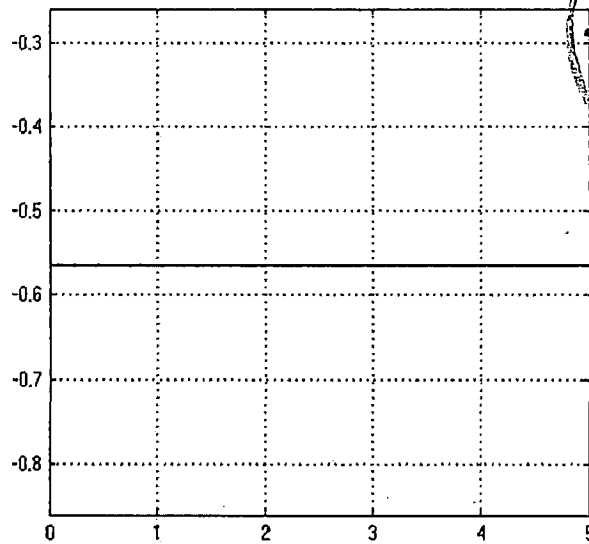


Fig 4.21 SG with RI block : Mechanical torque output of wind turbine in p.u. vs. time in secs

As said before, even in fig 4.21 the initial oscillations are damped out and a constant torque output is obtained.

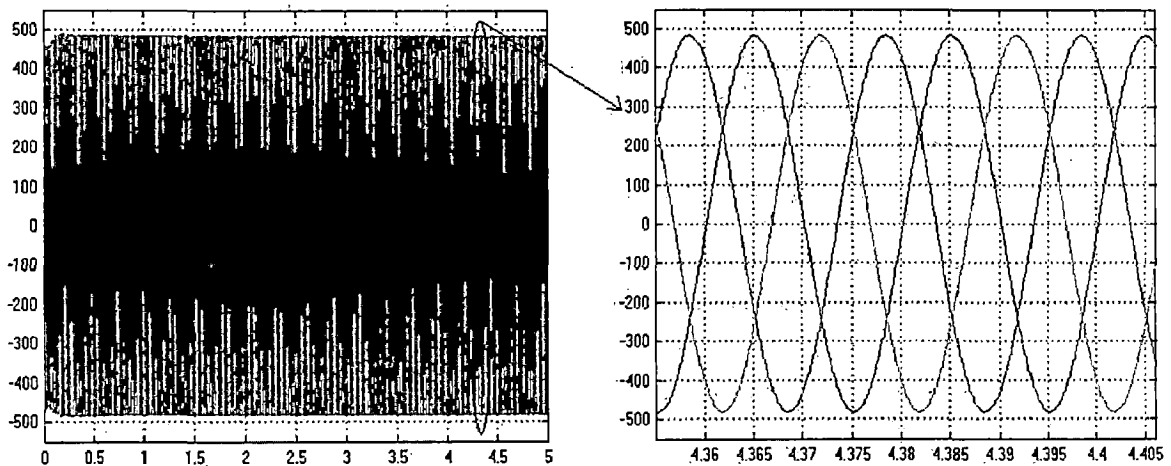


Fig 4.22 SG with RI block: Three phase load voltages in volts vs. time in secs

Fig 4.22 shows the voltage waveforms which clearly show perfectly desired sinusoidal voltages. It can be inferred from the figure that before the time $t=0$, as the rotor

of the generator is being supplied already an excitation voltage of 70 V initially as shown in fig 4.7, it produces a voltage of 450 V peak at the stator terminals. Now at t=0, when the field current of the rotor winding reaches its rated current of 13.66 A, the voltage output at the load terminal build up to about 500 V peak after the system reaches the steady state. But the rated voltage is 400 V rms. Therefore the rated peak voltage should be $400\sqrt{2}$ which is equal to approximately 565 V. The drop in the voltage by approximately 65 V is due to the stator resistances and inductances of the generator, LC filters, loading on the transmission line, nature and the amount of the load.

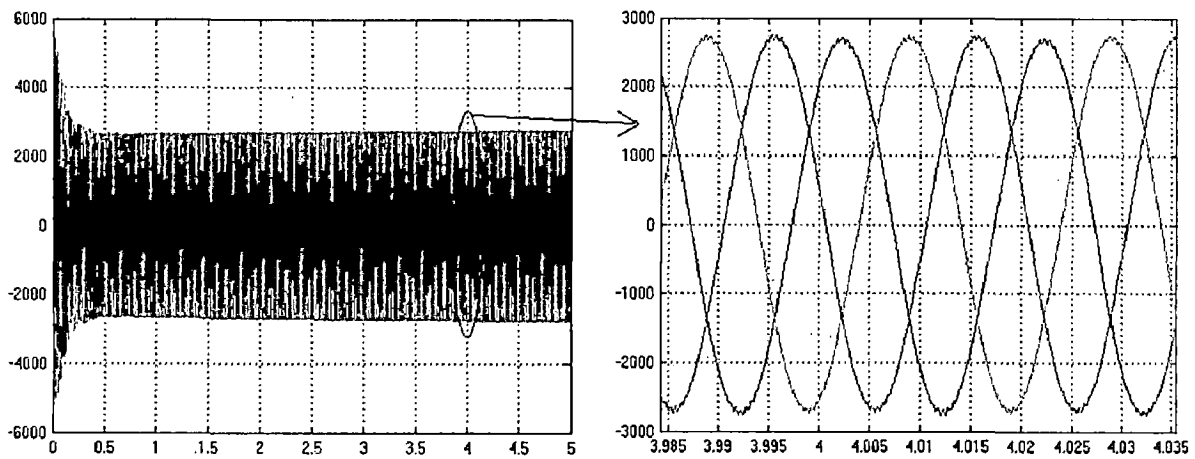


Fig 4.23 SG with RI block: Three phase currents in amps vs. time in secs

Fig 4.23 shows the current waveforms which are also obtained as perfect sinusoidal currents. Initially at t=0, when the system is initialized to achieve steady state, it is observed that huge currents flow into the grid due to the switching transients. The current reaches a magnitude of about 5200A where the rated current is only 2890 A theoretically as shown.

$$\begin{aligned}
 I_{rated} &= \frac{P_{rated}}{\sqrt{3} \times V_{L-L}} \\
 &= \frac{2 \times 10^6}{\sqrt{3} \times 400} \\
 &= 2890A
 \end{aligned}$$

During switching, the current waveforms may reach to n times (explained in section 5.5.1) the rated value due to the DC component which creeps in due to the sudden

change of state (explained in section 5.4). This DC component decays slowly depending on the decaying time constant, 0.3 seconds in this case. The reason for abnormal increase in currents is due to the inductive loads present in the system. The flux linkages associated with those inductances cannot be changed suddenly by the application of switching which is a sudden act. For maintaining these flux linkages constant, large changes of current will take place as above. The higher rate of decay is obtained due to the large inertia which is generally achieved through damper windings. The current then stabilizes itself to a steady state value of about 2800 A which is the rated/load current obtained in simulation.

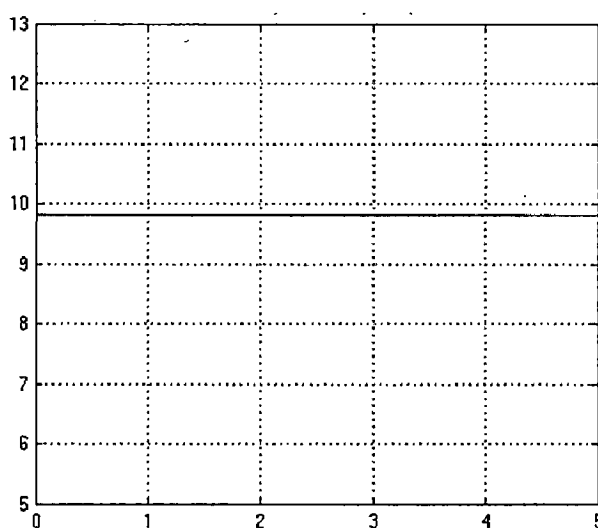


Fig 4.24 SG with RI block: Rotor speed in rads/sec vs. time in secs

Fig 4.24 shows the rotor speed in rads/sec with respect to the time in seconds. The generator rotor runs at its rated constant speed of 9.817 rads/sec in this case because it is assumed that the wind speed is constant at its rated value in this simulation. So at the rated wind speed, the generator runs at its synchronous speed. It is because the speed is constant, the power and torque are also constant. This rotor speed which is obtained, at the output of the generator, is given as a feedback to the input of the wind turbine so as to define the tip speed ratio which is to be maintained constant to maintain the power coefficient C_p constant. This enables Maximum power point tracking, i.e., at any wind speed (speed range of 2 m/s to 25 m/s), the system works at its maximum efficiency. This can be achieved for a variable speed turbine-generator system as shown in fig 3.5.

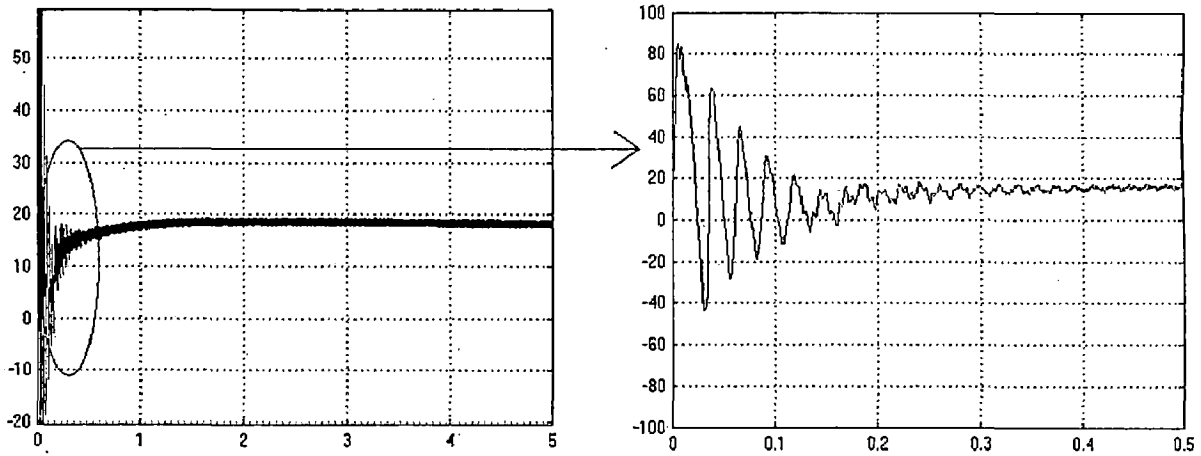


Fig 4.25 SG with RI block: Load angle in degs vs. time in secs

Fig 4.25 shows the load angle in degrees with respect to the time in seconds. The load angle in this case settles down at around 19° in the steady state. The steady state is achieved after the initial oscillations. The initial oscillations are due to the same reason explained before i.e., due to the change from initial state to the final steady state. When the generator tries to achieve the steady state, the generator's rotor oscillates and hence the load angle oscillates. It oscillates between -40° and 80° .

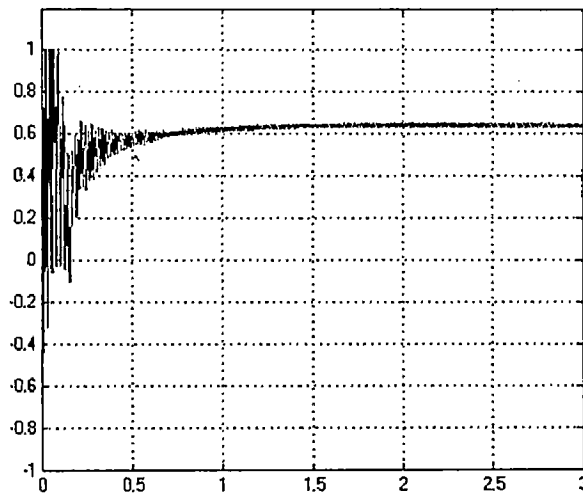


Fig 4.26 SG with RI block: Power factor $\cos \phi$ vs. time in secs

Fig 4.26 shows power factor $\cos \phi$ with respect to the time in seconds. The plot is obtained by performing the simulation on fig 3.11. From the above graph, the value of the power factor is obtained as 0.65 in the steady state which is 0.2 less than the specified

value. This reduction is due to the presence of more inductive load than the actual load. These inductive loads are present in both the single phase and three phase LC filters and all other non linear elements which are used in the frequency converter circuit. From this it can be inferred that the efficiency of the variable speed system is improved at the expense of loss in power factor. But as it is known that the reduction in power factor directly affects the efficiency of a system because of the reduced active power. Hence, it should be necessary to install the power factor correction devices like synchronous condensers, capacitor banks etc. Hence the cost of the system increases further more.

With all these simulations and results, it can be concluded that the complete model of variable speed wind turbine-generator drive is successfully designed as it is working properly without any acute abnormalities.

4.6 Grid power quality

A power quality problem is defined as any problem manifested in voltage, current or frequency deviations that result in failure or mis-operation of customer equipment. The voltage problem is taken care of by the excitation control system and the frequency is always constant because of the frequency converter.

There will be three types of power quality problems

- Occurrence of flicker
- Occurrence of harmonics
- Occurrence of voltage deviations such as voltage sags and over voltages

Problem of Flicker in variable speed wind turbines

The rapid power fluctuations are very scarce in variable speed turbines, because the rotor acts as a flywheel (storing energy temporarily as a buffer) due to its large inertia (which is specified for these generators in section 4.5) and hence flicker doesn't occur as said before in section 1.5.

Harmonic mitigation in variable speed wind turbines

The power electronic devices such as diodes and IGBTs have been used in the model which will cause severe harmonics. Those harmonics are mitigated with the help of single phase and three phase LC filters respectively used in the model itself, in fig 4.15.

Mitigation of voltage deviations in variable speed wind turbines

The voltages sags and over voltages which occur due to the variable speed operation of the synchronous generator are taken care of by the excitation control system as said before.

Hence, all the power quality problems are eliminated in the system itself which finally maintains grid power quality. Hence, the need for installing new power electronic devices such as SVCs, Statcoms, SSCs etc is eliminated saving the overall cost.

4.7 Variable speed hydro turbines

The same concept of this variable speed operation used in this work can be used for the hydro turbines as well. In such a case, the governor, which is generally used to maintain a constant speed of the synchronous generator coupled to that hydro turbine, can be eliminated. Hence, the governor's cost is reduced but the inclusion of the frequency converter increases the cost. It is hence, a compromise between the two. The optimization techniques can be used to select either the governor or a frequency converter, for best possible cost.

CHAPTER 5

FAULT ANALYSIS

5.1 Overview

This chapter is the result of the successive simulations on the model designed in the previous chapter for various fault conditions. This chapter briefly introduces about the fault analysis and about the purpose of fault calculation. The simulation results and discussion on various fault conditions has been presented.

Fault analysis is very important for the power system studies since they provide data such as voltages and currents during and after the various types of faults which are necessary in designing protective schemes of the power system. The purpose of fault calculation is discussed in more detail.

5.2 Purpose of fault calculation

Fault calculation is the analysis of power system electrical behaviour under faulted conditions, with particular reference to the effects of these conditions on the power system current and voltage values. Together with other aspects of system analysis, fault calculation forms an indispensable part of the whole function and process of power system design. Correct design depends essentially on a full knowledge and understanding of system behaviour and on the ability to predict this behaviour for the complete range of possible system conditions. Accurate and comprehensive analysis, and the means and methods of achieving it, are therefore of essential importance in obtaining satisfactory power system performance and in ensuring the continued improvement in performance which results from the development and application of new methods and techniques [9].

The applications of power system analysis cover the full range of possible system conditions, these being divisible into two main classes, namely conditions in which the power system is operating in a normal healthy state, and others in which it is subjected to one or more of a wide variety of possible fault conditions. The analysis of these conditions and their effects on the power system is of particular relevance to such considerations as:

- the choice of a suitable power system arrangement, with particular reference to the configuration of the transmission or distribution network
- the determination of the required load and short-circuit ratings of the power system plant
- the determination of the breaking capacity required of the power system switchgear and fuse gear
- the design and application of equipment for the control and protection of the power system
- the operation of the system with particular reference to security of supply and economic considerations
- the investigation of unsatisfactory performance of the power system or of individual items of power system plant.

5.3 Types of faults

There are different types of faults in the power system which can broadly be divided into symmetrical and unsymmetrical faults. The currents and voltages resulting from various types of faults occurring at different locations through out the power system network must be calculated in order to provide sufficient data for designing the protective scheme i.e. both the protective relays and circuit breakers.

Different types of faults in the power system are:

- 3-phase direct short circuit or 3-phase fault through fault impedance (i.e. LLL or LLLG),
- Double line to ground fault with or without fault impedance (LLG),
- Line to line direct short-circuit or short circuit with fault impedance (LL),
- 1-phase to ground fault with or without fault impedance (LG), and
- Any combination of the above faults, for eg., Line to line direct short-circuit or short circuit with fault impedance (LL) cum 1-phase to ground fault with or without fault impedance (LG) on the third phase.

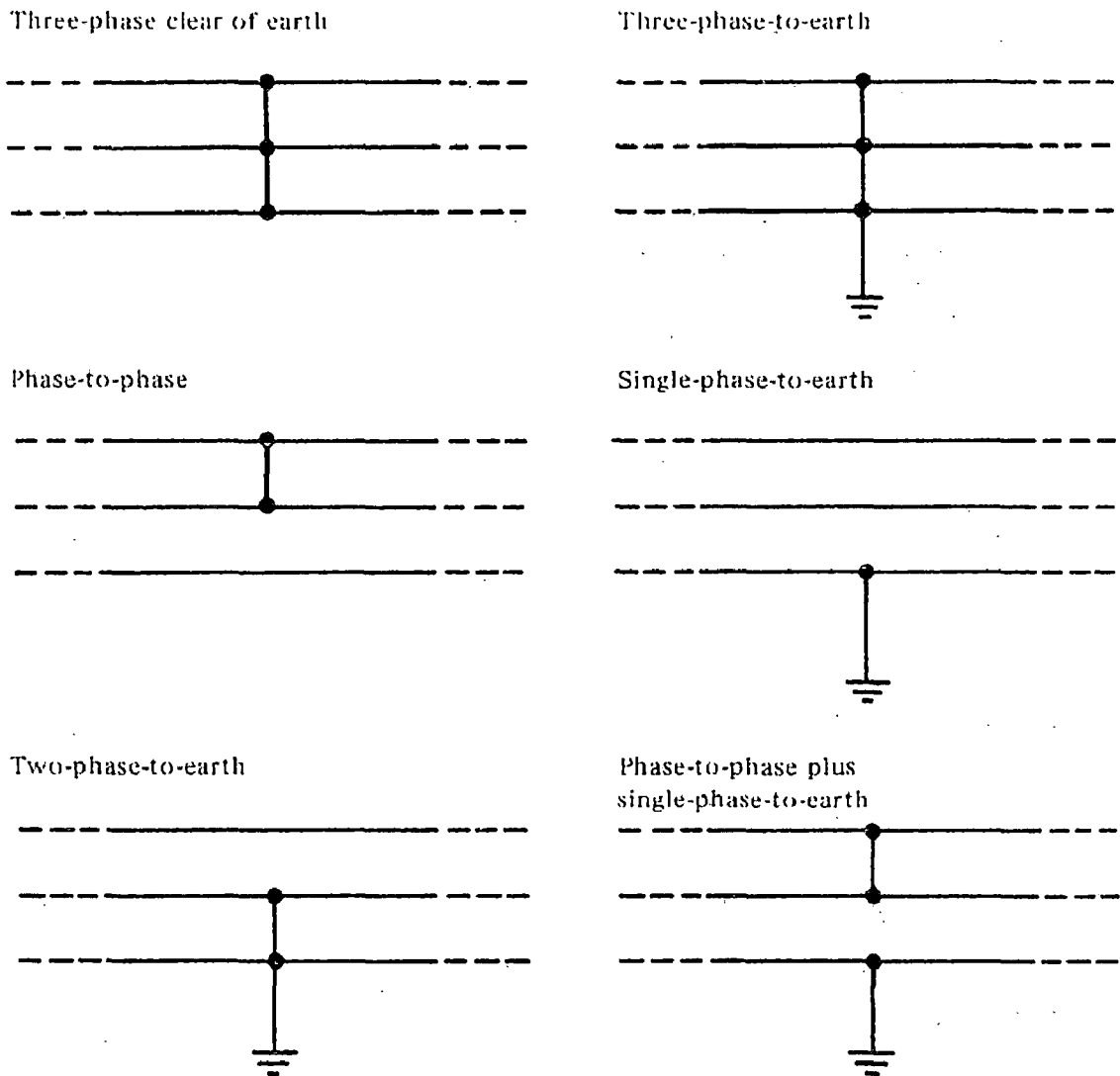


Fig 5.1 Representation of the faults in power system [16]

Out of the first four types of faults as listed above, the first one which is the least common but most severe, is a symmetrical fault i.e. after the fault, the system remains symmetrical, i.e. balanced. However, the next three faults are unsymmetrical, i.e. after the fault, the voltages and currents become unbalanced, thus it becomes a case of balanced network with unbalanced excitation. The last type of fault is also unsymmetrical fault of very rare case. In addition to the above, there may be several other types of faults such as opening of one or two conductor, load rejection i.e. opening of all the three conductors etc.

All the above five common possibilities of faults have been considered, and analysis has been done on the wind turbine model of chapter 4. The simulation results and discussion is done in section 5.5. The next section is about the switching transients, whose overview is necessary to explain the phenomena of faulted conditions.

5.4 Switching Transients

The switching transients are observed when load break switches, circuit breakers, disconnectors or fuses operate in the power system network and parts of the power system are separated from or connected to each other. These switching transients' magnitude is almost similar or larger when compared to the transients caused by the faults which are illustrated in the next section. The switching action can be either a closing or an opening operation in the case of a switching device. The reason for abnormal increase in currents is due to the inductive loads present in the system. The flux linkages associated with those inductances cannot be changed suddenly by the application of switching which is a sudden act. For maintaining these flux linkages constant, large changes of current will take place.

$$E_{\max} \sin(\omega t + \varphi) = RI + L \frac{dI}{dt} \text{-----(5.1)}$$

The equation (5.1) is the non-homogeneous differential equation of any RL circuit. By solving the above differential equation, the value of current can be obtained as

$$I(t) = e^{-(R/L)t} \left\{ \frac{-E_{\max}}{\sqrt{R^2 + \omega^2 L^2}} \sin\left[\varphi - \tan^{-1}\left(\frac{\omega L}{R}\right)\right] \right\} + \frac{-E_{\max}}{\sqrt{R^2 + \omega^2 L^2}} \sin\left[\omega t + \varphi - \tan^{-1}\left(\frac{\omega L}{R}\right)\right] \text{-----(5.2)}$$

The first part of equation (5.2) contains the exponential term which is the one that damps out. This is the DC component. The expression between the brackets is a constant and its value is determined by the instant of closing of the circuit. For $[\varphi - \tan^{-1}(\frac{\omega L}{R})] = 0$ or an integer times π , the DC component will become zero and the current immediately reaches the steady state. In other words, there will be no transient oscillations. But when the switch closes the circuit 90° earlier or later, the transient current will reach a maximum amplitude [16].

In the following analysis, the switching transients are observed at $t=0$ when the system is initialized to achieve steady state and at $t=3$ secs when the fault is cleared. This is because after an opening operation, when a power frequency current is interrupted, a transient recovery voltage (TRV) will appear across the terminals of the interrupting device. The configuration of the network as seen from the terminals of switching device determines amplitude, frequency and shape of the current and voltage oscillations. The TRV which stresses the interrupting device after the current interruption depends on the type of fault, the location of the fault and the type of circuit switched. Generally, the TRV will be highest in an LG fault. After a closing operation, transient currents will flow through the system as usual.

It is to be noted that the fault clearing consists of two operations, they are the opening and closing operations of the interrupting device and everything happens in milliseconds and hence that period is not shown anywhere in further simulations.

5.5 Simulation results and discussion

In this section, the results of the model for all the faults have been shown. It is to be noted that the fault of all types is initiated at $t=2$ secs and cleared at $t=3$ secs. It is also to be noted that generally, the phase colours are red, yellow and blue. But due to the colour inversion, while converting from the MATLAB/ Simulink format to JPEG format, red becomes green, yellow becomes blue and blue becomes red. Hence, from hereon the GBR colour format will be used instead of RYB format.

An important point is that when a fault of any type occurs, the nature of currents in the various phases varies with time in a complicated way. Analysis of the waveforms show that they consist of

- A fundamental-frequency component
- A DC component.
- A double-frequency component

The fundamental-frequency component is symmetrical with respect to the time axis. Its superposition on the DC component will give an unsymmetrical waveform. The degree of asymmetry depends upon the point of the voltage cycle at which the short circuit/ fault takes place as explained in section 5.4.

5.5.1 LLLG Fault

This is a rare fault and is most severe of all types of faults as seen in the waveforms below.

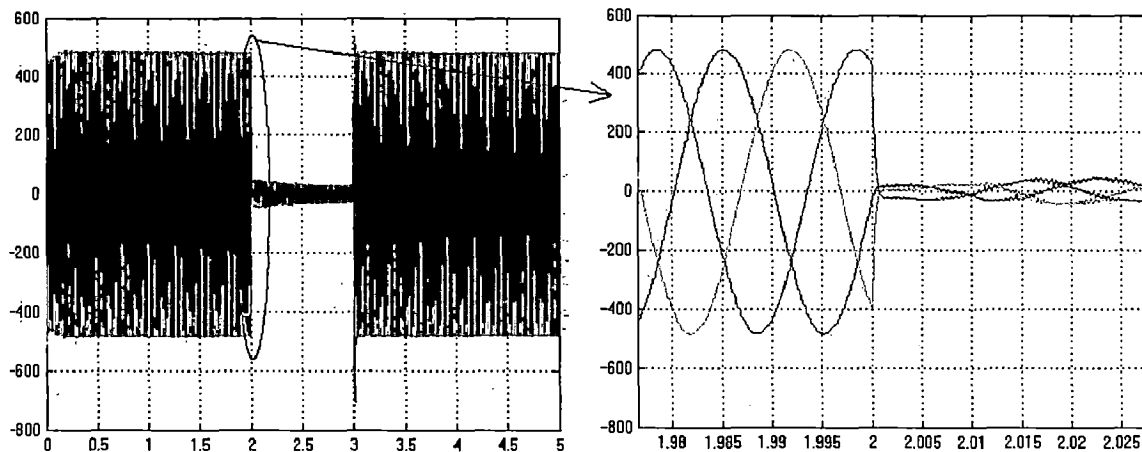


Fig 5.2 LLLG Fault: Three phase load voltages before, during and after the fault

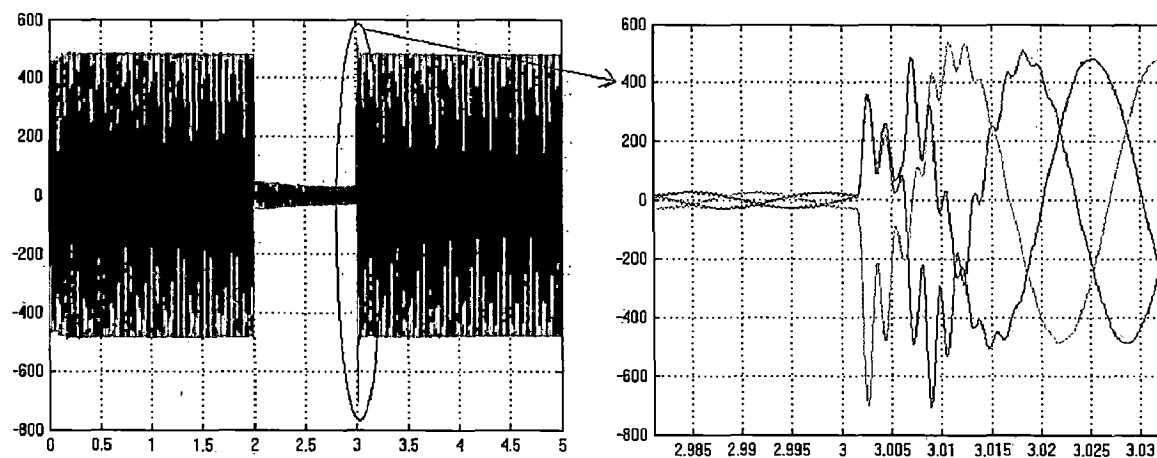


Fig 5.3 LLLG Fault: Three phase load voltages (for zooming)

Figs 5.2 and 5.3 shows the waveforms of voltages when an LLL or a LLLG fault occurs. As the name itself indicates, when this fault occurs, all the three phase lines gets short circuited. It is known that when a short circuit occurs, the phase voltages become zero. But in practice, as shown in figs above, the voltages will not become zero but will drop to very small values of magnitude less than 5 V due to the presence of fault resistances of magnitude 0.001Ω each.

At the instant of clearing the fault at $t=3$ secs, the disturbances occurring and the spikes are shown in fig 5.3. These spikes are caused because of the sudden interruption of

current flow which leads to a sharp rise in voltage across the load. This sharp rise in voltage leads to transients as above.

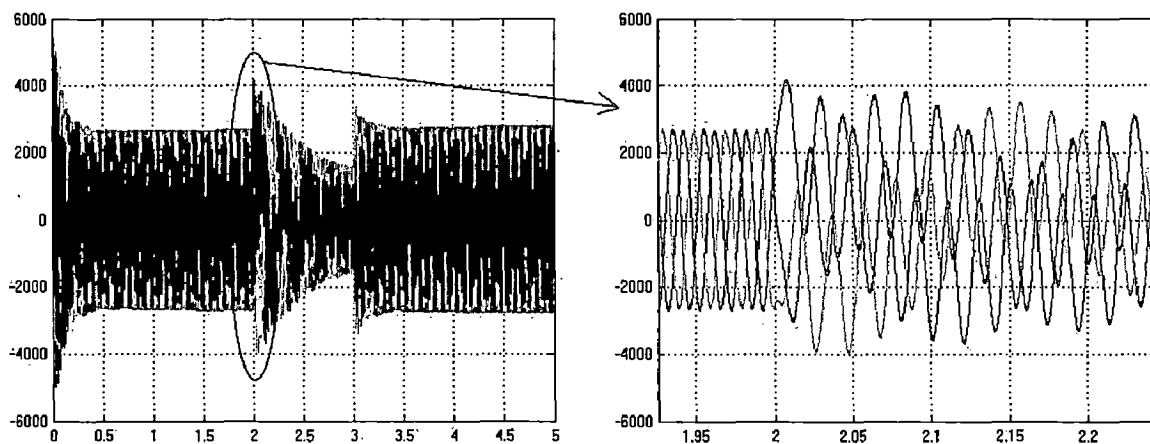


Fig 5.4 LLLG Fault: Three phase load currents before, during and after the fault

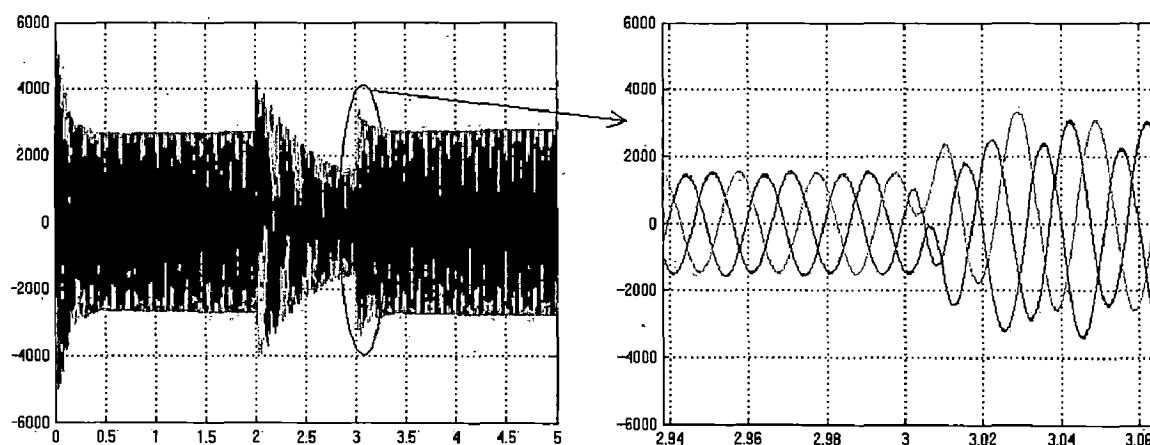


Fig 5.5 LLLG Fault: Three phase load currents (for zooming)

Figs 5.4 and 5.5 shows the current waveforms when an LLL or a LLLG fault occurs. At $t=2$, when the fault occurs suddenly, the current which is initially flowing into the grid encounters a short circuit in all the three phases. So it rises up to 4000 A from 2800 A. This is because when a system encounters such faults, the transient currents occur and they are soon damped out. These transient oscillations are damped out because their energy is dissipated in the resistive part of the circuit. The transient currents consist of three components. They are the sub-transient component, transient component and the steady state.

- The sub-transient period is first, and is associated with the largest currents i.e. of may be even 8 to 10 times of rated current. These currents decay in a matter of milliseconds. The magnitudes of these currents are dependant on the sub-transient reactance of the synchronous generator.
- The transient period comes next i.e. between sub transient and steady-state with currents of 3 to 5 times of rated current. These decay in tenths of a second, 0.9 seconds in this case. The magnitudes of these currents are dependant on the transient reactance of the synchronous generator. And the decaying time constant for the above two cases, depends on the stator resistance and their respective reactances of the synchronous generator.
- Then comes the steady-state which occurs after all the transients have had time to settle down.

After the transients settled down, the currents stabilize themselves at around 1500 A until the fault is cleared as shown above. The values of the steady state currents depend on the synchronous reactance of the synchronous generator. All the values of the above reactances are specified in Appendix C.

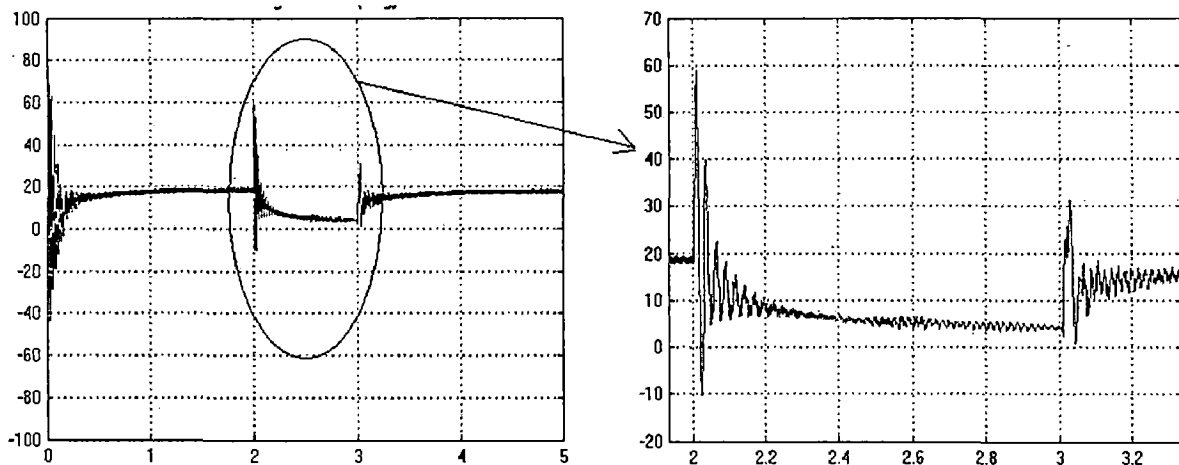


Fig 5.6 LLLG Fault: Load angle before, during and after the fault

Fig 5.6 shows the load angle behaviour. After the fault it sees only the fault impedance which is negligible when compared to the load impedance before the fault. Hence the angle reduces and settles at around 0° if the fault impedance is zero. When the fault is cleared, the angle again increases after several oscillations to its original value of 19° . This systematic change in the load angle is only observed for the symmetrical faults.

5.5.2 LL Fault

This fault comes second in the list of the most common type of fault which is the LG fault and it is more severe than an LG fault as seen in the waveforms below.

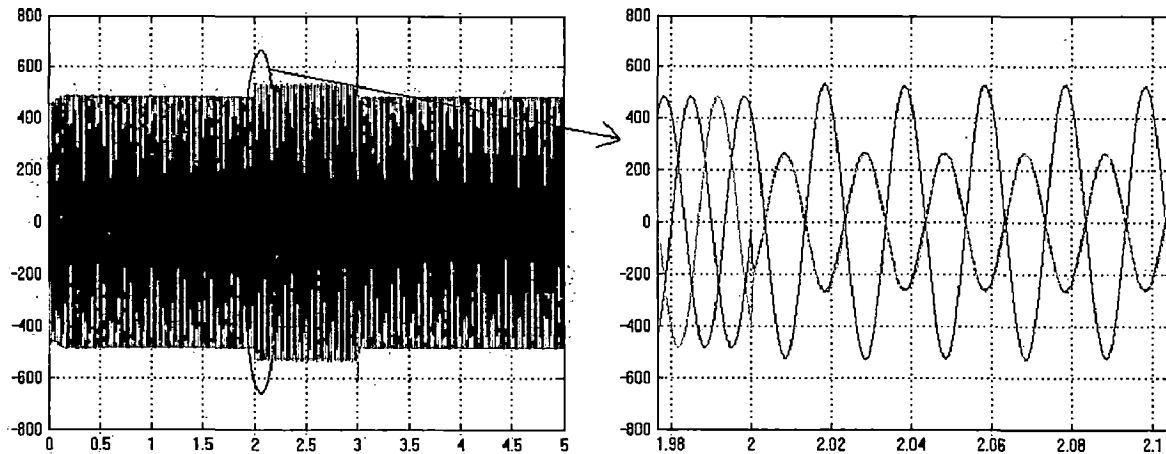


Fig 5.7 LL Fault: Three phase load voltages before, during and after the fault

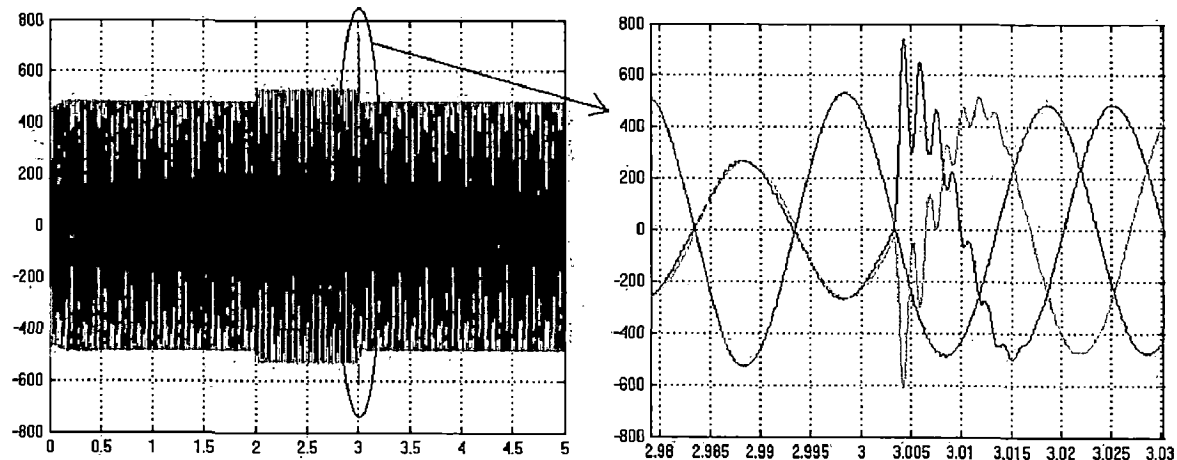


Fig 5.8 LL Fault: Three phase load voltages (for zooming)

Figs 5.7 and 5.8 shows the voltage waveforms when an LL fault occurs. It is clearly seen that voltages of two phases will have a drop from 500 V to 230 V which is slightly less than the half of the original voltage and it is also observed that the third phase voltage increases to about 530 V from 500 V. This is because, in the faulted phases, higher current circulates than normal due to the short circuit but the magnitude is limited to a certain value due to the system impedance. And in the healthy phase, less current than normal flows. So to maintain the overall power balanced, those changes in

voltages take place. An observation here is that the two phase voltages get in phase with each other as expected since a short circuit occurred.

At the instant when the fault is cleared i.e. at $t=3$ secs, the spikes in the voltages of both the faulted phases are observed and the value of the third phase reaches normal value.

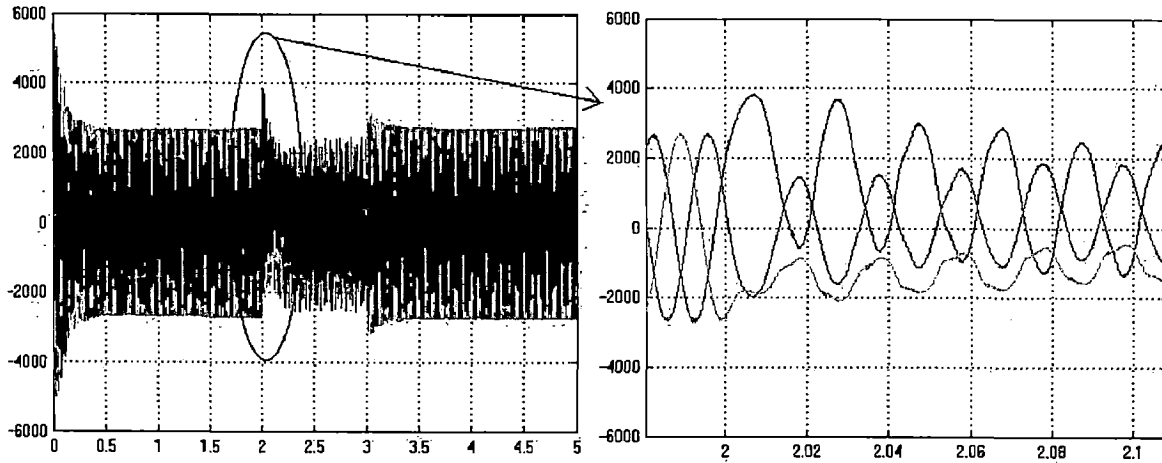


Fig 5.9 LL Fault: Three phase load currents before, during and after the fault

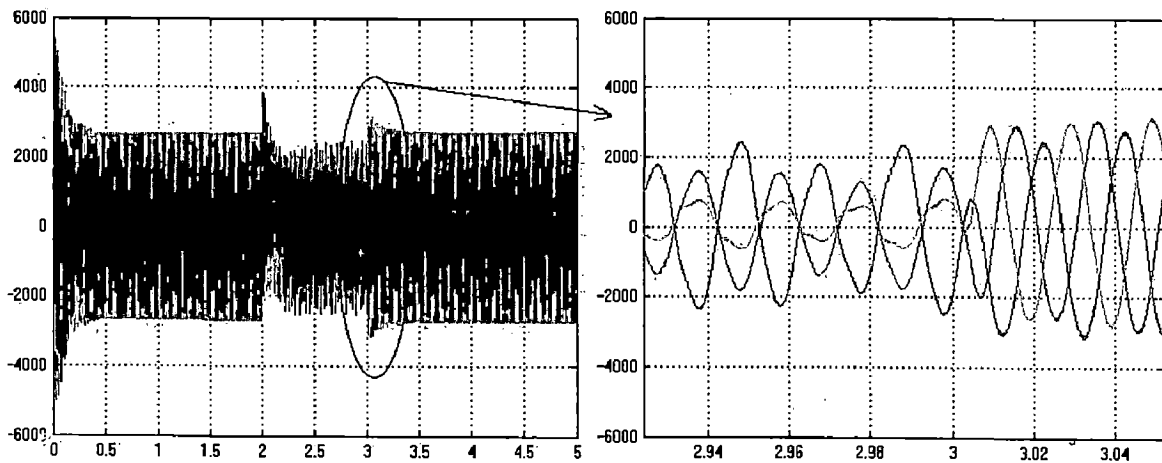


Fig 5.10 LL Fault: Three phase load currents (for zooming)

Figs 5.9 and 5.10 shows the current waveforms when an LL fault occurs. The transients are observed at the instant of occurrence and clearance of the fault as usual. If carefully observed, during the fault, three phases will carry three different currents. As said before, the high currents are circulated in the faulted phases but are limited to the

system cum fault impedance. To further explain, this is an asymmetrical fault and the asymmetrical current can reach a peak value of nearly twice that of the symmetrical steady state current, depending on the time constant L/R of the supply circuit. When the time constant of the supply circuit is high, the transient and sub transient reactance of the synchronous generator cause an extra high first peak of the short circuit current. This can be seen in the fig 5.10 above.

Fault occurs in blue and green phases as seen. In the above graphs, the magnitude of blue phase current is high (about 2300 A), and the magnitude of the green phase current is low (about 800 A). The circulation current is the sum of both these currents (because the two phases are in same phase after the fault) which is equal to 3100 A. The healthy phase current is also affected because of the high current in other two phases and it will settle to the steady state value of 1500A which is the steady state current which depend on the synchronous reactance of the generator as said in section 5.5.1.

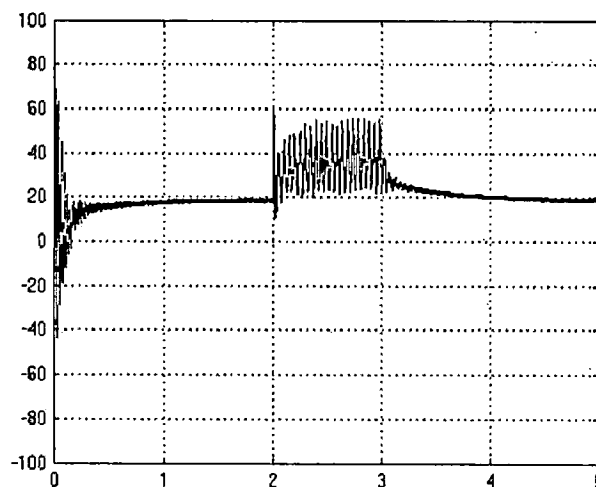


Fig 5.11 LL Fault: Load angle before, during and after the fault

Fig 5.11 shows the load angle when the LL fault occurs. Since this kind of fault is an unsymmetrical fault unlike the LLL fault which is symmetrical, a particular pattern is not followed by the load angle. But the generator sees some kind of disturbance at the load and hence the oscillations result through out the duration of the fault as shown in the figure above. The load angle oscillates in between 20° and 55° .

5.5.3 LG Fault

This is the most common type of fault and is least severe. Hence this fault is also termed as a short line fault.

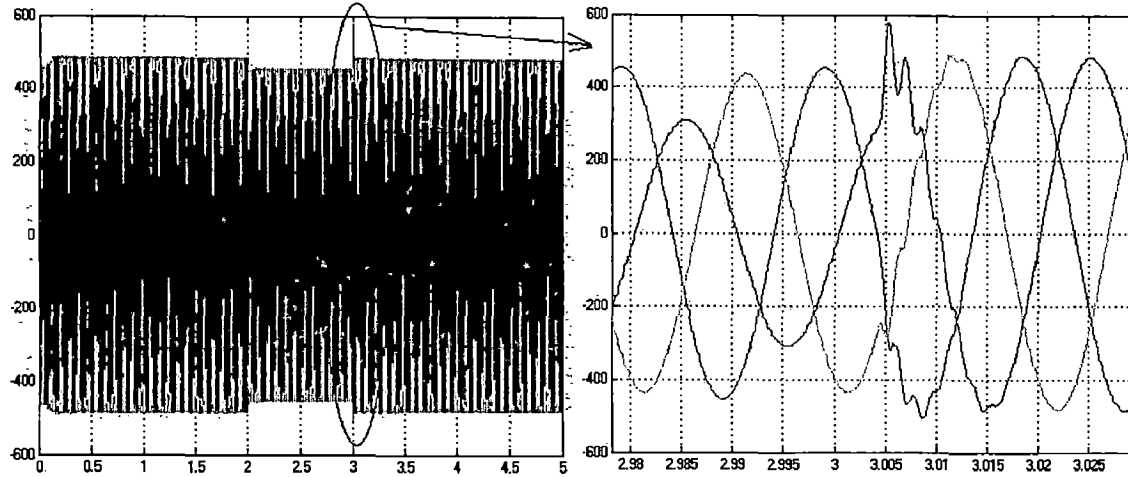


Fig 5.12 LG Fault: Three phase load voltages before, during and after the fault

Fig 5.12 shows the voltage waveforms when an LG fault occurs. As per the model the fault has been created in the green phase. It is observed that the voltage of the blue phase drops from 500 V to 250 V i.e. approximately to half of the original value. The faulted phase voltage is also reduced by about 80 V while not much change in voltage is observed in the third phase. Here the measured voltages are phase to phase voltages and it is difficult to interpret the waveforms. If they were phase to ground voltages, it would have been easily concluded that the faulted phase voltage would have fallen to nearly zero volts because of the grounding.

After the fault is cleared, a very steep abnormal voltage oscillation is observed similar or higher than the voltage spikes of other faults. This puts a high stress on the still-hot arc channel of the interrupting device used for fault clearing and can cause a thermal break down of the arc channel.

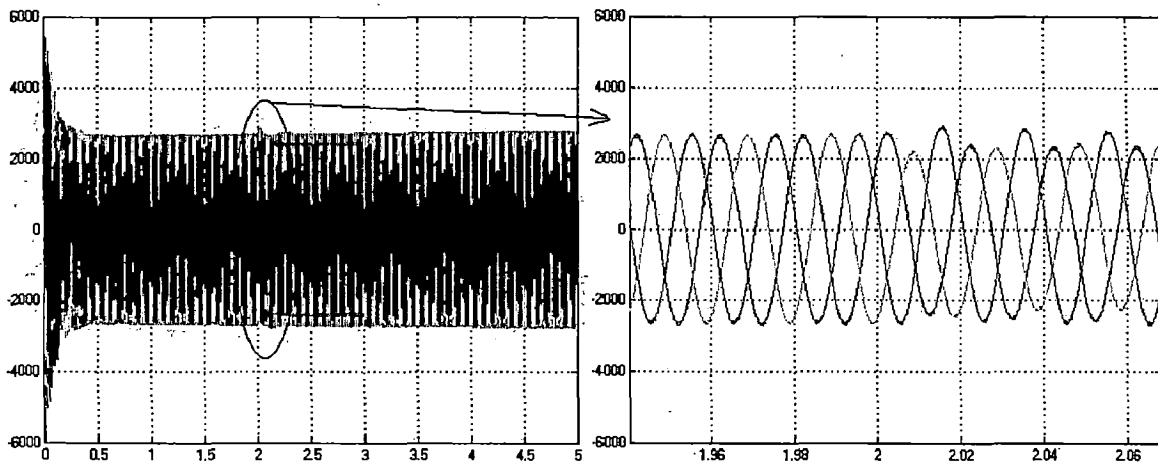


Fig 5.13 LG Fault: Three phase load currents before, during and after the fault

Fig 5.13 shows the current waveforms when an LG fault occurs. It has been observed that the interrupting devices used occasionally failed to interrupt short circuit currents smaller than the current values they were designed and tested for. A careful analysis has revealed that in many cases, the fault occurred on a high voltage transmission line, a few kilometers away from the interrupting device. It was later discovered that the fault was an LG fault. As the simple analysis cannot be done for an LG fault like other faults, few standards came into existence for the short line LG fault test. At present, the short line LG fault test is considered to be one of the most severe short circuit duties for high voltage circuit breakers, the reason is because of the building up of the transient recovery voltage TRV across the terminals of the interrupting device[18].

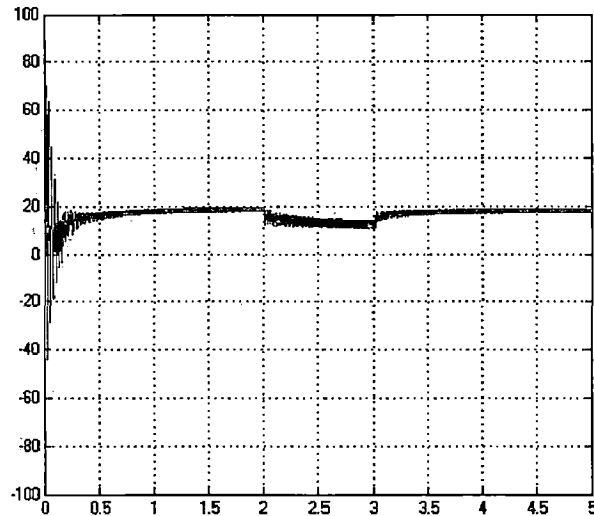


Fig 5.14 LG Fault: Load angle before, during and after the fault

Fig 5.14 shows the load angle when the LG fault occurs. Since this kind of fault is also an unsymmetrical fault, a particular pattern is not followed by the load angle. But the generator sees some kind of disturbance at the load and hence the oscillations result through out the duration of the fault as shown in the figure above.

5.5.4 LLG Fault

This type of fault is almost similar to the LL fault with slight differences. The waveforms are shown below.

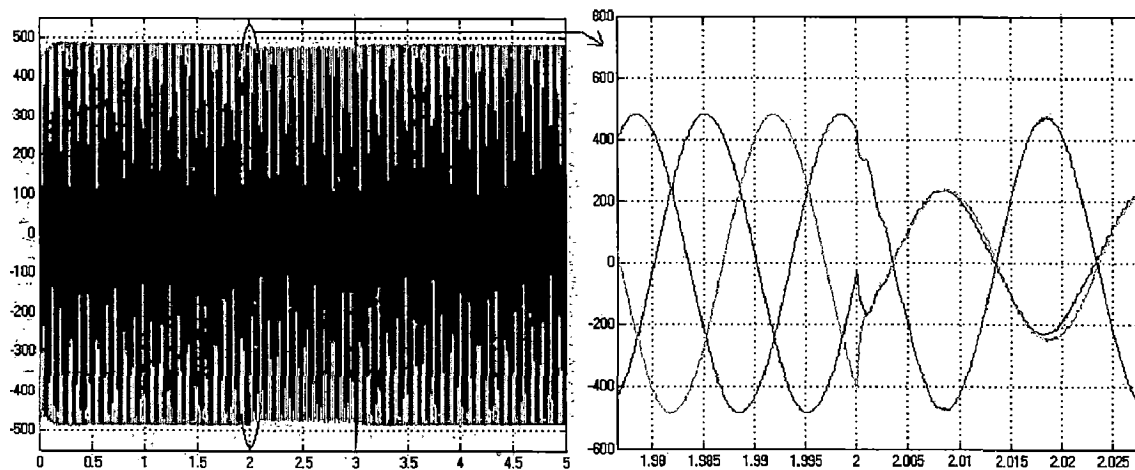


Fig 5.15 LLG Fault: Three phase load voltages before, during and after the fault

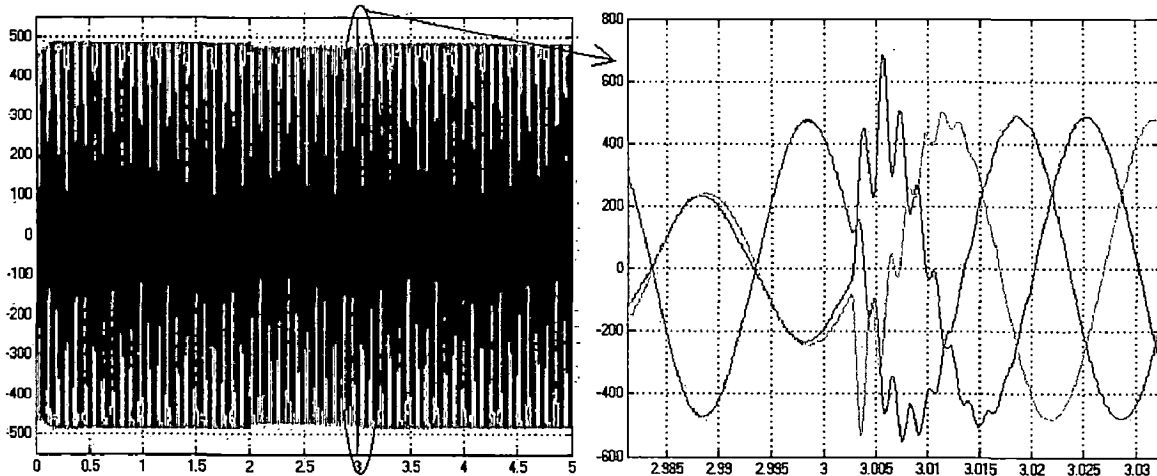


Fig 5.16 LLG Fault: Three phase load voltages (for zooming)

Figs 5.15 and 5.16 shows the voltage waveforms when an LLG fault occurs. This fault is similar to the LL fault. It is clearly seen that voltages of two phases will have a drop from 500 V to 230 V which is slightly less than the half of the original voltage as in LL fault and there is no change in the third phase voltage. This is because, in the faulted phases, higher current circulates than normal due to the short circuit but the magnitude is limited to a certain value due to the system's impedance. And in the healthy phase, normal current flows because the faulted currents are sent into the ground and it does not effect the third phase. An observation here is that the two phase voltages get in phase with each other as expected since a short circuit occurred similar to an LL fault.

At the instant when the fault is cleared i.e. at $t=3$ secs, the spikes in the voltages of all the three phases are observed.

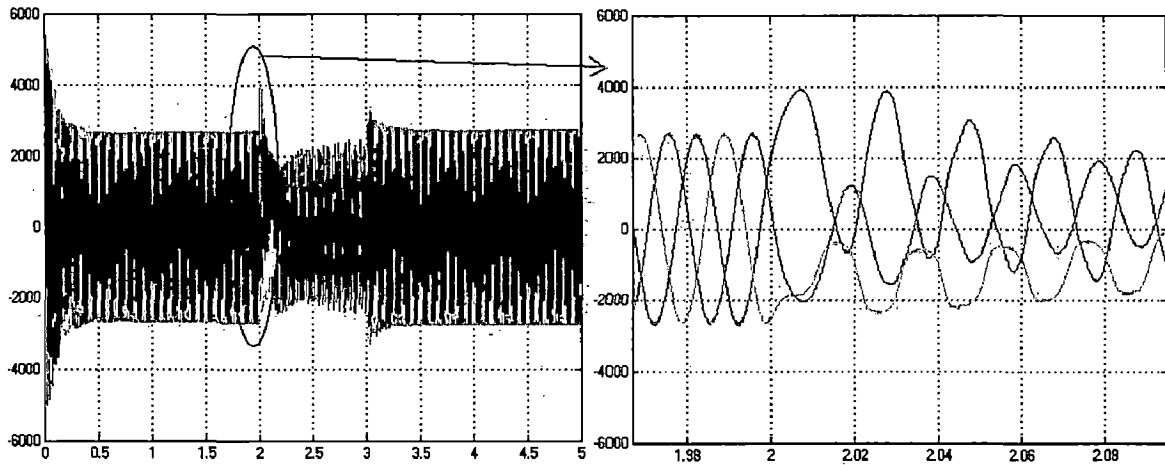


Fig 5.17 LLG Fault: Three phase load currents before, during and after the fault

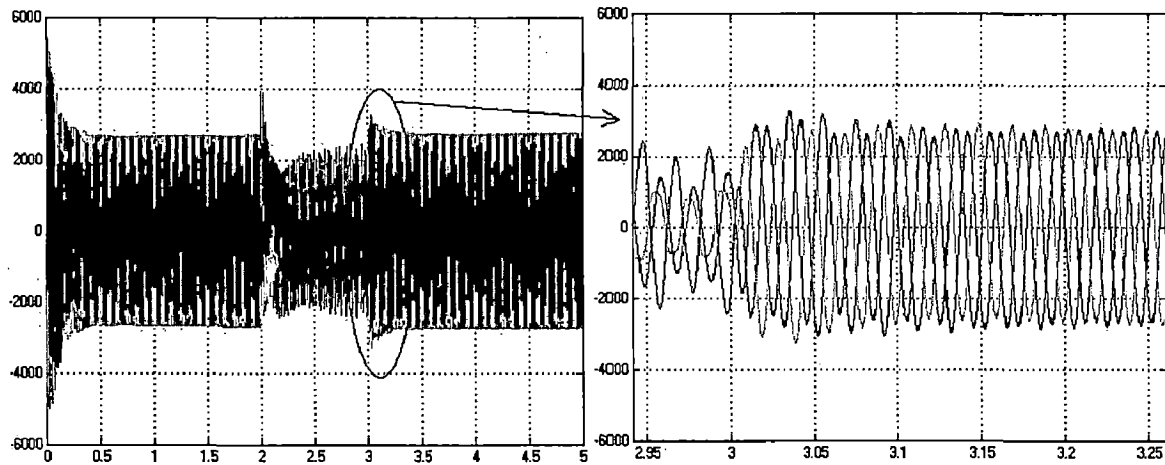


Fig 5.18 LLG Fault: Three phase load currents (for zooming)

Figs 5.17 and 5.18 shows the current waveforms when an LLG fault occurs. The transients are observed at the instant of occurrence and clearance of the fault as in LL fault. Here also, during the fault, three phases will carry three different currents. As said before, the high currents are circulated in the faulted phases but are limited to the system's impedance. Fault occurs in blue and green phases as seen. In the above graphs, the magnitude of blue phase current is high (about 2300 A), and the magnitude of the green phase current is low (about 800 A). The circulation current is the sum of both these currents which is equal to 3100 A.

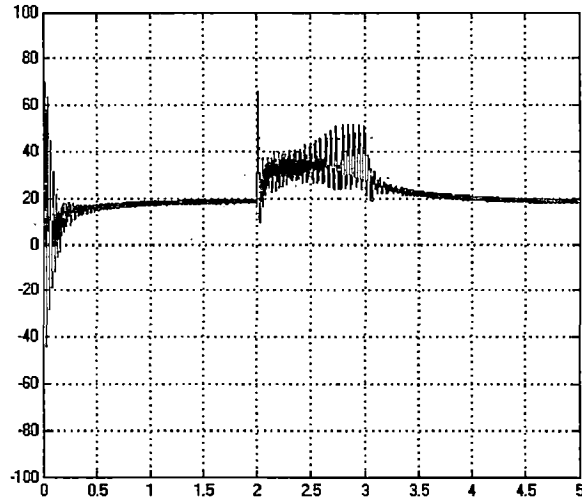


Fig 5.19 LLG Fault: Load angle before, during and after the fault

Fig 5.19 shows the load angle when the LLG fault occurs. Since this kind of fault is also an unsymmetrical fault unlike the LLL fault which is symmetrical, a particular pattern is not followed by the load angle. But the generator sees some kind of disturbance at the load and hence the oscillations result through out the duration of the fault as shown in the figure above. The load angle oscillates in between 20° and 50° .

5.5.5 LL Fault and LG Fault on the third phase

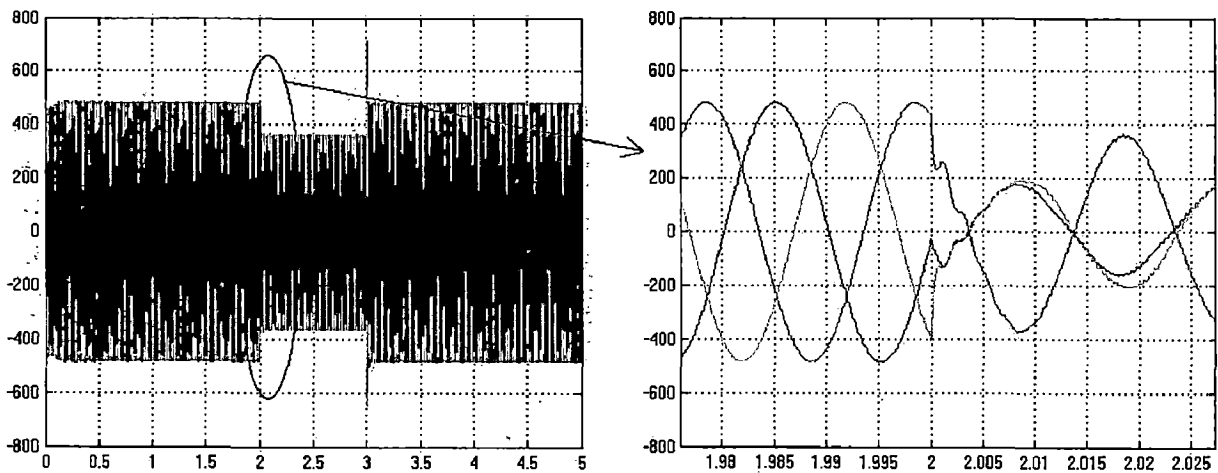


Fig 5.20 LL&LG Fault: Three phase load voltages before, during and after the fault

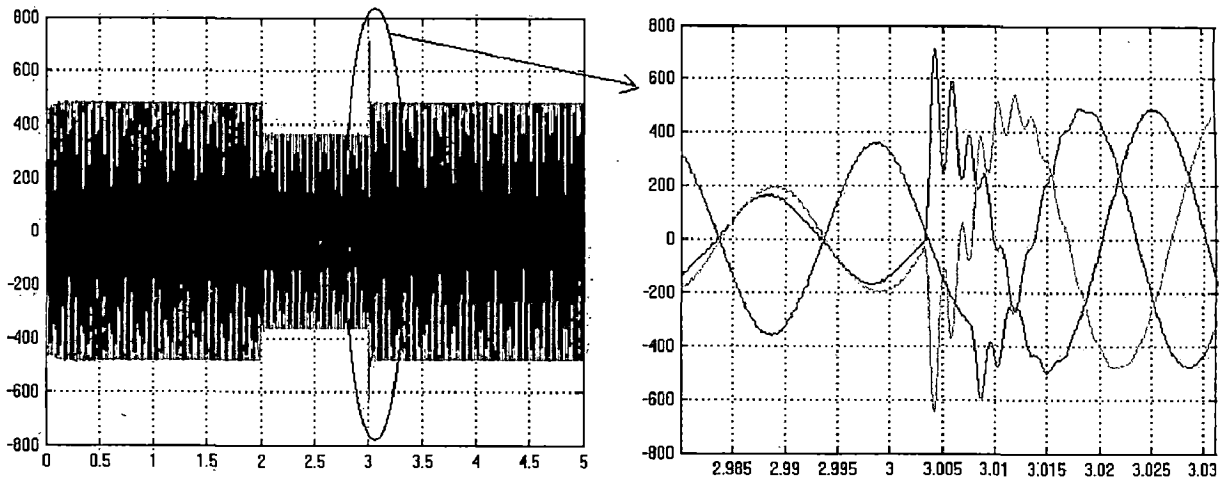


Fig 5.21 LL&LG Fault: Three phase load voltages (for zooming)

Figs 5.20 and 5.21 shows the voltage waveforms when an LL and LG fault on the third phase occurs. As in LL fault and LG fault above, here the combined effects of both are seen. The LL fault occurs in the blue phase and green phase and hence as the circulating current will be high, and to maintain the power constant, the voltage drops to about 200 V in both phases from 500 V. An observation here also is that the two phase voltages get in phase with each other as expected since a short circuit occurred. As the LG fault occurs on the third phase, and as its effect is relatively less, the voltage drops to about 380 V.

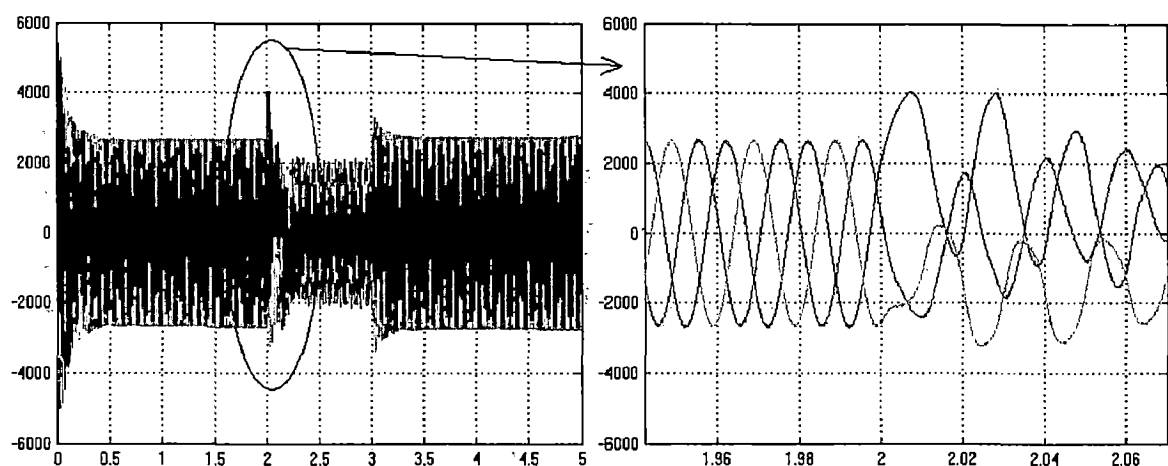


Fig 5.22 LL&LG Fault: Three phase load currents before, during and after the fault

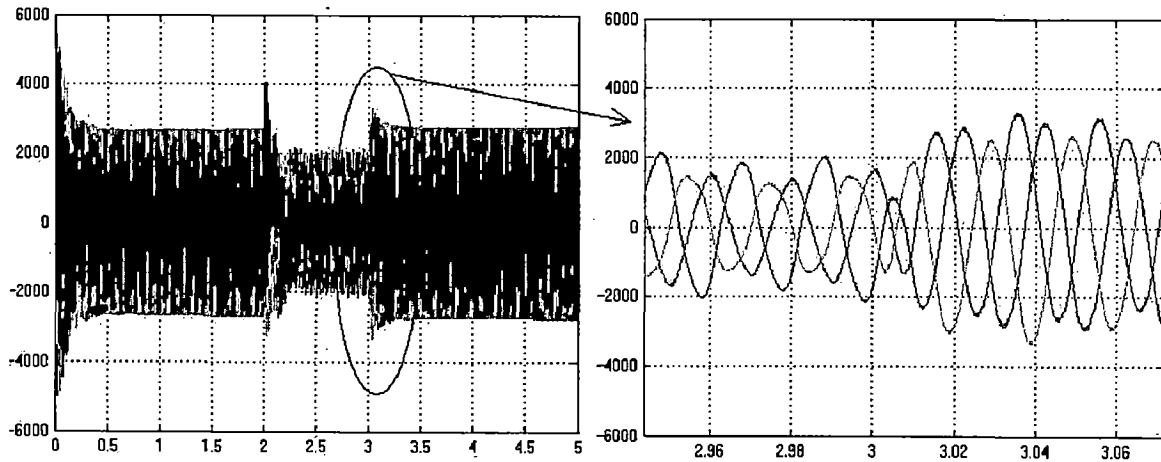


Fig 5.23 LL&LG Fault: Three phase load voltages (for zooming)

Figs 5.22 and 5.23 shows the current waveforms when an LL and LG fault on the third phase occurs. As in LL fault above, here also the three phases currents have three different values. Faulted phases are blue and green. Magnitude of fault current in blue phase is around 2000 A and in green it is 1100 A. Therefore the fault current is the sum of these two i.e. 3100 A. In the third phase also, as the LG fault occurs, the current of 1500 A flows and the remaining current of 300 A goes to the ground.

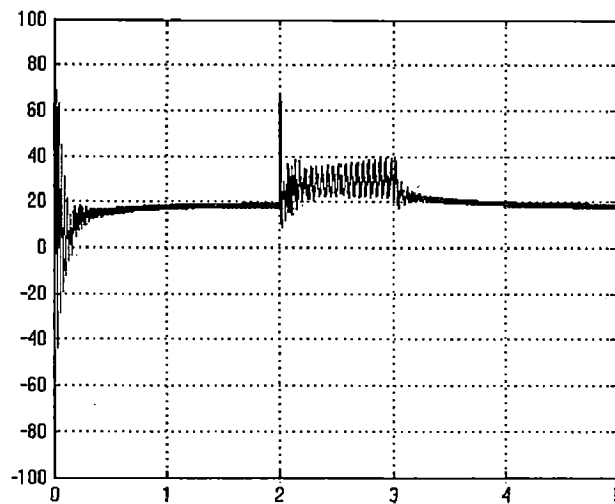


Fig 5.24 LL&LG Fault: Load Angle Before, During and After the Fault

Fig 5.24 shows the load angle when an LL and LG fault on the third phase occurs. As said before, the fault here also is an unsymmetrical fault. The generator sees some

kind of disturbance at the load and hence the oscillations result through out the duration of the fault as shown in the figure above. The load angle oscillates in between 20° and 40°.

5.5.6 Short circuit fault current calculation

This section is drafted just to show that the above obtained values in various faulted conditions are correct. It is to be noted that the comparison of this sort is practically not correct because the above values are obtained under dynamic condition and the values obtained in this section are under static condition.

The theory has been shown in section 5.4.

When the short circuit occurs at $t=2$ or $[\varphi - \tan^{-1}(\frac{\omega L}{R})] = 0$,i.e. when the voltage is at the zero crossing, the DC component is zero and peak short circuit current is due to the AC component only.

$$\begin{aligned} I_{sc} &= \frac{V_{peak}}{X_d''} \\ &= \frac{549}{0.13} \\ &= 4223 A \end{aligned}$$

Where X_d'' is the sub-transient reactance of the synchronous generator.

V_{peak} is the peak value of the terminal voltage which is measured theoretically to be 549 V approximately at the stator terminals. Where as the practical value obtained in the simulation under dynamic conditions is 500 V which is measured at the load terminals. Certain voltage drop will be there in the additional loads of the rectifier and inverter circuit block.

So in all cases, theoretically, the sub-transient peak currents should be around 4223 A for the model used. The practically obtained value is 4000 A.

After all the transients are died out, the only steady state short circuit current will flow in the system as said before which is given by

$$I_{ss} = \frac{V_{peak}}{X_d}$$

$$= \frac{549}{0.35}$$

$$= 1568.6A$$

So theoretically, the steady state peak currents should be around 1568.6 A for the model used. The practically obtained value is 1500 A.

Where X_d is the synchronous reactance of the synchronous generator. The values of the sub transient reactance and the synchronous reactance of the generator model are specified in Appendix C.

5.6 Results in a tabulated form

S.No	Parameters	MATLAB/ Simulink value
1	Load current	2800 A
2	Rotor speed	9.817 rad/sec
3	Torque	115000 Nm
4	Power factor	0.65
5	Load voltage.	500 V peak
6	Short circuit fault current	4000 A
7	Steady state fault current	1500 A

Table 5.1 Results in a tabulated form

CHAPTER 6

CONCLUSIONS AND FUTURE SCOPE

6.1 Conclusions

A generic model for the Type D class of variable speed wind turbines with a synchronous generator and full power conversion has been presented. The use of the model to analyze the performance of the wind turbine during the faults has been demonstrated.

It has been highlighted that by using the full power conversion, the variable speed operation is possible and the wind turbine will be immune to severe sags in grid voltage due to the complete decoupling of the operation of the synchronous generator from the grid.

The various results obtained for the simulations of different operating conditions and parameters are shown in chapters 4 and 5. From the discussions of these results, the following points can be concluded for the whole model.

- The whole model has been built in MATLAB/Simulink environment and its accuracy is verified successfully by considering individual components and finding out the output results of those individual components. The specifications of these components have been given individually by the trial and error method until the results finally got converged to stable values.
- The characteristics of the synchronous generator have been studied for both fixed speed case and for the variable speed case (full power conversion case or decoupled case).
- The synchronization is initialized at time $t=0$ in all the cases and it is observed that as the phase shift between grid voltage and internal voltage of the generator increases at the instant of synchronization, the fluctuation in rotor speed, output power, output torque and the stator current also increase. This fluctuation is negligible for best synchronization, i.e. when grid voltage and internal voltage are in phase with each other and also when the generator rotor's inertia is high. Both the above conditions are applied to obtain the best synchronization.

- The power quality is maintained in the system itself eliminating the need for installing new PE devices directly saving the cost.
- Finally, the fault analysis has been carried out for the purpose of identifying the fault voltages and currents for future protection through circuit breakers, relays and other reasons such as choosing of a suitable power system arrangement etc.

6.2 Future Scope of work

The initial work such as building and simulating for practical conditions of the up coming variable speed wind turbine-generator drives has been completed through this dissertation. But there is a lot of scope and demand for these kinds of machines for future power generation. So this work can be continued in the future to study the following points which give more reliability to the decision of using variable speed technology.

- Parallel operation of these wind turbines is important because there are problems relating to this for example if 30 turbines are installed over a stretched area as in fig 1.3, the wind speed at a particular time will not be the same for all the turbines. Hence, some turbines generate less power, some more and some do not. In that case, the grid compatibility is very important. So parallel operation of variable speed wind turbines is one of the hot topics.
- Now-a-days, permanent magnet synchronous generators are being widely used with variable speed wind turbines and a lot of research is also being done. At present, the application of these generators is limited to only lesser MW wind turbines, the highest being only 1 MW. So a similar work can be carried out using permanent magnet synchronous generators for higher MW turbines using variable speed technology.
- The use of frequency converter can be eliminated if a dynamically pole changing synchronous generator is used. But the poles cannot be fractional and only even number of poles can be achieved. Through a new technology known as the written pole technology, the dynamical pole changing can be achieved with fractional poles also [23].

REFERENCES

- [1]. **Ackermann, T.**, “Wind power in power systems”, John Wiley & Sons, Ltd., 2005
- [2]. **Behnke, M.R. and Muljadi, E.**, “Reduced order dynamic model for variable speed wind turbine with synchronous generator and full power conversion topology”, in Future Power Systems, 2005, an International Conference on 16-18 Nov. 2005 Page(s): 6 pp.
- [3]. **Bimbhra, P.S.**, “Power Electronics”, Third edition, Khanna publishers, 2005
- [4]. **Chen, Z.**, “Compensation Schemes for a SCR Converter in variable speed wind power systems”, in IEEE Transactions on Power Delivery, vol. 19, No. 2, April 2004
- [5]. **Chen, Z. and Spooner, E.**, “Grid power quality with variable-speed wind turbines,” in IEEE Transactions on Energy Conversion, vol. 16, pp. 148–154, June 2001.
- [6]. **Chen, Z. and Spooner, E.**, “Wind turbine power converters: A comparative study”, Power Electronics and Variable Speed Drives, 21-23 September 1998, Conference Publication No. 456 IEE 1998
- [7]. **Conner, B. and Leithead, W.E.**, “Performance assessment of variable speed wind turbines”, Opportunities and Advances in International Electric Power Generation, International Conference on (Conf. Publ. No. 419) 18-20 March 1996 Page(s):65 - 68
- [8]. **Eduard, M. and Butterfield, C.P.**, “Pitch-controlled variable-speed wind turbine generation” in IEEE Transactions on industry applications, Vol. 37, No. 1, January/February 2001.
- [9]. **Electricity Training Association**, “Power system protection”, volume 1, revised by Institution of Electrical Engineers, 1995

- [10]. **Jin-Woo, J.**, “Sine- Δ PWM Inverter”, Ph.D Thesis, Mechatronic systems laboratory, Department of Electrical and Computer Engineering, the Ohio State University
- [11]. **Mullane, A., Lightbody, G., Yacamini, R. and Simon, G.**, “The simulation and control of a grid connected variable speed wind turbine” in Proceedings of the Irish Signals and Systems Conference, pages 472–479, Jun. 2000.
- [12]. **Müller, H., Pöller, M. and Basteck, A., Tilscher, M. and Pfister, J.**, “ Grid compatibility of variable speed wind turbines with directly coupled synchronous generator and hydro-dynamically controlled gearbox”, in Sixth International workshop on Large-scale integration of wind power and transmission networks for offshore wind farms, Delft, the Netherlands, October 2006.
- [13]. **Naveen, G.**, “Parallel operation of grid connected permanent magnet synchronous generators for Small Hydro Power plants”, M.Tech Dissertation, Alternate Hydro Energy Centre, Indian Institute of Technology, Roorkee
- [14]. **Pieter, S., Tim, G.**, “Torque control for variable speed wind turbines” in European wind energy conference, London, 22-25 November, 2004.
- [15]. **Pöller, M. and Sebastian, A.**, “Direct drive synchronous machine models for stability assessment of wind farms”, in a publication of DIgSILENT GmbH, Heinrich-Hertz-Str, Germany
- [16]. **Van der sluis, L.**, “Transients in power systems”, John Wiley & Sons, Ltd., 2001
- [17]. www.4energia.ee/files/File/Enclosure%201.1%20Product%20overview.pdf
- [18]. www.denysschen.com/catalogue/density.asp
- [19]. www.energyadvocate.com/fw91.htm
- [20]. www.ftexploring.com/energy/wind-enrgy.html

[21]. www.jxj.base10.ws/magsandj/rew/2003_01/inside_wind.html: Fixed vs. Variable speed turbines

[22]. www.mathworks.com/access/helpdesk/help/toolbox/physmod/powersys: MATLAB-works-support

[23]. www.meridiumpower.ca/C/body_c.html

[24]. www.windpower.org/en/tour/wres/cp.htm

[25]. www.vestas.com/NR/rdonlyres/E94ED277-D654-4A5C-AD73-6DA09A649BA2/0/

Hoyle_UK.pdf

APPENDIX A

DESIGN OF SNUBBER CIRCUITS

In this work, the snubber circuits are used in the rectifiers and the inverters. Snubbers are basically used to avoid unnecessary switching on of a diode or IGBT in this work. They are also used to absorb the transients in voltages and currents which may apply across the diodes or IGBT's and destroy them. Snubbers are also used to avoid unwanted $\frac{dv}{dt}$ triggering and $\frac{di}{dt}$ triggering of the device.

A snubber circuit consists of a series combination of resistance and capacitance in parallel with the device. In the absence of snubber, a sudden voltage appears across the device and turns it on unwantedly or destroys it. Now when the snubber is present, when a sudden voltage appears, the capacitor behaves as a short circuit and therefore, the voltage across the device is zero initially. With the passage of time, voltage across the capacitor builds up at a slow rate such that $\frac{dv}{dt}$ across it and therefore across the device is less than the specified maximum $\frac{dv}{dt}$ rating of the device.

Before the device is fired by gate pulse, the capacitor charges to the full voltage applied across it. When the device is turned on, the capacitor discharges through the device and sends a current equal to (full voltage)/ (resistance of the local path formed by the capacitor and the device). As this resistance is quite low, the turn on $\frac{di}{dt}$ will tend to be excessive and as a result the device may be destroyed. In order to limit the magnitude of this discharge current, a resistance is inserted in series with the capacitor as show in fig A1. Now when the device is turned on, initial discharge current is relatively small and the turn on $\frac{di}{dt}$ is reduced [3].

To design a snubber circuit, it must be made sure that the resistance, capacitance and the load parameters should be such that the $\frac{dv}{dt}$ across the capacitor during its

charging is less than the specified $\frac{dv}{dt}$ rating of the device and the discharge current at the turn on of the device is within reasonable limits. Generally these parameters form an under damped circuit so that the $\frac{dv}{dt}$ is limited to acceptable values. The design of snubber circuit parameters is quite complex but approximate formulas have been used to find out the values of the capacitor and the resistance.

In this work, the rectifier uses the diodes and the snubber circuit for each diode is approximated as follows:

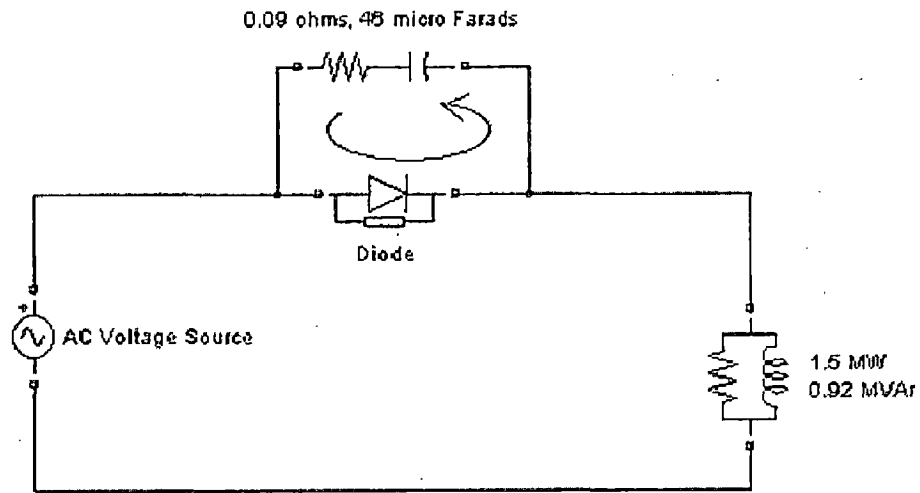


Fig A1: Representation of the snubber circuit of a single diode of the rectifier

The snubber resistance R_s and the snubber capacitance C_s have been designed from the following relations.

$$\begin{aligned}
 C_s &< \frac{P}{1000(2\pi f)V^2} \\
 &< \frac{2.35 \times 10^6}{1000 \times 2 \times \pi \times 50 \times 400^2} \\
 &< 0.0000467 \\
 &< 46.7 \mu F \\
 &= 46 \mu F
 \end{aligned}$$

$$\begin{aligned}
 R_s &> 2 \frac{T_s}{C_s} \\
 &> \frac{2 \times 2 \times 10^{-6}}{46 \times 10^{-6}} \\
 &> 0.0869 \Omega \\
 &= 0.09 \Omega
 \end{aligned}$$

Where T_s is the time period of the discrete system

Voltage V is the rms value and

Power P is in VA.

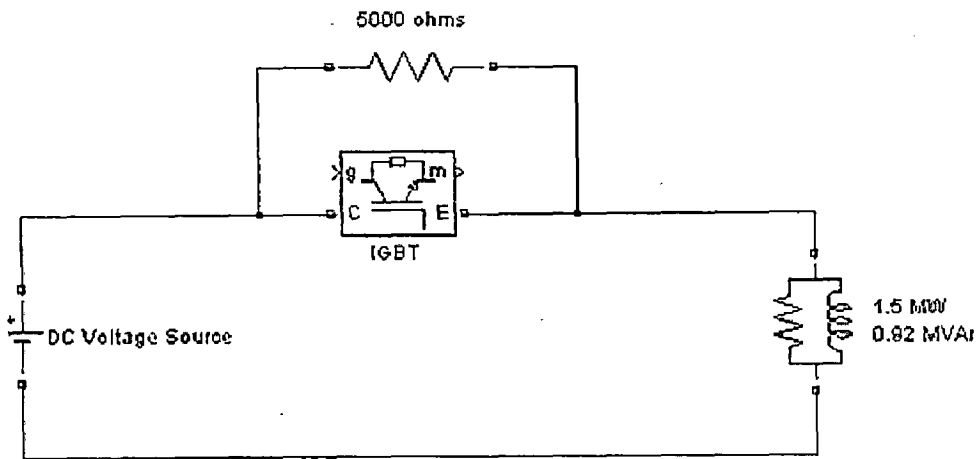


Fig A2: Representation of the resistive snubber circuit of a single IGBT of the inverter

The inverter also uses snubbers but the impedance of the capacitance is taken as zero, i.e. the snubbers used by the inverter are the resistive snubbers. As the inverter's IGBTs are triggered by the gate pulses which are generated from the output of the inverter itself (feed back circuit), it is very difficult to find out the exact time of trigger of each IGBT. Hence, it is complex to design the capacitance value for the snubber circuit because the capacitor takes some time to get fully charged and it may be possible that during this time only a gate pulse may occur. For instance, if the capacitor is charged only to one fourth of the full voltage by the time the gate pulse appears, the discharge current it generates may not be sufficient for the IGBT to turn on. Hence as abnormal operation may result producing harmonics in voltages. So to avoid this problem, the capacitance value is kept infinite so that its impedance is zero and only a

resistance of high value appears across the IGBT. This high resistance is enough to avoid $\frac{dv}{dt}$ triggering and $\frac{di}{dt}$ triggering.

The set up is shown in fig A2. Before the turn on of the IGBT, a sufficient voltage is developed across it by the presence of the resistance in its parallel, so that when the IGBT is triggered by a gate pulse to turn on, the sudden high current which is normally supposed to flow through it in the absence of the resistance is avoided by the voltage drop across the resistance and IGBT developed in the local circuit in the opposite direction. So a less current always flows through the IGBT protecting it from getting destroyed too.

APPENDIX B

CONCEPT OF THE CONTROL SYSTEM OF INVERTER

The most efficient method of controlling the output voltage is to incorporate pulse width modulation control (PWM control) within the inverters. In this method, a fixed DC input voltage is supplied to the inverter and a controlled AC output voltage is obtained by adjusting the on-and-off periods of the inverter devices. The PWM control has the following advantages:

- The output voltage control can be obtained without any additional components.
- With this type of control, lower order harmonics can be eliminated or minimized along with its output voltage control. The filtering requirements are minimized as higher order harmonics can be filtered easily.

The main drawback of this method is that the IGBTs used in this method must have very low turn-on and turn-off times. Therefore, they are very expensive.

The commonly used PWM control techniques are:

- (a) Single-pulse width modulation (SPWM)
- (b) Multiple-pulse width modulation (MPWM)
- (c) Sinusoidal pulse width modulation (sin PWM)

In this work, the sinusoidal pulse width modulation technique is used. In this method of modulation, several pulses per half-cycle are used. Instead of maintaining the width of all pulses the same, the width of each pulse is varied proportional to the amplitude of a sine-wave evaluated at the centre of the same pulse. By comparing a sinusoidal reference signal with a triangular carrier wave of a particular frequency, the gating signals are generated as shown in Fig A4. The frequency of reference signal, 50Hz in this case, will determine the inverter output frequency and its peak amplitude and then in turn the RMS output voltage. The number of pulses per half-cycle depends on the triangular carrier frequency.

By varying the modulation index M , the RMS output voltage can be varied. It can be observed that the area of each pulse corresponds approximately to the area under the

sine-wave between the adjacent midpoints of off periods on the gating signals [3].

The control system used in the work consists of a voltage comparator where the comparison takes place and a PWM pulse generator which will generate the required pulses as shown in the fig A3.

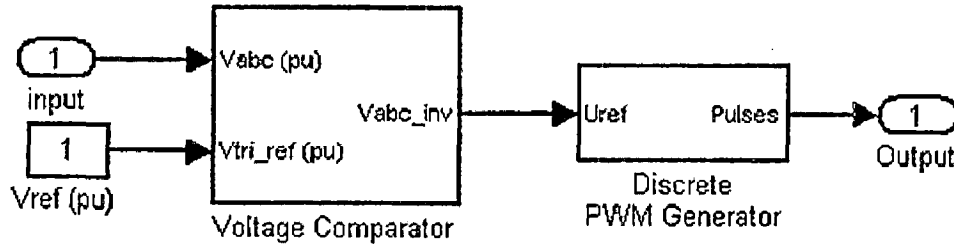


Fig A3: Inside the control system block of fig 4.15

The voltage comparator takes the per unit value of the three phase output voltages as its input ($V_{control}$) whose frequency is 50 Hz and compares it with triangular carrier waveform as shown in the fig A4.

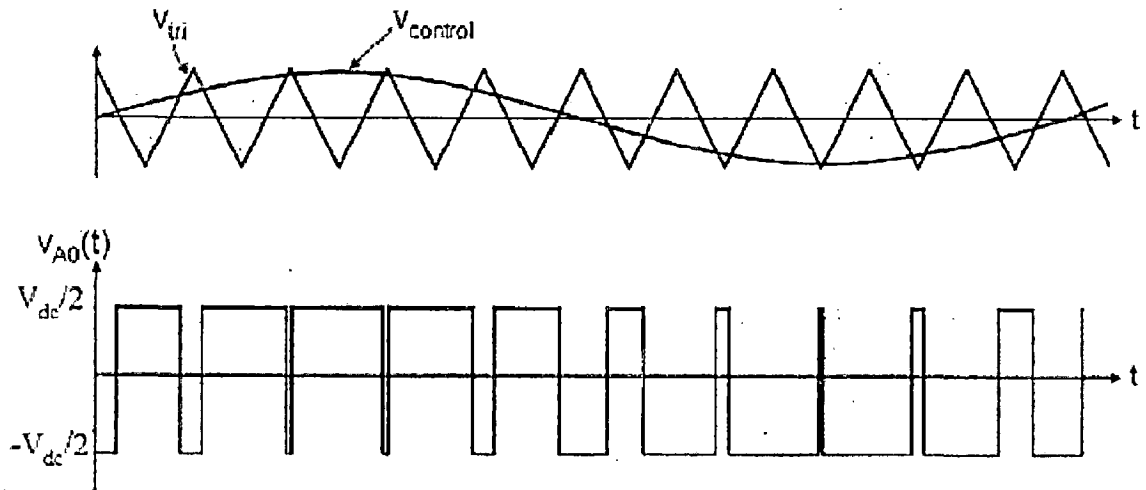


Fig A4: PWM wave forms

As depicted in Fig. A4, the inverter output voltage is determined in the following:

When $V_{control} > V_{tri}$, $V_{A0} = V_{dc}/2$

When $V_{control} < V_{tri}$, $V_{A0} = -V_{dc}/2$

The quasi square wave output of the inverter is then filtered using a 3 phase LC filter to produce perfect sinusoidal voltage waveforms of constant frequency 50 Hz. So the sine wave output of the inverter after filtering, is then again given to the voltage comparator in per unit where it is again compared with a triangular carrier waveform particular frequency and magnitude to produce the output as shown above. This output is again filtered and the feedback cycle continues which is shown in fig 4.15.

The inverter output voltage has the following features:

- PWM frequency is the same as the frequency of V_{tri}
- Amplitude is controlled by the peak value of $V_{control}$
- Fundamental frequency is controlled by the frequency of $V_{control}$

APPENDIX C

PARAMETERS

1. Excitation system parameters

- Time constant of filter (T_R) = 20×10^{-3} s
- Maximum and minimum regulator output limits (V_{AMAX}, V_{AMIN}) = 1, 0 p.u.
- Voltage regulator gain (K_A) = 300 p.u.
- Voltage regulator time constants (T_A) = 0.001 s
- Exciter time constant (T_E) = 0 s
- Exciter constant related to self-excited field (K_E) = 1 p.u.
- Excitation control system stabilizer gain (K_F) = 0.001 p.u.
- Excitation system stabilizer time constant (T_F) = 0.1 s
- Transient gain reduction time constants (T_B, T_C) = 0, 0 s

2. Transformer parameters

- Nominal power = 2 MW
- Frequency = 50 Hz

Winding 1:

- Connection = Delta
- Primary voltage phase to phase = 400 V rms
- Primary winding resistance = 0.0027 p.u.
- Primary winding reactance = 0.08 p.u.

Winding 2:

- Connection = Star, grounded
- Secondary voltage phase to phase = 230 kV rms
- Secondary winding resistance = 0.0027 p.u.
- Secondary winding reactance = 0.08 p.u.

Magnetization resistance = 500 p.u.

Magnetization reactance = 500 p.u.

3. Transmission line parameters

- Frequency (used for R L C specifications) = 50 Hz
- Positive and zero sequence resistances = $0.01273 \Omega / km$, $0.3864 \Omega / km$
- Positive and zero sequence inductances = $0.9337 \times 10^{-3} \text{ H/km}$, $4.1264 \times 10^{-3} \text{ H/km}$
- Positive and zero sequence capacitances = $12.74 \times 10^{-9} \text{ F/km}$, $7.751 \times 10^{-9} \text{ F/km}$
- Length of the line = 100 kms

4. Grid parameters

- Grid voltage phase to phase = 230 kV rms
- Phase angle of phase A = 0 deg
- Frequency = 50 Hz
- Internal connection = Star, grounded
- Three phase Short circuit level at base voltage = 10000 MVA
- X/R ratio = 10

5. Load parameters

(a) On High voltage side

- Active power (P) = 15 MW
- Inductive reactive power (QL) = 9.2 MVA_r

(b) On Low voltage side

- Active power (P) = 1.5 MW
- Inductive reactive power (QL) = 0.92 MVA_r

6. Additional parameters of the synchronous machine

- D-axis synchronous reactance (X_d) = 0.35Ω
- D-axis transient reactance (X_d') = 0.17Ω

- D-axis sub-transient reactance (X_d'') = 0.13 Ω
- Q-axis synchronous reactance (X_q) = 0.35 Ω
- Q-axis transient reactance (X_q') = 0.23 Ω
- Q-axis subtransient reactance (X_q'') = 0.05 Ω
- Transient open-circuit (T_{do}') or short-circuit (T_d') time constant = 4.49 s
- D-axis subtransient open-circuit (T_{do}'') or short-circuit (T_d'') time constant = 0.0681 s
- Q-axis subtransient open-circuit (T_{qo}'') or short-circuit (T_q'') time constant = 0.0513 s